ASSESSMENT OF THE NITRIDING PROCESS PARAMATERS TO IMPROVE THE WEAR RESISTANCE OF SELECTED STEELS

by

Onur YAMAN

B.S., Mechanical Engineering, Middle East Technical University, 2007

Submitted to the Institute for Graduate Studies in
Science and Engineering in partial fulfillment of
the requirements for the degree of
Master of Science

Graduate Program in Mechanical Engineering
Boğaziçi University

2009

To my Family

ACKNOWLEDGEMENTS

I express sincere appreciation to Assistant Professor Ercan Balıkçı for his invaluable guidance and help during the preparation of this dissertation.

I have very much benefited from the discussions with my dear friends Dr. Özgür Özdemir, Barış Tanzer, Hasan Sicim, and Aidin Dario.

I also express my appreciation to Volkan Eşme from Işın Teknik and to Ercan Kurtuluş from Kurtuluş Makina for material and machining support.

I am grateful to my mother, father, and sister for their support during my whole life.

ABSTRACT

ASSESSMENT OF THE NITRIDING PROCESS PARAMATERS TO IMPROVE THE WEAR RESISTANCE OF SELECTED STEELS

Liquid nitriding is one of the most popular heat treatment methods due to its application temperature which is generally in the ferritic region. This results in a good dimensional control after nitriding. Still, it is possible to apply nitriding in austenitic region to increase compound and nitriding case thickness. Nitriding increases surface hardness and wear resistance of specimens sharply. In this thesis, to see these effects of nitriding, three different alloys have been chosen and nitrided in two different salt baths for four different nitriding durations at four different process temperatures according to a predetermined nitriding test matrix. This matrix has been designed to see the effects of initial material microstructure and composition, nitriding temperature, nitriding duration, and nitriding bath composition. Afterwards, the specimens have been tested on a pin-on-disc wear setup, built according to ASTM G99-95a specification. Weights and lengths of all specimens have been measured consistent with given directions in ASTM G99-95a specifications to compare their wear resistance. Furthermore, microstructural characterizations have been completed by using OM, SEM, EDS, XRD, microhardness, and surface roughness analyses after nitriding to identify the properties of compound and diffusion layer.

The evaluation of the data gathered gives an insight in to the nitriding. According to the results, time and temperature have similar effects on nitriding. The increase in nitriding time and bath temperature increases the compound layer and nitriding case thickness. However, the comparison of these two parameters shows that the effect of temperature on nitriding case is more than that of nitriding duration in consistent with Fick's law of diffusion. Analysis of bath composition has shown that higher cyanate content, which is responsible for nitriding, make low temperature nitriding applications possible since nitriding in a bath consisting of high amount of cyanate results in a thick compound layer and nitriding case at low nitriding

temperatures. Further data analysis shows that initial chemical composition of specimens has affected nitriding case thickness and microhardness directly. Low carbon steels have thicker nitriding case due to easy diffusion of nitrogen. On the contrary, alloys with high chromium and aluminum reduce nitrogen diffusivity. Nitriding case thickness of these specimens has been found to be relatively thin, although they have high surface hardnesses.

Pin-on-disc wear results have shown that wear resistance of low alloy steels have increased after nitriding. Wear test results of specimens have clarified that wear on disc which tested with pins having thicker compound layer brings about more volumetric loss than those having thin compound layer on pin specimens. According to results, it is concluded that increase in the compound layer thickness results in a higher wear resistance. However, very thick compound layer has triggered abrasive wear on the disc and pin due to its brittle structure.

ÖZET

FARKLI MALZEMELERE UYGULANAN NİTRASYON PROSESİNDEKİ PARAMETRELERİN AŞINMA DİRENCİN ARTTIRMASINI ÜZERİNDEKİ ETKİLERİNİN ARAŞTIRILMASI

Sıvı nitrürleme işlemi, düşük uygulama sıcaklığından dolayı giderek yaygınlaşan bir ısıl işlem metodudur. Ferritik bölgedeki düşük proses sıcaklığı, nitrürleme işleminden sonra parçaların boyutlsal olarak kontrol edilebilmesini sağlar. Buna ek olarak, beyaz tabaka ve nitrürleme derinliğinin arttırılması istenen durumlarda, nitrürleme prosesi östenitik bölgede de uygulanmaktadır. Nitrürleme prosesi malzemelerin aşınma dirençlerini ve yüzey sertliklerini yükseltir. Bu nedenle, bu tezde, sıvı nitrürlemenin aşınma ve sertlik üzerindeki etkileri çalışılmıştır. Bu etkileri belirlemek için üç farklı özellikte malzeme seçilip sıvı nitürleme işlemine tabi tutulmuştur. Bu uygulama sırasında, dört farklı sıcaklık, dört farklı süre ve iki farklı tuz banyosu kullanılmıştır. Nitrürlenen örnekler ASTM G99-95a test tarifine göre hazırlanmış test düzeneğinde test edilmiştir. Belirtilen test tarifi, aşınma performansını hacimsel kayıp olarak ölçtüğü için, örneklerdeki malzeme kayıplarının hassas bir şekilde belirlemek önemlidir. Bu nedenle örnek malzemeler testlerden önce ve sonra olmak üzere boy ve ağırlık değişimleri belirlenmiştir. Daha sonra, örnekler, mikroyapı analizine tabi tutulmuştur. Mikroyapı analizinde, OM, XRD, SEM, ve EDS metodları kullanılarak nitrürleme sonucunda oluşan beyaz tabaka ve difüzyon tabakası özellikleri belirlenmiştir. Mikroyapı testlerinden sonra mikrosertlik ölçümleri yapılmış ve nitrürlemenin malzeme sertliğini ne kadar değiştirdiği belirlenmiştir.

Bu ölçümler ışığında yapılan değerlendirmeler sonucunda, nitrürleme sıcaklığının ve zamanının, beyaz tabaka ve nitrürleme kalınlıklarında etkili oldukları belirlenmiş olup, sıcaklıkta ve süredeki artış, beyaz tabaka ve difüzyon derinliklerini arttırdığı belirlenmiştir. Ancak sıcaklığın etkisi Fick kanununa uygun şekilde zamandan daha etkili bulunmuştur. Buna ek olarak, banyodaki tuz miktarının nitrürlemenin sonuçlarını olumlu etkilediği belirlenmiştir.

Daha fazla nitrojen içeren banyolarda, daha düşük sıcaklıkta bile yeterli difüzyon ve beyaz tabaka derinlikleri elde edilebilmiştir. Aynı zamanda, malzemenin içeriğinin de etkileri incelenmiş ve yüksek miktarda krom ve aliminyum içeren malzemelerde difüzyon derinliğinin kısıtlı kaldığı ancak sertliğin gayet yüksek olduğu belirlenmiştir.

Aşınma testleri, nitrürlemenin düşük alaşımlı çeliklerin aşınma direncini arttırdığı görülmüştür. Sonuşlara göre kalın beyaz tabakalı pinlerle aşınma testine tabii tutulan disklerdeki hacimsel kayıp, ince beyaz tabakalı pinlerle test edilen disklere göre daha falza bulunmuştur. Sonuçlara göre beyaz tabaka kalınlığı artıkça aşınma direncini arttığı belirlenmiştir. Ancak fazla kalın beyaz tabaka kırılarak abrasif aşınmaya neden olduğu tespit edilmiştir.

TABLE OF CONTENTS

LIST OF FIGURES

LIST OF TABLES

LIST OF SYMBOLS / ABBREVIATIONS

FCC	Face-Centered Cubic
BCC	Body-Centered Cubic
BCT	Body-Centered Tetragonal
HCP	Hexagonal Closed-Pack steep
γ'	Gamma prime - Fe_4N
ε	Epsilon – $Fe_{2-3}N$
Z	Fe_2N
A_1	Eutectoid line
γ	Austenitic iron
α	Ferritic iron
Fe_3C	Cementite phase
LTCHT	Low-temperature chemical heat treatment
APCS	Automated process control systems
c	Concentration
x	Distance from the surface
c_s	Surface concentration of nitrogen diffusing into the surface
c_o	Initial concentration of nitrogen in the solid
c_x	Concentration of nitrogen at distance x from the surface
D	Diffusion coefficient
t	time
D_o	Constant for a given diffusion system
Q	Activation energy for the diffusion process
R	Ideal gas constant
T	Absolute temperature
atm	Atmospheric pressure
AC	Alternating current
NaCN	Sodium cyanide

KCN	Potassium cyanide
NaCNO	Sodium cyanate
KCNO	Potassium cyanate
AMS	Aerospace Material Specifications
σ_d	Local endurance limit
σ_e	Residual stress distribution after nitriding
N	Fatigue cycles
DIN	Deutsches Institut für Normung
ASTM	American Society for Testing and Materials
SAE	Society of Automotive Engineers
rpm	Revolution per minutes
HB	Brinnel hardness
HV	Vickers hardness
$HV_{0.1}$	Vickers hardness with 100g load
HRC	Rockwell C Hardness
OP	Optical microscopy
SEM	Scanning electron microscopy
EDS	Energy dispersive spectroscopy
XRD	X-Ray diffraction method
wt	weight
vol	volume

1. INTRODUCTION

A series of performance criteria such as hardness, fatigue resistance, wear resistance, and tribological requirements are very important in today's machine technology. Among these, wear is particularly a great problem for mating components. Hence, several surface engineering methods have been employed to overcome this problem.

Surface hardening techniques are used to improve the wear resistance of parts without affecting their interior properties. The combination of hard surface and resistance to breakage upon impact is useful in many mechanical applications. A tough interior absorbs the impact that occurs during operation, while a hard surface resists wear. The surface hardening methods make the low-carbon and medium-carbon steels adequately combat wear problems at minimal cost [1]. Since these methods are generally performed at low temperatures, distortion problem is also eliminated. Moreover, imposed compressive stresses on the surface prevent cracking problem while working under severe service conditions. Surface hardening methods can be divided into two groups. The first group involves an intentional buildup or addition of a new layer on the surface. The second group includes methods causing no dimensional change but creates a thin hardened case on the surface. This group comprises the carburizing, nitriding, nitrocarburazing, boriding, siliconizing, and chromizing.

Nowadays, nitriding is more popular than other surface hardening methods due to its relatively low application temperature. The process of nitriding consists of heating steels in a nitrogenous environment usually at a temperature between 400^{o}C and 590^{o}C for a period of time depending upon the desired depth of the nitriding case. In this temperature range, steels are in the ferritic phase field. Furthermore, it is possible to apply nitriding in austenitic region above 590^{o}C to increase compound and nitriding case thickness for some special applications. On the contrary, many other surface hardening methods are only applied in austenitic state, such as carburizing, or boriding. However, the process temperature range in the ferritic state brings about excellent dimensional control at the end of the nitriding process, since no crystal

structure transformation is observed during cooling in contrast to the FCC to BCC or BCT transformation observed when cooling the austenite.

The nitriding develops a hard, wear, fatigue, and corrosion resistant surface and a steep hardness profile in the nitriding case on a tough matrix [2]. These properties make nitriding one of the most common methods to improve surface hardness and hence wear resistance of materials. Thus, in this thesis, the aim is to assess the effect of nitriding parameters on surface hardness and wear resistance of selected steels.

A surface exposed to a nitriding medium will generally form two distinct layers: The outer section is called compound layer or white layer (γ' - Fe_4N and/or ε – Fe_3N) and the inner section is diffusion layer or diffusion case. Both of these zones together comprise what is generally referred to as “the nitriding case”.

A typical nitriding case thickness varies between 100 μm and 500 μm. Deeper case depths are possible; however, they require significantly long process cycles due to the slow diffusion rate of nitrogen into steel [3]. The case depth is defined as the total case thickness determined by chemically etching a specimen, or as the depth at which a specified hardness is obtained. The case hardness depends mainly on core hardness of raw material and decreases gradually from the surface to the core [4].

Nitriding treatment also improves the fatigue properties of engineering components. The compressive stress introduced into the surface brings about an improved surface strength and can overcome notch effects easily. Thus, fatigue improvement as high as 100 per cent may be possible [5, 6].

Nitriding can be fundamentally applied in three different ways: gas nitriding, liquid (bath) nitriding, and ion nitriding. In this research, among these three nitriding types, liquid nitriding has been investigated in detail, since rapid heating and processing and ease of obtaining good nitrided layers on low carbon and low alloy steels in repeated production are

possible by liquid nitriding. The term “liquid nitriding” has become a generic term for a number of different fused-salt processes, all of which are performed at temperatures around the ferritic phase field. Operating at these temperatures, the treatments are based on chemical diffusion and influence metallurgical structures primarily through absorption and reaction of nitrogen with the matrix.

The nitriding process has been known and performed nearly from the beginning of 20th century [7]. Essentially, this is a simple process. Mainly, its application temperature is in the ferritic phase field. Furthermore, because of no phase transformation expectation, a critical cooling path on the time – temperature – transformation diagram is not required to consider like in most other heat treatments. This simple process includes heating the workpieces in a nitrogen rich environment to a suitable temperature below the eutectoid line on the iron-cementite phase diagram shown in Figure 1.1 [8]. After completion of the nitriding process, no additional heat treatment to the part is required.

1.1. Development of the Nitriding Process

The historic development of the nitriding started in the early 1900s. Dr. Adolph Fry in Europe was the discoverer of the attraction of nitrogen and iron to one another under heat [9]. He developed the iron – nitrogen equilibrium phase diagram in 1906, which is still valid with small modifications (See Figure 1.2). When solid iron and nitrogen gas are heated together, the nitrogen will diffuse into the surface of the steel. This creates a structural change in the surface of the steel which is perceived as the surface hardness. In his works, this increase was measured from 282 to 470 HB in steel containing 0,39 wt per cent carbon and 2,88 wt per cent chromium.

He also worked on the effects of adding other alloying elements such as vanadium, tungsten, manganese, molybdenum, and titanium and found that all of these elements would also produce stable, high nitrogen content nitrides [9].

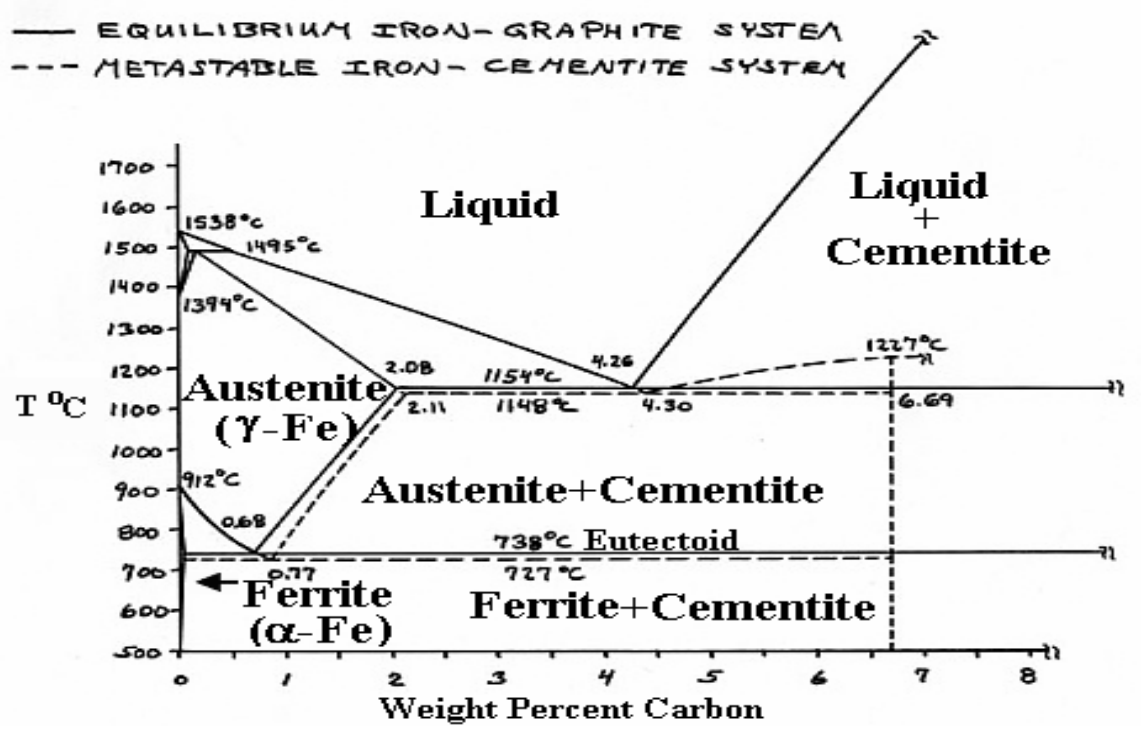

Figure 1.1. Iron – Cementite equilibrium phase diagram [8]

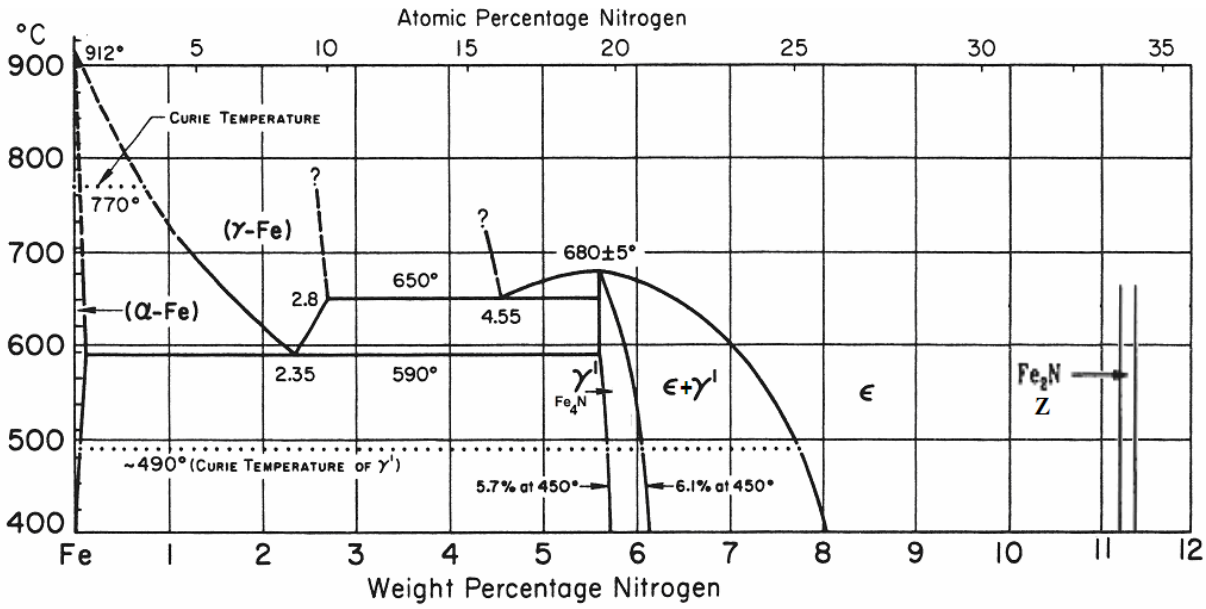

Figure 1.2. Iron – Nitrogen equilibrium phase diagram [7]

Studies on nitriding continued in the following years. Totten et al. [7] reported that in 1928, McQuaid and Ketchum worked on the practical applications and cost analysis of nitriding. Then, in 1929, Robert Sergeson published [5] the effect of varying the aluminum content of the nitralloy along with the effect of nickel. Studies on the effect of temperature on the physical properties of the nitriding steels, equipment preheat-treatment, and decarburization effects on nitrided steel were started by V.O. Homberg and J.P. Walsted [10]. The phenomenon of "compound layer" and its effects on component performance was suggested by their work.

At the same period Adolph Machlet, while working for American Gas Company in Elizabeth, New Jersey, USA, was also studying solubility of nitrogen into iron under various heating conditions [5]. Another researcher, Pierre Aubert, presented both the research and practical applications for nitriding usage in Europe in 1927 [9]. These applications contain railway steels, machine tools, and other applications in both the automotive and aviation industries. Some benefits of nitriding from his presentation are listed below:

- High surface hardness with practically no distortion
- No change in core material properties
- Higher wear resistance than those achieved with other surface treatments
- Maintained the hardness advantages after tempering
- No shelf life aging since parts were free of internal stress
- Corrosion resistance

After Homberg and Walsted, Dr. Floe had conducted some studies on the "compound layer" effects and on various methods to change the composition, reducing, or changing thickness of this thin, hard layer. His work today is known as "The Floe Process" [11].

Process control, evaluation of metallurgical results, alloy steel developments, and most other studies in science have been lighting the way for today's processing environments. The historical development in the nitriding process in the world can be summarized as given in Table 1.1, which is taken from the research of Bannykh [12] and updated in [9].

Table 1.1. The history of the nitriding process [5,12]

Name and duration of the period	**Result achieved**
1905 - 1940. First systematic works in the field of nitriding and development of industrial processes	• Creation of the scientific foundation of the nitriding process, i.e., the theory of pure (atomic) and reaction (reactive) diffusion, • Concepts of the mechanism of formation of the structure of the nitriding case and its phase composition, • Effect of the treatment temperature on the structure and properties of the layer. • Development of industrial nitriding processes, determination of the chemical composition of nitralloys. Stepped nitriding regimes, processes of anti-corrosion nitriding.
1940 - 1960 Classical gas nitriding	• Industrial use of stable nitriding processes. • Creation of effective methods combining nitriding and quenching processes (nitroquenching). • Beginning of Lakhtin's active research in the field of nitriding.
1960 - 1980 Low-temperature chemical heat treatment (LTCHT)	• A qualitative change in the saturation process: joint saturation of the surface layer of steel with nitrogen and carbon. • Appearance of various processes of LTCHT. Refining of the structural model of the nitrided layer, appearance of the concept of the nitrogen potential of the atmosphere. • Creation of the process and equipment for ion nitriding.
1980 – 2003 New directions in the advancement of LTCHT	• Automation of LTCHT processes, computer simulation of diffusion processes in gas nitriding, creation of hardware for automated process control systems (APCS). • Appearance of new concepts and methods for determining the nitrogen potential used to create new APCS in gas media. • The concept of saturation in new atmospheres (products of incomplete catalytic oxidation of ammonia). • Duplex processes based on nitriding, and nitriding in high-pressure atmospheres. • Oxynitride process, during which a controlled postoxidation treatment is carried out to further enhance the surface corrosion resistance. Ferritic nitrocarburizing (a controlled process using nitrogen and carbon to enhance surface characteristics of low-alloy steels)

2. SURFACE HARDENING METHODS

Surface hardening methods make it possible to use inexpensive, low and medium-carbon steels in applications requiring high performance without distortion or cracking problems associated with thorough hardening methods.

As listed in Table 2.1, surface hardening methods are divided into two groups:

- Hardening by an intentional buildup or addition of a new layer
- Hardening by surface and subsurface modification without any intentional buildup or dimensional change

Using of thin films, coatings, or weld overlayers are included in the first group. This group is less cost effective, especially for large production quantities and especially when the entire surface of the specimen is needed to be hardened. Additionally, fatigue resistance is the biggest constrain of this group.

The second group is divided into two subgroup; namely, hardening by diffusion and selective hardening methods. The principle behind the hardening by diffusion methods is to modify the chemical composition of a specimen's surface generally via introduction of carbon, nitrogen, boron, or other interstitial elements. This group is more cost effective when the entire surface of the specimen is needed to be hardened and production volume is large. On the contrary, selective surface hardening methods do not cause any chemical compositional change since these methods do not introduce additional elements into the whole surface of the material. By these methods, only localized hardening is possible. Selective hardening generally involves modification of the microstructure (via techniques listed in Table 2.1) on the surface and subsurface regions to increase the wear resistance and hardness of the materials [13].

Table 2.1. Surface hardening methods (adopted from ASM Metals Handbook, Vol 4) [1]

Group 1 **Intentional Buildup - Additional Layer**	
Hardfacing	Fusion hardfacing
	Thermal spray
Coatings	Electrochemical plating
	Chemical vapor deposition (electroless plating)
	Thin films (physical vapor deposition, sputtering, ion plating)
	Ion mixing
Group 2 **Hardening by Surface and Subsurface Modifications**	
Diffusion methods	Carburizing
	Nitriding
	Nitrocarburizing
	Aluminazing
	Chromizing
	Siliconizing
Selective hardening methods	Flame hardening
	Induction hardening
	Laser hardening
	Electron beam hardening
	Ion implantation
	Selective carburizing and nitriding
	Use of arc lamps

Since this thesis investigates liquid bath nitriding which is a diffusional surface hardening method, only the diffusional methods will be discussed here.

2.1. Diffusional Surface Hardening Methods

Surface hardening of materials by diffusion depends on mass transformation either within a specified solid or from liquid, gas, or another solid phase which results in chemical modification of a surface. Thermochemical processes are used to ease the diffusion of hardening elements into the surface and subsurface of a workpiece. Diffusion of hardening elements into the surface creates a case whose depth is dependent on application time, temperature, material type, and hardening method.

According to the Fick's 2nd Law of Diffusion [11] (See Equation 2.1), most of the diffusion cases occur in non-steady state where concentration of the solute atoms within a material changes with time. The solution for the Fick's diffusion equation for nitriding process is given in Equation 2.2 where c_s is the surface concentration of nitrogen diffusing into the surface, c_o is the initial concentration of nitrogen in the solid, c_x is the concentration of nitrogen at a distance x from the surface D is diffusion coefficient and t is time.

The process temperature has a major role on the diffusion coefficient. Equation 2.3 shows that diffusion coefficient increases exponentially as a function of absolute temperature. In this equation, D_o (m^2/s) is a constant for a given diffusion system, Q is the activation energy for the diffusion process (kJ/mol), R is the ideal gas constant (8,31 J/mol.K), and T is the absolute temperature (K).

$$\frac{dc}{dt} = D\frac{d^2c}{dx^2} \tag{2.1}$$

$$\frac{c_s - c_x}{c_s - c_o} = erf\left[\frac{x}{2\sqrt{Dt}}\right] \tag{2.2}$$

$$D = D_o e^{-\frac{Q}{RT}} \tag{2.3}$$

The solution of both Equations 2.2 and 2.3 for a fixed time and temperature indicates that x varies with t and D which is material dependent (Equation 2.4).

$$x \approx \sqrt{Dt} \tag{2.4}$$

There are many types of diffusion hardening processes and each of them has different factorial dependences. Thus, each type possesses certain process characteristics and gives rise to various case depths and case hardness. A summary of diffusion hardening methods are given in Table 2.2, and a brief description of them are provided in the following paragraphs.

2.1.1. Carburizing

Carburizing is a heat treatment process which is the addition of carbon atoms to the surface of iron or steels. This process is basically performed between 850°C and 950°C where steels are in the austenitic form. The reason for selecting this temperature range is the high carbon solubility of steels in this range. Due to a concentration difference, carbon atoms in the carburizing medium penetrate into the surface of the specimen. Carbon atoms dissolve into interstitial sites in iron to form a carbon rich layer. Then, the specimen is rapidly cooled by quenching to form martensite. There are four different types of carburizing [1, 14, 15]: gas carburizing, liquid carburizing, solid carburizing, and plasma (ion) carburizing.

These methods differ in the way of introducing carbon atoms into the metal surface. Advantages and disadvantages of the carburizing methods are given in Table 2.3. Because of the disadvantages, applications of this process remain limited to the treatment of high cost parts or to high production rates. Therefore, pay-off is needed to arrange the production cycle and load preparation in cost extend appropriately.

2.1.2. Nitriding

Nitriding is mostly applied to low-carbon steels which are capable of forming nitrides with nitrogen. Nitriding is frequently used in industrial applications such as gears, rocker arms, pistons, and rings in automotive industry, spindles for many machine tools that require high degree of dimensional accuracy in manufacturing industry [16, 17]. Typical applications

Table 2.2. Typical characteristics of diffusional surface hardening methods [1]

Process	Nature of case	Process Temp. (°C)	Typical case depth	Case hardness (HRC)	Typical base metals	Process characteristics
Carburizing						
Solid	Diffused carbon	815-1090	125µm-1.5mm	50-63*	Low-carbon steels, low-carbon alloy steels	Low equipment costs, difficult to control case depth accurately
Gas	Diffused carbon	815-980	75 µm-1.5mm	50-63*	Low-carbon steels, low-carbon alloy steels	Good control of case depth, suitable for continuous operation, good gas controls required, can be dangerous
Liquid	Diffused carbon and possibly nitrogen	815-980	50 µm-1.5mm	50-65*	Low-carbon steels, low-carbon alloy steels	Faster than pack and gas processes, can pose salt disposal problem, salt baths require frequent maintenance
Ion	Diffused carbon	815-1090	75 µm-1.5mm	50-63*	Low-carbon steels, low-carbon alloy steels	Excellent process control, bright parts, faster than gas carburizing, high equipment costs
Nitriding						
Gas	Diffused nitrogen, nitrogen compounds	480-590	12µm-0.75mm	50-70	Alloy steels, nitriding steels, stainless steels	Hardest cases from nitriding steels, quenching not required, low distortion, process is slow, is usually a batch process
Salt	Diffused nitrogen, nitrogen compounds	510-565	2.5µm-0.75mm	50-70	Most ferrous metals. Including cast irons	Usually used for thin hard cases <25 µm, no compound layer, most are proprietary processes
Ion	Diffused nitrogen. nitrogen compounds	340-565	75µm-0.75mm	50-70	Alloy steels, nitriding steels, stainless steels	Faster than gas nitriding no compound layer, high equipment costs, close case control
Nitrocarburazing						
Gas	Diffused carbon and nitrogen	760-870	75µm-0.75mm	50-65*	Low-carbon steels, low-carbon alloy steels, stainless steels	Lower temperature than carburizing (less distortion), slightly harder case than carburizing gas control critical

Table 2.2. Typical characteristics of diffusion treatments [1] (continued)

Process	Nature of case	Process Temp. (°C)	Typical case depth	Case hardness (HRC)	Typical base metals	Process characteristics
Liquid (cyaniding)	Diffused carbon and nitrogen	760-870	2.5-125μm	50-65*	Low-carbon steels	Good for thin cases on noncritical parts, batch process, salt disposal problems
Ferritic	Diffused carbon and nitrogen	565-675	2.5-25μm	40-60*	Low-carbon steels	Low-distortion process for thin case on low-carbon steel, most processes are proprietary
Other						
Aluminizing (pack)	Diffused aluminum	870-980	25μm-1mm	< 20	Low-carbon steels	Diffused coating used for oxidation resistance at elevated temperatures
Siliconizing by chemical vapor deposition	Diffused silicon	925-1040	25μm-1mm	30-50	Low-carbon steels	For corrosion and wear resistance, atmosphere control is critical
Chromizing by chemical vapor deposition	Diffused chromium	980-1090	25-50μm	Low-carbon < 30; High-carbon 50-60	High- and low carbon steels	Chromized low-carbon steels yield a low-cost stainless steel, high-carbon steels develop a hard corrosion resistant case
Titanium Carbide	Diffused carbon and titanium, TiC compound	900-1010	2,5-12.5μm	> 70*	Alloy steels, tool steels	Produces a thin carbide (TiC) case for resistance to wear, high temperature may cause distortion
Boriding	Diffused boron. boron compounds	800-1150	12,5-50μm	40- > 70	Alloy steels, tool steels, Cobalt and nickel alloys	Produces a hard compound layer, mostly applied over hardened tool steels, high process temperature can cause distortion

*Requires quench from austenitizing temperature.

of nitriding are Nitrides in a metal have increased their popularity as a result of high hardness and wear, oxidation, and corrosion resistance [18]. Aluminum, chromium, vanadium, and molybdenum are nitride creators. Nitrides of these elements in steel prevent sliding of slip

planes, so increase the surface strength and hardness. Process temperature is usually kept in the ferritic range between 495^{o}C and 590^{o}C to obtain a desired diffusion depth in a 0.25 - 100 hour period. However, nowadays, nitriding in austenitic phase field is popular.

Table 2.3. Advantages and disadvantages of the carburizing [18]

Advantages	**Disadvantages**
- Bright surface after treatment - Possibility of high temperature carburizing - Low gas and energy consumption - Important reduction in cycle time - Pollution free process and equipment, environmentally safe - Easily integrated in production lines - No superficial intergranular oxidation responsible for reduction in fatigue resistance	- Process sometimes complex and expensive - Production starting up sometimes long and delicate - The load have to be carefully prepared - Low density of loading - Low penetration in small diameter holes

As given in Table 2.2, nitriding is carried out in three different industrial ways: gas nitriding, nitriding in salt bath, and ion (plasma) nitriding.

Each type has its own advantages and disadvantages. Nitriding types and properties of nitrided surfaces are explained in detail in Sections 2.4 and 2.5.

2.1.3. Nitrocarburazing

Nitrocarburizing is a variation of the nitriding process. Where nitrogen, carbon, and to a very small extent, oxygen atoms are diffused into the surface of steel parts as a result of a thermochemical diffusion process. As nitriding, nitricarburizing is applied in gas, liquid, and plasma forms. On the surface of the specimen, a compound layer and a nitriding case is created at the end of the nitrocarburizing process as in the nitriding process. This process is frequently applicable to low-alloy and low-carbon steels in order to increase surface hardness

and corrosion resistance of the material. Generally, it is applied in the ferritic phase field of the iron – carbon equilibrium phase diagram between 525^{o}C and 650^{o}C [5].

2.1.4. Carbonitriding

Carbonitriding is a surface hardening process which uses the mixture of hydrocarbons and ammonia in the carburizing atmosphere [14]. Ammonia decomposes to release nitrogen to diffuse into austenitic steel. By this process, high surface hardness is reached by quenching that forms martensite. Due to the nature of the nitrogen enhancement, it is possible to use low carbon steels to achieve equal surface hardness comparable to high-alloy, carburized steels without drastic quenching requirements. Thus, distortion and crack accumulation are lessened [1].

2.1.5. Boriding

This process is commonly known as boronizing, in which boron will vaporize and diffuse into the steel and other alloys to create an extremely hard compound layer on the surface of the steel. This extremely hard surface results in improved wear resistance. This process is performed between 800^{o}C and 1150^{o}C. High process temperature can cause distortion problem. After the completion of boriding process, parts can be used directly without additional treatment. The boriding products are dependent on the process temperature, process duration, and environment [19, 20].

2.1.6. Siliconizing

This process is applied at high temperatures, generally to low alloy steels by diffusing of silicon into solid metal in order to improve corrosion or wear resistance [21].

2.1.7. Chromizing

This process similar to siliconizing is used to produce a chromium rich coating. Chromizing is very complex in low alloy steel applications. Layers occurred after chromizing contain a thin outer layer nearly 5 μm, where chromium content is greater than 80 wt per cent. It is mainly used for corrosion protection. Underneath the outer layer, there are large columnar ferritic grains containing 15 – 30 wt per cent chromium [22].

2.2. Nitriding Process

Wear is an unrecoverable loss of material due to friction. A large amount of money is wasted because of this failure mode [23]. The wear performance of materials has been improved owing to the improvements in surface coating technologies and surface engineering. Surface modification technologies make it possible to improve the performance of a material only at a required zone.

Among several surface modification technologies, nitriding is one of the most effective methods used to increase the corrosion, fatigue, and especially the wear resistance of steels without dimensional distortion due to its application temperature which is in the ferritic phase field of steels.

Nitriding began as a gas process, developed for and used only in Nitralloy-type alloys [24]. It produced a brittle compound layer requiring costly removal. In the 1950's, salt-bath nitriding for the first time demonstrated that the process could be successfully applied to low alloy and even plain carbon steel in a relatively short duration (3 - 12 h) than the previous nitriding applications [11]. At that time, the safety and health hazard of this process due to cyanide content were not classified completely. These concerns led many users away from this technology. Recently, the salt bath process has undergone significant improvements both in technology and safety.

Now, cyanide free salt baths are used to overcome environmental problems. By these methods, it is possible to obtain components having excellent wear, corrosion, and fatigue resistance in many applications. However, on account of the relatively high melting point of the salt bath, this type of nitriding is limited to only those steels, which can be heated above approximately 570°C without loss of core hardness. It should also be considered that the salt bath is a finite source of active nitrogen. Therefore, to keep the bath composition at the required level, salt baths require regeneration procedures at strictly defined time intervals during which the salt bath is inoperable [24].

The next development in the nitriding process was short duration gas nitriding, which gave the same advantages as the salt bath process but this process was free of ecological problems [24]. However, limited process control was the main problem of this process, and hence, this process is not capable of yielding fully repeatable and predictable results.

Ion (plasma) nitriding was introduced in Europe on an industrial scale in the 1970s. This method was regarded as a major step forward in the nitriding technology, although it could only be used by a highly skilled and experienced operator who knew how to deal with several difficulties, such as the sensitivity of the process to part geometry and load arrangement in the furnace. In the meantime, gas nitriding remained undeveloped due to inadequate process control and to the existence of a brittle compound layer.

A great effort has always been spent to save on material and processing costs in industry. This means that the part must be engineered to very tight tolerances and, at the same time, costly final machining must be limited or even totally eliminated. This is the major advantage that nitriding offers. Table 2.4 presents some of the processing features of the nitriding.

2.2.1. Thermodynamics of Nitriding

A variety of industrial applications makes the iron-nitrogen system very important. The system involves highly metastable regions as seen in the iron-nitrogen phase diagram in

Figure 1.2. Nitrogen is dissolved in iron interstitially at equilibrium conditions only in a small region on the left side of the diagram (α-Fe and γ-Fe).

Table 2.4. Technological features of nitriding process [24]

Features	Remarks
Material compatibility	Wide variety of steel grades, including austenitic stainless, maraging, and precipitation hardening
Typical treatment temperature range	460 - 600°C
Accompanying heat treatment	No additional treatment required
Finish machining	In most cases, does not require finish grinding
Distortion	Minimum to nil due to low treatment temperature and absence of transformation in bulk material
Surface cleanliness	After nitriding, part ready to be assembled
Surface hardness	Depending on steel grade, may exceed 70 HRC
Corrosion resistance	Compound layer enhances corrosion resistance, (with the exception of stainless steels)

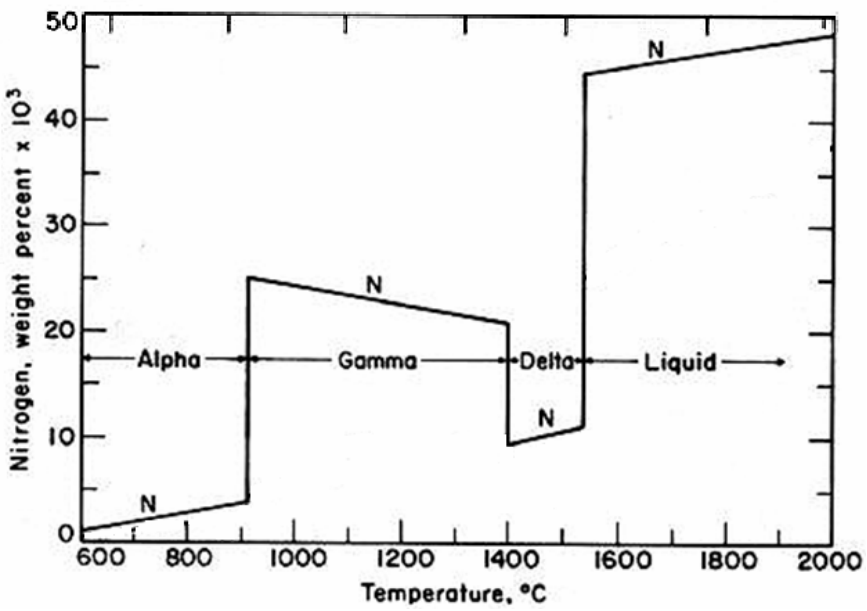

Figure 2.1. Solubility of nitrogen in pure iron [25]

The reason for relatively lower process temperature of the nitriding than that of other diffusional hardening processes can be understood by the investigation of Figure 2.1 which gives that the solubility of nitrogen in austenite at 910°C is 0,026 wt per cent, and in Figure 1.2, it is indicated that the solubility of nitrogen is not defined for a solubility larger than 0,026 wt per cent at this temperature at 1 atm, and the boundaries are given by dashed lines. Therefore, it is pointed out that any equilibrium that exists at atmospheric pressure must be metastable [26].

In addition to the nitrogen content, the carbon content of the steel has also several effects on the nitriding. Around nitriding temperatures, steels continue to being tempered. Additionally, most of the alloying elements in steels are strong carbide formers as well as nitride formers. This results in segregation of nitride former to the carbides during tempering. This makes process difficult since carbon diffuses toward the core of the steel and a carbon-rich layer builds up before the nitride reaction front where carbon as an alloying element forms cementite [26].

2.2.2. Diffusion Kinetics of Nitriding

The nitriding process is generally performed between 500°C and 590°C which is below the eutectoid temperature for steels. Furthermore, there are special applications performed till 630^{o}C. Operating at these temperatures, the treatments are based on chemical diffusion which influences metallurgical structures. This diffusion process consists of the movement of nitrogen atoms into the ferrite lattice leading to a reaction of nitrogen with iron and other alloying elements. Due to smaller diameters of carbon and nitrogen atoms than that of iron atoms, these atoms go between iron atoms to form an interstitial solid solution. They can diffuse without any need for vacancies in the steel. Their diffusion rate is much higher than that of substitutional atoms [26].

As can be seen from Figure 1.2., the solubility of nitrogen in ferrite is low to form iron nitrides. Nitrogen dissolves in iron up to 0.1 wt per cent at 590^{o}C, after that γ' (Fe_4N) – a face-

centered cubic phase starts to form. If the nitrogen concentration exceeds about 6 wt per cent at 590^{o}C, a new compound phase, ε ($Fe_{2-3}N$) – hexagonal phase forms. After 11.0 wt per cent nitrogen concentration yet another compound phase, Z (Fe_2N) appears at the same temperature. As the nitrogen content increases, there is a tendency for spalling which is a surface failure where a large solid body flakes off due to the brittle nature of the ε and Z phases [27].

When the rate of diffusion of nitrogen into steel is sufficiently decelerated, a layer of nitrides builds up on the surface of the steel. This is a clearly visible layer known as "the compound layer" or "the white layer" as shown in Figure 2.2. The thickness of the compound layer is usually around 0 – 0.03 mm. Nonetheless, nitrogen can diffuse deep into the core of the material, creating a zone below the compound layer that is called as "the diffusion zone" or "the diffusion layer". Both of these layers make up "the nitriding case". Consequently, a layered microstructure is observed after any nitriding process. However, the characteristics of the layers depend on process parameters. Thus, the surface properties of a nitrided material can be differentiated by changing nitriding medium, nitriding duration, nitriding temperature, and the material being nitrided.

2.3. Nitrided Surface Layers

The compound layer builds up to thicknesses between nil to 30 μm. This layer is a thin layer of extremely hard iron nitride containing ε - Fe_3N and/or γ' - Fe_4N compound phases. The gamma prime (γ' - Fe_4N) with FCC structure is more ductile than the epsilon phase (ε - Fe_3N) with HCP structure. Although this layer is acceptable if it is kept thin, some specifications suggest this layer be removed. Because of being extremely hard and brittle, this layer can crack during operation, and then the broken particles increase wearing of the system [28].

The thickness of this layer is controlled by the process temperature, duration, and environment. To obtain the compound layer on the surface, nitriding temperature should be at

least minimum 500°C and nitriding potential of the atmosphere should be adequate [7]. A thick compound layer provides a higher degree of corrosion resistance since it covers the surface of the specimen and so protects it from oxidation. A thick compound layer is also prone to more porosity and it is an excellent choice when holding the lubricant at the wear interface is desired to absorb the lubricant inside the pores and subsequently to form a lubrication layer. However, a porous zone will raise the initial wear in case of the adhesive and abrasive wear due to its brittle microstructure.

Investigations have shown that the adhesive wear resistance of the compound layer is strongly affected by the volume of nitrides [20]. In most cases, the resistance increases with increasing nitride content. Similar behavior exists when nitrided parts are abrasively worn.

Underneath the compound layer, there is a diffusion layer. This layer is thicker than the compound layer and will increase in thickness as the process time is increased. Depending on the initial structure and composition of the core material, the nitrogen in the diffusion layer is dissolved in the iron lattice and/or precipitated as very fine nitrides. Thickness of this layer generally ranges from 100 μm to 500 μm.

2.4. Types of Nitriding

As explained briefly in Table 2.2, there are mainly three different types of nitriding, which are namely liquid nitriding, gas nitriding, and ion nitriding. All of these nitriding operations are explained in the following sub-sections.

2.4.1. Liquid Nitriding

The term liquid nitriding has become a generic term for a number of different fused-salt processes. In the literature [1, 28], it is stated that liquid nitriding basically consists of cyanide (Sodium cyanide – NaCN, or Potassium cyanide – KCN) and cyanate (Sodium cyanate – NaCNO, or Potassium cyanate – KCNO) salts. Therefore, besides nitrogen, carbon also

diffuses into the steel during this operation. Thus, this process is frequently called as liquid nitrocarburizing [28 - 30].

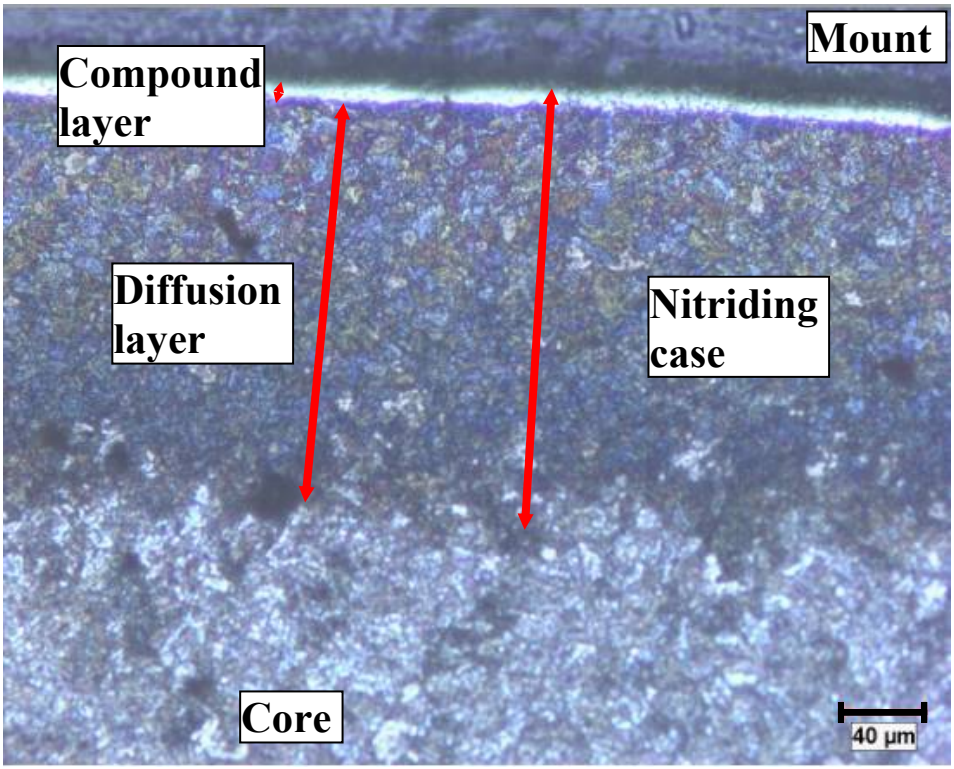

Figure 2.2. Microstructure of liquid nitrided steel

In liquid nitriding, while the cyanide content of the bath decreases, the cyanate and carbonate contents increase as a result of aging which is the oxidation of the cyanide to cyanate. The cyanate content in all nitriding baths is responsible for the nitriding action, and hence the cyanate ratio is critical and varies for the types of liquid bath nitriding [1]. Although a vast number of different types of liquid nitriding can be found in the literature [1], aerated low-cyanide liquid nitriding is investigated in detail in this research since nitriding of specimens have been performed by using this method.

2.4.1.1. Aerated Low-Cyanide Liquid Nitriding. Low-cyanide aerated bath processes have been developed in time due to the environmental problems. Aerated low-cyanide nitriding is a

cyanate salt bath process which does not contain any lithium or sulphur and may consist of a small amount of (1-3 wt per cent) cyanide. Decrease of cyanide content brings about high cyanate content in bath so nitriding activity is higher in these types of nitriding baths. The main nitriding medium is of potassium salts with some sodium in low-cyanide salt baths. As a result of catalytic reactions given in Equation 2.4 and Equation 2.5, nitrogen and a small amount of carbon is supplied to the steel surface. The supplied elements penetrate into the steel and form nitrides and carbides as shown in Figure 2.3. The penetrated carbon and nitrogen atoms build up to such concentrations to form γ'- (Fe_4N), ε - ($Fe_{2-3}N$), and Fe_3C-cementite phases at the processing temperature.

$$8NaCNO \rightarrow 2Na_2CO_3 + 4NaCN + CO_2 + (C)_{Fe} + 4(N)_{Fe} \quad (2.4)$$

$$8KCNO \rightarrow 2K_2CO_3 + 4KCN + CO_2 + (C)_{Fe} + 4(N)_{Fe} \quad (2.5)$$

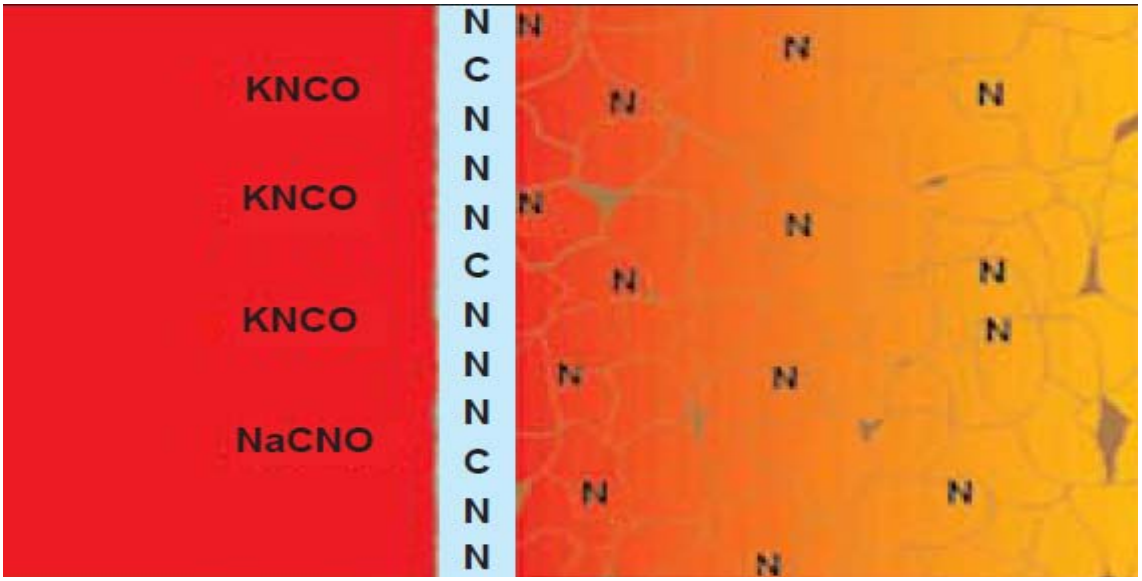

Figure 2.3. Reactions at the surface of a workpiece [31]

2.4.1.2. Other Liquid Nitriding Methods. There are also other liquid nitriding methods applied in industry. They are basically liquid pressure nitriding, aerated bath nitriding, and aerated cyanide-cyanate nitriding. The reason for these different liquid nitriding applications are to

accelerate the chemical activity of the process, increase the types of material to which nitriding can be applied, and improve the surface and material properties after nitriding.

Further information about liquid bath nitriding is given in the following and specifications U.S Patent 3022204, U.S. Patent 3208885, U.S. Patent 4019928, U.S. Patent 4006643, and AMS 2753 and AMS 2755B [1].

2.4.2. Gas Nitriding

Gas nitriding is a case-hardening process by which nitrogen is introduced into the surface of an alloy by holding the metal at a suitable temperature in contact with a nitrogenous gas environment. Quenching is not required for the production of a hard case. The nitriding temperature for all steels is between 500°C and 570°C. Limitations and advantages of this process are shown below in Section 2.5. Especially, NH_3 exhaust gas is the biggest problem in this type of nitriding causing health hazards [32, 33].

2.4.3. Ion (Plasma) Nitriding

Plasma (Ion) nitriding is an extension of gas nitriding processes using plasma-discharge physics. In vacuum, high-voltage electrical energy is used to form plasma, by means of plasma, nitrogen ions are accelerated to impact on the workpiece. This ion bombardment heats the workpiece, cleans the surface, and provides active nitrogen. This process is applied in a variety of gas atmospheres of N_2, H_2, Ar, and NH_3 gases, and the application temperature is between 350°C and 600°C.

2.5. Advantages and Disadvantages of Nitriding Processes

All of nitriding processes have various advantages and technical drawbacks. The advantages and disadvantages of nitriding types are listed in Table 2.5 below.

Table 2.5. Advantages and disadvantages of nitriding types. Adopted from [24]

Advantages and disadvantages of currently used nitriding methods		
Process	Advantages	Disadvantages
Salt bath nitriding	• Rapid heating and processing • Ease of obtaining good nitrided layers on low carbon and low alloy steels in repeatable production	• No in-process control • Processes limited to those steels which can be heated to higher temperatures, without losing core hardness. • Short processes only • Requires thorough washing to remove salt residues which may cause corrosion • Health hazard and waste disposal problems
Ion (plasma) nitriding	• Simple, mechanical masking of surfaces to be free of nitriding • Ease of surface activation through cathodic sputtering • Low temperature processes possible • Short saturation cycles	• Problems with temperature measurement and uniformity • Risk of overheating if not closely monitored • Results sensitive to part geometry and arrangement in furnace retort • Requires highly skilled and experienced operator
Gas nitriding	• Simple control techniques	• Controlling parameter: (ammonia dissociation rate) inadequate for control of layer properties • In many cases process produces a brittle compound layer which requires removal • Masking requires copper plating or painting with protective paste • Stainless steels require special activation techniques • Health hazard due to NH_3

2.6. Properties of a Nitrided Surface

2.6.1. Surface Roughness

Nitriding always increases surface roughness of a specimen. During the heating period of nitriding, the nonuniform nucleation and growth of nitride grains in the compound layer is

one important factor of this increase. Besides temperature, initial surface roughness of the part has a significant role in final surface roughness as shown in Figure 2.4. Surface roughness after nitriding increases by the increase of initial surface roughness. In the same figure, it is indicated that the carbon content of the alloy is another major factor affecting final surface roughness. The higher carbon content brings about a higher surface roughness after nitriding. Indeed to reduce friction wear and to increase corrosion resistance of the specimen, there should be some roughness and porosity on the surface to absorb the lubricant or corrosion inhibitor [7].

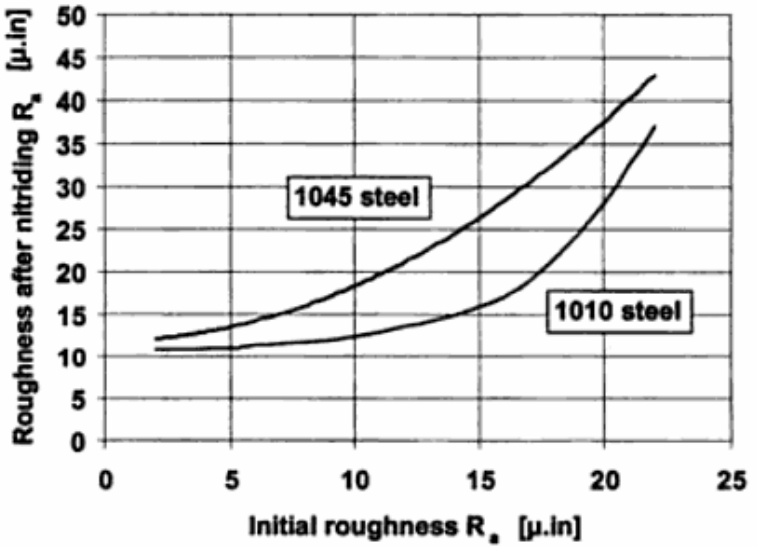

Figure 2.4. Effect of initial surface roughness on final roughness [34]

Porosity, which affects the surface roughness of specimen after nitriding, is formed in the outer zone of the compound layer by trapped atoms of nitrogen which recombines to N_2. Porosity is a common feature in all nitriding processes. The pore formation is explained by Yurtışık [26]. Nitrogen atoms diffusing through the compound layer can bind together to form molecular nitrogen, predominantly in the compound layer and to a lesser extent, in the diffusion layer at energetically favorable sites, for example grain boundaries, and this leads to the formation of the porosity in the case [7, 25]**.** The porosity formation is influenced by the temperature of the process.

2.6.2. Wear Resistance

The wear resistance of a material is one of its most significant mechanical properties when material forms part of a machine that is subject to a mode of sliding contact. The parameters governing the wear resistance are multiple, including both external parameters (depending on relative speed, contact pressure, lubricant, etc.) and internal parameters depending on properties of the material itself (such as hardness, density, and rigidity). Nitriding mainly increases wear resistance of a material by raising the hardness of the material.

The wear resistance of a nitrided layer changes with distance from the surface (See Figure 2.5). The wear resistance is reduced in the porous zone of the compound layer because of the lower fatigue strength, reduced density, and the notch effect of the pores. The wear resistance of the poreless portion of the compound layer is significantly higher than that of the diffusion layer and the core material. If the compound layer is free of pores, wear resistance is same throughout the surface of the material. In the diffusion layer, wear resistance decreases to the value of the core material with increasing distance from the surface; this is because of the reduction of the density of the nitride precipitates due to decrease of diffused nitrogen into the matrix.

The wear behavior of a nitriding case is often assumed to be a complex reaction of the nitriding layer to wear loading. Therefore, wear resistance and mechanisms must be discussed in conjunction with the structure of the nitriding layer. The compound layer resists the adhesive and abrasive wear. On the contrary, the wear resistance of the diffusion layer is relatively lower than that of the compound layer.

2.6.3. Corrosion Resistance

As nitriding can be used for wear resistance, it also brings about some improvement in corrosion resistance in the case of most steels [20]. However, when the latter is a major requirement, nitriding alone is insufficient. Meeting wear, fatigue, and corrosion resistance

requirements by way of nitriding is a complex problem because of many and varied factors influencing the overall result. Of paramount importance is the thickness and morphology of the nitrided layer, dependent on process conditions, i.e. temperature, time, and nitriding potential. This last factor is considered to be the basic parameter of the nitriding process, determining the nitrogen concentration and resulting phase composition in the surface layer [35]. Additionally, it is reported that Fe_4N (γ') formed in the surface layer after ion nitriding is relatively stable in corrosive medium. The hardened surface layer is also uniform and continuous throughout the surface. These factors contribute to the improvement in the corrosion resistance of the material [36].

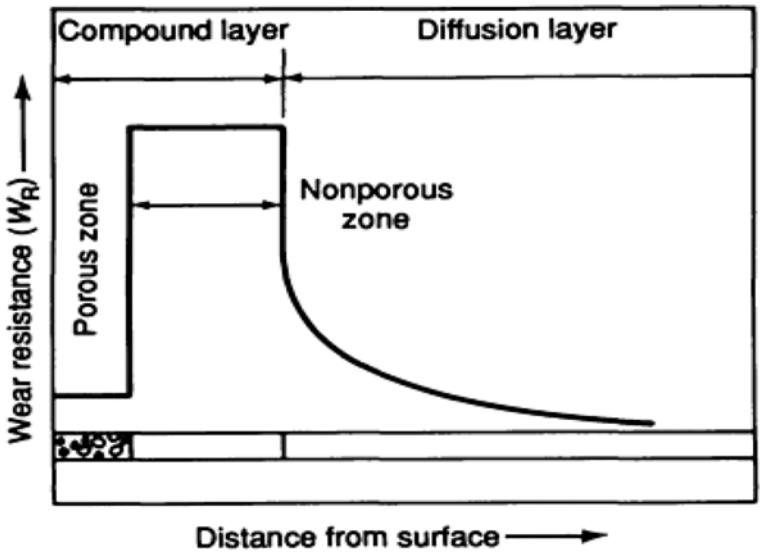

Figure 2.5. Wear resistance change of nitrided specimen from the surface to the core [34].

Nevertheless, the corrosion resistance of stainless steels is adversely affected by nitriding. This is to be expected since corrosion resistance is due to presence of chromium in solid solution in the steel. Nitriding precipitates chromium as chromium nitride and this leads to depletion of Cr and so the decrease of corrosion resistance. Although there is a decrease in corrosion resistance, the corrosion resistance of stainless steels is still higher than that of other nitrided steels.

2.6.4. Fatigue Resistance

Surface treatment of parts causes a residual stress. A compressive residual stress occurs in the case and this stress turns into a tensile residual stress through the core of the material. The increase of the fatigue strength comes from the combined effects of higher case hardness and compressive residual stress in the case. As shown in Figure 2.6, compressive residual stress brings about an increase in local endurance limits (σ_d) which is a function of hardness gradient of the nitrided specimen and residual stress distribution (σ_e) after nitriding. Accordingly, local endurance limit decrease towards the core of the material since hardness decrease in this direction. The fatigue strength differences between nitrided and nontreated specimens are shown on Figure 2.7 [7].

2.7. Friction and Wear Failures

Wear occurs while using various machinery and equipment and may cause great economic losses. Therefore, this issue is very important in machine design [37]. Because of contact surfaces, friction results in force and power losses, and machining tolerance problems. That's why wear is needed to be taken into consideration during design [38].

2.7.1. Friction

Friction can be defined as the resistance of objects moving relative to each other. In general, friction is defined as the movement of material under absolute vacuum on a cleared environment from all kinds of foreign material. Nevertheless, most of the current systems work in normal atmospheric conditions. However, clean working surface in atmospheric conditions includes oxide layer. Therefore, friction of the surfaces cleaned from foreign substances under the atmospheric conditions is accepted as dry friction [37, 38].

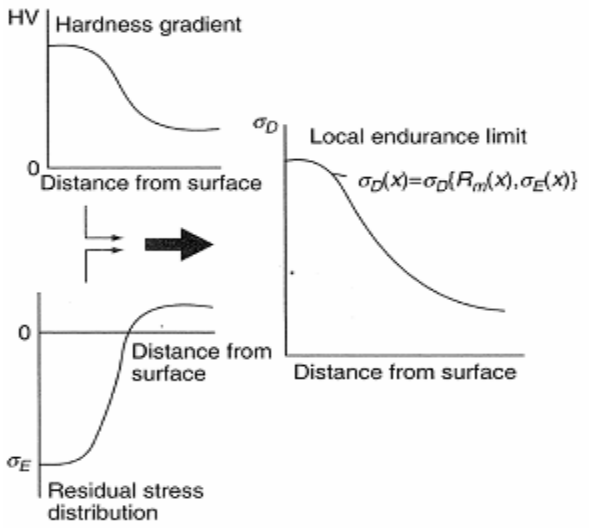

Figure 2.6. Local endurance limit of surface hardened specimens ($R_m(x)$ is hardness distribution and σ_e is the residual stress distribution) [7]

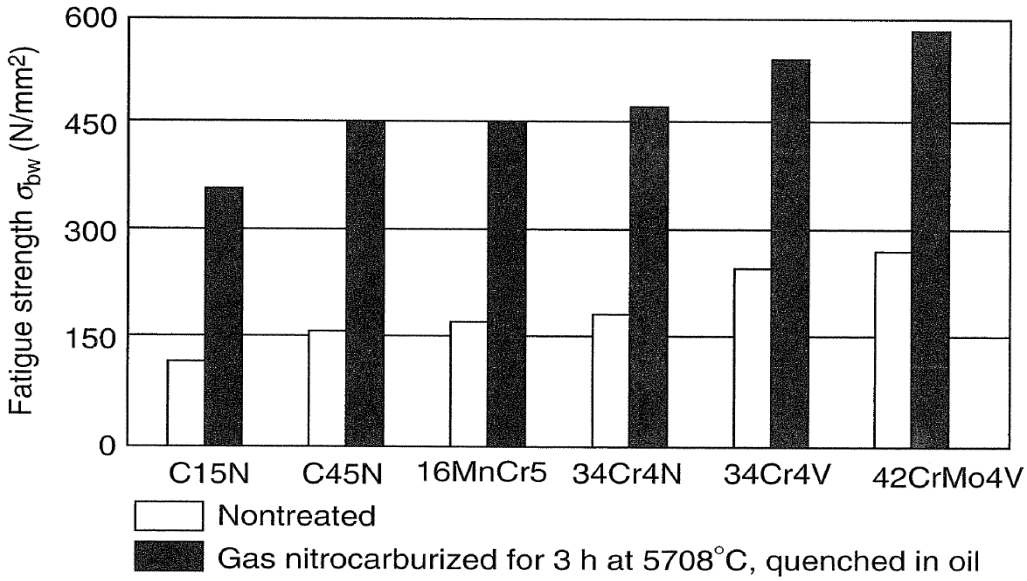

Figure 2.7. Bending fatigue strength of nitrocarburized steels [7]

2.7.2. Wear

German DIN 50320 norm defines wear as small and undesired material loss from the surface, resulted from the contact of a material with another material which is in gas, liquid, or solid phase due to mechanical effects [38]. Similarly, according to ASTM G 40 standard, wear is defined as the damage to a solid surface, generally involving progressive loss of material, due to relative motion between the surface and a contacting substance(s).

Material loss from the specimens in contact occurs in three different ways: local melting, chemical reactions, and material breakage from the surface.

Mainly, wear is started due to the direct contact of two sliding surfaces. The main factors increasing wear are listed below.

- Materials in contact: crystal structures, hardness, modulus of elasticity, surface roughness
- Environmental effects: temperature, humidity, lubricant
- Load
- Movement: sliding speed and sliding path
- Design
- Contact area and degree of movement

2.7.3. The Wear Mechanisms

2.7.3.1. Adhesive Wear. Adhesive wear is the most frequently seen wear type; however, this type wear does not accelerate failures. Generally, adhesive wear is seen as a result of the rupture of particles from one surface and transportation and sticking to another surface when mutually interacting parts are in relative movement.

Two surfaces contacting under pressure are bonding together due to heat from friction and cold welding. The bonding from friction may be stronger than the intergranular bond strength [37]. In these cases, particles break from the lowest strength bonds. If the breakage

occurs on material except for welding area, material transportation occurs from one surface to another. Repeating of this process for several times, adhesive wear causes significant performance failures.

2.7.3.2. Abrasive Wear. The removal of materials with hard particles is called as abrasive wear. These hard particles may be present at two different conditions: the first one is the surface of a second material (two-body wear) and the second one is as loose particles between two surfaces (three-body wear) [39]. Dust particles from the environment and combustion product in the engine are good examples for abrasive wear particles.

The two factors affecting abrasive wear are the hardness differences between materials and abrasive particles and pressure causing this contact.

2.7.3.3. Fatigue Wear. Fatigue wear are seen as a result of repeated stressing by the two moving surfaces. Tribological strains mostly results from mechanical stresses on the surfaces. The accumulation of fatigue wear is simulated in Figure 2.8. A particle is caught by the mating parts. This particle creates a dent on the surface and then a crack is initiated by dent on the surface. Although, there won't be any additional damage on the surface, a crack is initiated and spreads due to the repeated stressing. Finally, the surface failure occurs and some area from the surface breaks off.

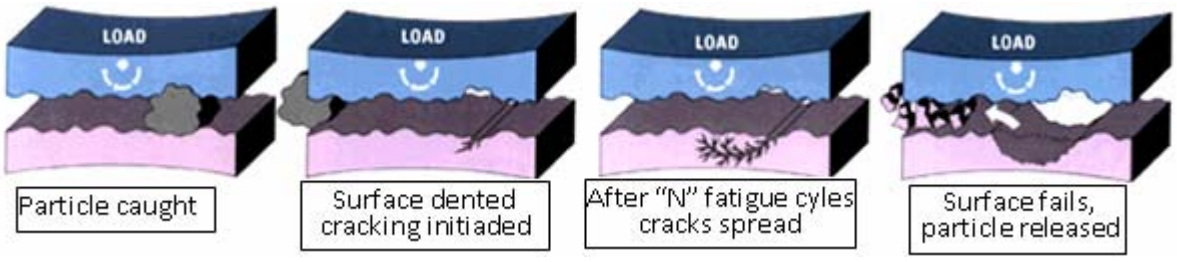

Figure 2.8. Simulation of fatigue wear on bearing surfaces [40]

2.7.3.4. Corrosion Wear. The degradation of material by means of both corrosion and wear mechanism is called as corrosion wear. Total material losses can be resulted from this combined effect of wear and corrosion together, and the effects of this combination are more severe than when the effects are present alone [41].

2.7.4. Friction and Wear Setups

The friction or wear properties of materials are measured by tribometers. Testing can be carried out in various environments to simulate real life scenarios. In tribometer, different shape workpieces, such as a sphere, a pin or flat workpiece is loaded onto the test specimen with a precisely known force. The pin is mounted on a stiff lever which is designed as a frictionless force transducer. Friction force is measured by this transducer and friction coefficient of the workpiece is calculated. Volume of the lost material during test is used to calculate wear of the pin and disc materials. This simple method facilitates the study of friction and wear behavior of almost every solid state material combination with or without lubricant.

Furthermore, the control of speed, frequency, contact pressure, time, and environmental parameters (temperature, humidity, and lubricant) during the test allows simulation of the real life conditions of wear situation. Additionally, they can conduct both linear reciprocating and rotating modes [34, 42, 43].

2.7.4.1. Pin-On-Disc Tribometer. A tribometer in which one or more relatively moving pin specimen is loaded against a flat disc specimen surface such that the direction of loading is parallel to the axis of rotation of either the disc or the pin-holding shaft, and a circular wear path is described by the pin motion.

Either the disc rotates or the pin specimen holder rotates so as to produce a circular path on the disc surface. An arrangement wherein the pin specimen is loaded against the curved circumferential surface of a flat disc is not generally considered to be a pin-on-disc machine [43].

Pin-on-disc type tribometer is capable of 5,000 rpm and is readily modified to permit pin-on-disc, roller-on-disc or pad-on-disc testing. The use of interchangeable test specimen holders gives wide ranging test capability. The ability to accept large diameter test discs, up to 200 mm in diameter, permits multi-track testing on a single specimen. An insulated test specimen holder and a localized pin heater permit testing with pins at temperatures to approximately 370°C.

2.7.4.2. High-Speed Roller Tribometer. High-speed roller tribometer has a capacity to reach 30,000 rpm. The main spindle is powered by synchronous variable speed AC drive motor. Two configurations are offered, one with a magnetic bearing near the test end to permit loading and unloading of the test roller at desired main spindle test speeds. An alternative configuration using a high-speed, ball bearing supported spindle and pneumatically actuated plate to raise/lower the test roller pair is also offered. The free or test end of the high speed spindle is generally designed to permit installation and removal of 100 mm diameter test journals in the evaluation of the various tribomaterial pairs [34].

2.7.4.3 Start/Stop Wear Tester. Start/stop wear tester is a 20,000 rpm room temperature wear tester used to evaluate coatings subjected to unidirectional sliding under a variety of loads during acceleration, dwell and deceleration. Measured parameters include the starting/coast down torque, steady state torque and speed. The nominal test journal diameter is 35 mm. Various static loads may be applied to the test specimen.

2.7.4.4. High-Speed Bearing Type Tribometer. This high-speed bearing type tribometer is capable of 70,000 rpm and temperatures to 750^{o}C, when used with the oven. The spindle is mounted on oil mist lubricated rolling element bearings and is driven by an air turbine. The spindle housing incorporates a water cooling jacket, buffered seals to keep spindle oil out of the test chamber and a heat shield to maintain bearing spindle temperature at acceptable levels. The test journal is 35 mm in diameter. The high temperature oven is made in two separate halves to permit easy opening when changing test specimens. Load is applied to the test specimen through the test bearing holder.

2.8. Nitriding Steel Selection

The steel selection is very important during design. The following criteria must be carefully considered [7]:

- Complexity of the part geometry and final product
- Operation conditions: compressive loads, tensile loads, impact loads, and cyclic loads
- Abrasive conditions
- Corrosion
- Thermal cycling
- Adequate lubrication
- Further machining after nitriding

After above conditions are satisfied, nitriding can be applied to various classes of steels.

Historically, at the beginning of nitriding process application, it is generally thought that nitriding can only be applied to steels containing aluminum, chromium, molybdenum, vanadium, and silicon elements since these elements are the most influential elements on the hardness of materials as shown in Figure 2.9. In fact, steels containing these alloying elements can really be nitrided easily. However, all steels with iron form nitrides. Thus, all steels can be nitreded, but they are comparably softer than the special nitriding steels, some of which are shown in Table 2.6.

The most generally used steels for nitriding are given below [1]:

- Aluminum-containing low-alloy steels
- Medium-carbon, chromium-containing low-alloy steels of the 4100, 4300, 5100, 6100, 8600, 8700, and 9800 series
- Hot-work die steels containing 5 wt per cent chromium such as H11, H12, and H13
- Low-carbon, chromium-containing low-alloy steels of the 3300, 8600, and 9300 series

- Air-hardening tool steels such as A-2, A-6, D-2, D-3, and S-7
- High-speed tool steels such as M-2 and M-4
- Nitronic stainless steels such as 30, 40, 50, and 60
- Ferritic and martensitic stainless steels of the 400 and 500 series
- Austenitic stainless steels of the 200 and 300 series
- Precipitation-hardening stainless steels such as 13-8 PH, 15-5 PH, 17-4 PH, 17-7 PH, A-286, AM350, and AM355
- Nitriding steels DIN series

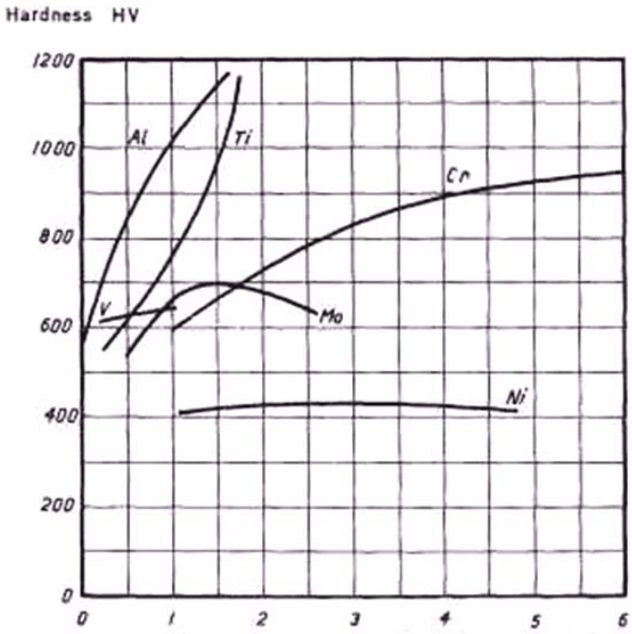

Figure 2.9. Effect of alloying element additions on hardness [1]

2.9. Objectives

The primary objective of this research is to assess the hardness and wear performance of selected steels after nitriding by investigating the influence of nitriding bath composition, alloy composition, nitriding duration, and temperature.

Table 2.6. Steels that have been designed and developed as nitriding steels [1]

wt per cent	C	Si	Mn	P	Cr	Mo	Ni	V	Al	W	Co
Alloy Steels											
SAE 4132	0,34				1						
SAE 4137	0,35	0,25	0,8		1						
SAE 4142	0,42				1						
SAE4140	0,4	0,25	0,85		1						
SAE 9840	0,36				1		1				
SAE 4150	0,5				1						
28NiCrMoV85	0,3				1,3		2	0,1			
32NiCrMo145	0,32				1		3,3				
30CrNiMo8	0,3				2		2				
34CrNiMo6	0,34				1,5		1,5				
SAE 4337	0,38				0,8		1,5				
SAE 4130	0,26				1						
Nitralloy Series											
Nitralloy	0,20-0,3	0,10-0,35	0,40-0,65	0,05 max	2,90-3,5	0,40-0,7	0,4 max	0,10-0,3			
Nitralloy M	0,30-0,5	0,10-0,35	0,40-0,8	0,05 max	2,50-3,5	0,70-1,2	0,4 max				
Nitralloy 135	0,25-0,35	0,10-0,35	0,65 max	0,05 max	1,40-1,8	0,10-0,25	0,4 max		0,90-1,3		
Nitralloy 135M	0,35-0,45	0,10-0,35	0,65 max	0,05 max	1,40-1,8	0,10-0,25	0,4 max		0,90-1,3		
Cold tool steel											
F2	1,45			0,3			0,3	3			
Special purpose tool steels											
H13	0,5	1		5	1,4		1,4				
	1,2			0,2			0,1	1			
	0,9			0,2			0,3	1			
Dimensionally stable tool steels											
D2	1,55			11,5	0,8			1			
D3	2			12							
A2	1			5	1		0,2				
O1	0,95		10,5			0,1	0,5				
O2	0,9		20,4			0,2					
D6	2,1			11,5			0,2	0,7			

Table 2.6. Steels that have been designed and developed as nitriding steels [1] (continued)

wt per cent	C	Si	Mn	P	Cr	Mo	Ni	V	Al	W	Co
D2	1,65			11,5	0,6		0,1	0,5			
S1	0,59			1,1			0,2	1,9			
Die block steels											
L6	0,55				0,55	5	0,5	1,7	0,1		
L6	0,55				0,2	0,3	1,7	0,1			
Hot-work tool steels											
H12					0,36	5,2	1,4			0,4	1,3
H13	0,4				5	1,3		1			
H11	0,4				5	1,3		0,6			
H21	0,3				2,7			0,4		8,5	
H19	0,4				4,3	0,4		2		4,3	4,3
H10	0,32				2,8	2,8		0,5		0,3	
High-speed steel tungsten base											
T5	0,75				4	0,6		1,6		18	9,5
T4	0,8				4	0,7		1,6		18	5
T1	0,75				4			1		18	
T15	1,5				5			5		12,5	5
M42	1,08				4	9,5		1,2		1,5	8
M41	0,92				4	5		1,8		6,5	5
M3	1,2				4	5		3		6,5	
M2	0,87				4	5		1,8		6,5	
M2	1				4	5		1,8		6,5	
M7	1				4	8,7		2		1,8	
M1	0,83				4	2		1,2		1,8	
Nitriding Steels											
DIN 1.8521 15CrMoV5-9	0.13-0.18	≤0.40	0.80–1.10	≤0.025	1.20–1.50	0.80–1.10	0	0.20–0.30	0	0	0
DIN1.8515 31CrMo12	0.28–0.35	≤0.40	0.40–0.70	≤0.025	2.80–3.30	0.30–0.50	0	0	0	0	0
DIN 1.8519 31CrMoV9	0.27–0.34	≤0.40	0.40–0.70	≤0.025	2.30–2.70	0.15–0.25	0	0.10–0.20	0	0	0
DIN 1.8550 34CrAlNi7	0.30–0.37	≤0.40	0.40–0.70	≤0.025	1.50–1.80	0.15–0.25	0.85–1.15	0	0.80–1.20	0	0
DIN 1.8509 41CrAlMo7	0.38–0.45	≤0.40	0.40–0.70	≤0.025	1.50–1.80	0.20–0.35	0	0	0.80–1.20	0	0
DIN 1.8507 34CrAlMo5	0.30–0.37	≤0.40	0.40–0.70	≤0.025	1.00–1.30	0.15–0.25	0	0	0.80–1.20	0	0

3. EXPERIMENTAL

Three different alloy steels have been chosen for nitriding trials in this research according to their core hardness and chemical composition. These nitrided alloys then have been used as pin in the wear tests.

The first alloy is one of the most commonly used steel in various applications: DIN 1.7225 (42CrMo4). Core hardness of this steel, when austenized at 845°C, oil quenched to 65°C, and tempered at 540°C, is 300 $HV_{0.1}$ (Vickers hardness by applying 100g load) which corresponds to 285 HB. The second alloy is DIN 1.6523 (20NiCrMo2) steel. This steel is the softest among the selected steels for this particular application with core hardness of 185 $HV_{0.1}$ (185 HB) when normalized by austenizing 2 h at 915 °C and cooling in still air. The third selected steel is DIN 1.8550 (34CrAlNi7). This is called as "nitriding steel" in the literature and has a core hardness of 268 $HV_{0.1}$ (255 HB).

The chemical compositions of the alloys are given in Table 3.1. The main idea behind selection of these particular steels in terms of their chemical composition is to see the influence of various alloying elements on nitriding. Comparison of the selected alloys is expected to provide an insight into the effects of the following elements:

- DIN 1.7225 ⟷ DIN 1.8550: Effects of aluminum, chromium, and nickel
- DIN 1.6523 ⟷ DIN 1.8550: Effects of aluminum, chromium, and carbon
- DIN 1.7225 ⟷ DIN 1.6523: Effects of nickel, chromium, and carbon

Nitriding trials have been performed in two different salt baths; both of them are cyanide free. Bath Type 1 consists of 80 wt per cent potassium cyanate (KCNO), and Bath Type 2 consists of 40 wt per cent potassium cyanate (KCNO). The balance of the both baths is sodium carbonate.

Table 3.1. Chemical composition, hardness, and surface roughness of selected pin and disc alloys

Function ⟶		Pin			Disc
Alloy designation system	DIN Material no	1.8550	1.7225	1.6523	1.2379
	DIN Type	34CrAlNi7	42CrMo4	20NiCrMo2	X155CrVMo12-1
	UNS	K52440	G41400	G86200	T30402
	AISI		4140	8620	D2
	ASTM	A355	A322	A322	A 681
Element, wt per cent	C	0,36	0,41	0,19	1,54
	Si	0,26	0,26	0,18	0,51
	Mn	0,68	0,83	0,74	2,28
	P	0,01	0.032	0,022	0,02
	S	0,01	0,03	0	0,013
	Cr	1,56	1,04	0,41	12,4
	Mo	0,22	0,19	0,16	0,86
	V	0	0	0	0,92
	Ni	0,94	0	0,43	0
	Al	1,19	0	0	0
Core Hardness ($HV_{0.1}$)		268	300	185	263
Surface Roughness	Before (μm)	0,56	0,52	0,70	0,30
	After (μm)	0,73	0,78	0,77	

Four different nitriding temperatures, 520°C, 570°C, 590°C, and 630°C, have been selected to see the effect of temperature on the microstructure, hardness, and wear resistance of nitrided specimens. While the first three are in the ferritic region, the treatment at 630^{o}C is in the austenitic region, and provides an insight into the high temperature nitriding process. Due to the nature of the nitriding, the selected temperatures are relatively lower than those of

the other surface engineering methods (See Table 2.2). This leads to dimensional stability after nitriding.

Four different nitriding durations 0,5 h, 1 h, 1,5 h, and 2 h have been arranged to allow buildup of nitride layers, with various thickness.

The nitriding operations have been performed according to a test matrix shown in Table 3.2. A short nitriding duration at a low nitriding temperature (e.g.; 0,5 h at 520°C) and a long nitriding duration at a high nitriding temperature (e.g.; 2 h at 590°C and 630°C) have not been chosen since adequate diffusion cannot be satisfied at low temperatures and in short nitriding durations, and a very brittle microstructure builds up on the surface of the material as a result of high temperatures and long nitriding durations.

Table 3.2 Nitriding test matrix

Bath	Time (h)	Temperature (^{o}C)	Alloy
Type 1 (80 wt per cent potassium cyanate)	0,5	570	DIN 1.7225
	1		
	2		
Type 2 (40 wt per cent potassium cyanate)	0,5	590	DIN 1.6523
		630	
	1	520	DIN 1.8550
		590	
		630	
	1,5	630	
	2	520	
		590	

The disc material is chosen as DIN 1.2379 whose chemical composition is given in Table 3.1. Hardness of this material is measured as 263 $HV_{0.1}$ (250 HB). For this particular application, all disc surfaces have been ground with 120, 180, and 240 grit grinding papers on Metkon (Metkon is a laboratory device manufacturer located in Bursa, Turkey) Gripo grinding and polishing machine and surface roughness have been measured to be 0,3 μm Ra by Taylor – Hobson Surtronic 3+ surface roughness machine. This value is reported by ASTM G 99-95a standard to be adequate for wear tests.

3.1. Metallographic and Chemical Composition Studies

The nitrided parts have been analyzed in terms of microstructure to identify compound layer thickness, diffusion depth, and surface quality.

In order to perform these metallographic analyses, small sections have been cut from the nitrided and unnitrided specimens on a Metkon precision diamond blade cutting machine. Afterwards, all sections have been mounted on a Metkon hot mounting press. Then, to get a smooth surface, all specimens have been sequentially ground with 120, 240, 320, 400, 600, and 800 grit grinding papers on a Metkon Gripo grinding and polishing machine. Subsequently to get rid of grinding scratches, specimens have been polished respectively on a velvet, saturated with 15 μm, 10 μm, 5 μm, and 1 μm alumina solution on the same grinding and polishing machine.

Finally, all polished surfaces have been chemically etched with a 5 per cent Nital (5 vol per cent HNO_3 + 95 vol per cent ethanol) solution to reveal the microstructure of the specimens.

Nikon Eclipse LV 150 optical microscope having 50-1000X magnification has been used to analyze the microstructural features of the specimens as well as to determine the thickness of the compound layer and diffusion depth. Additionally, parts have been analyzed by a Philips XL 30 ESEM – FEG Scanning Electron Microscope (SEM). On this microscope,

in addition to taking microphotographs, Energy Dispersive Spectroscopy (EDS) analyses have been conducted with about 5 μm electron beam diameter to identify the chemical composition of nitrided specimens and worn region of discs.

3.2. XRD Studies

Types of nitrides formed on the surface of the nitrided specimens has been investigated by a Rigaku D/MAX-Ultima+/PC X-ray diffraction equipment. CuKα radiation with 1.5418 Å wave length has been used to analyze nitriding phases with 2θ within 25-80^{o}.

3.3. Hardness and Microhardness Measurement

Microhardness measurements have been conducted to determine the hardness profile in the nitrided parts. Measurements have been taken from ground and polished specimens. Microhardness measurements have been carried out with Leitz Microhardness Measurement Machine applying 100 g load ($HV_{0.1}$). At the nitrided zone, microhardness has been measured with 10 μm spacing and towards the core of the specimens, spacing between measurements has been increased till measuring a stable hardness profile.

Core hardness of unnitrided pin and disc materials has been measured on Reicherter Brinell hardness measurement machine. The measurements have been converted to Vickers Hardness and tabulated in Table 3.1.

3.4. Surface Roughness Measurements

Surface roughness of machined pins has been measured before and after nitriding to determine effects of nitriding on surface properties. Taylor – Hobson Surtronic 3+ surface measurement machine was used to determine the roughness of pin specimens.

3.5. Wear Tests

The wear resistance is determined by wear tests. A home-made Pin-on-Disc type wear test setup, as seen in Figure 3.1, has been built according to ASTM G 99-95a standard. This system consists of a drive spindle and chuck for holding the revolving disc, a lever-arm device to hold the pin, and attachments to allow the pin specimen to be positioned against the revolving disc specimen with a controlled load. In this type of a test setup, the wear track on the disc is a circle, involving multiple wear passes in the same track. The main idea behind this wear setup is to simulate the real working condition of the developed nitrided alloys under a controlled medium. By this test, sliding wear has been measured. It has been expressed by the dimensional and weight change of specimens before and after wear tests.

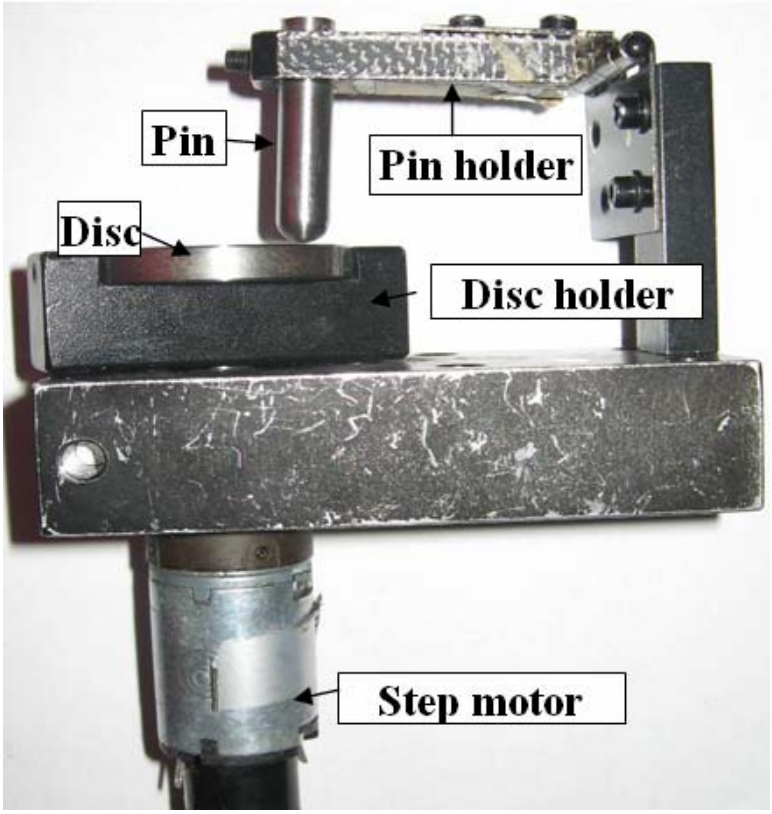

Figure 3.1. Photo of pin-on-disc wear test setup used for wear tests

The applied load, wear setup characteristics, sliding speed, sliding distance, and the material properties are the parameters that the amount of wear in any system depends on. Therefore, these parameters are needed to be determined carefully.

In this thesis, a step motor, capable of maintaining a constant speed of 150 rpm under load has been used. As shown in Figure 3.2, the geometry of the pin specimen has been chosen as 10 mm diameter and 60 mm long rods with a 5 mm radius hemispherical end. The selected pin alloys have been machined on Supermax GT200-B turning machine at 2000 rpm from cylindrical bars having 20 mm of diameter and 65 mm length. The discs have been cut on the same machine from a long bar having 50 mm diameter and 7 mm thickness.

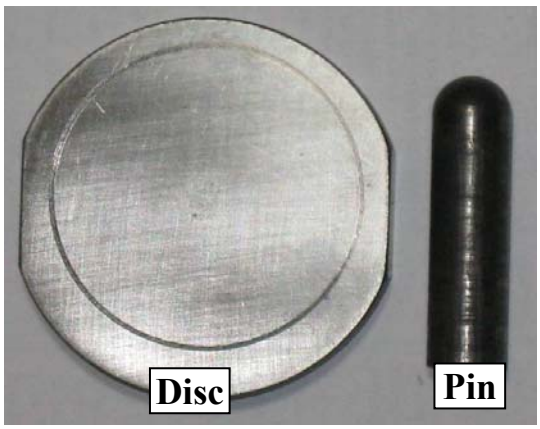

Figure 3.2. The pin and disc used for wear tests. A circular wear track is shown on the disc surface.

Four Newtons of contact force have been used during wear tests to keep continuous contact between the pin and disc. Relative sliding speed between the contacting surfaces to see the sliding effects has been chosen as 0,3 m/s and setup has run for 200 m of sliding distance to simulate the total working conditions. Specimens have been measured to the nearest 10 μm length and to the nearest 0,001 g weight before and after wear tests to determine the volume loss of the specimens.

After completion of the wear tests volumetric losses have been calculated by using disc volume loss formula, Equation 3.1, which employs the dimensions of the track. The disc volume losses have been checked by using Equation 3.2 which calculates lost volume using the lost mass and density of the disc material.

$$\text{disk volume loss, mm}^3 = \frac{\pi(\text{wear track radius, mm})(\text{track width, mm})^3}{6(\text{sphere radius, mm})} \tag{3.1}$$

$$\text{disc volume loss, mm}^3 = \left(\frac{\text{mass loss, g}}{\text{density, } \frac{\text{g}}{\text{cm}^3}} \right) \times 1000 \tag{3.2}$$

4. RESULTS AND DISCUSSIONS

Users of the nitriding process intend to gain improved material properties particularly the hardness and the wear resistance within the developed nitriding case. Principle factors affecting the case features are (a) the nature of the nitriding medium, (b) temperature and duration of nitriding, (c) amount and nature of nitride forming elements in solid solution in the steel such as aluminum and chromium, and (d) amount and nature of other elements in the steel such as carbon and silicon. Results of the experimental work carried out within the scope of this thesis to assess these factors have been presented and discussed in the following sections.

4.1. Results of the Nitriding Trials

Nitriding trails have yielded different compound layer thickness and diffusion depth (presented in Table 4.1) as a result of varied experimental parameters.

4.1.1. Characterization of the Nitriding Case and Phases in the Case

4.1.1.1. Microscopy and EDS Studies. The micrographs of unnitrided specimens have been used to set a base for comparison with nitrided specimens. Optical micrographs and SEM of unnitrided specimens are given in Figure 4.1 and Figure 4.2. Figure 4.1a shows a coarse pearlitic structure in a fully annealed specimen of DIN 1.7225 alloy steel where the cementite lamellae appear dark while the ferrite remains white. Figure 4.1b presents DIN 1.8550 steel which is fully martensitic. However, microstructure of DIN 1.6523 steel is composed of mainly primary ferrite and paerlite (See Figure 4.1c).

The effects of nitriding on the microstructure of the steels can be seen by investigation of the optical micrographs of the specimens shown in Figures 4.3 – 4.8. Microstructural photos are shown in these figures to present examples for nitrided specimens with minimal

Table 4.1. Thicknesses of nitriding layer for all specimens

Specimen No	Alloy	Compound layer thickness (μm)	Nitriding case thickness (μm)	Bath type	Temperature (^{o}C)	Time (h)
1	DIN 1.7225	4	130	Type 1 (80 wt per cent potassium cyanate)	570	0,5
2	DIN 1.6523	6	137			
3	DIN 1.8550	4	110			
4	DIN 1.7225	10	150			1
5	DIN 1.6523	12	166			
6	DIN 1.8550	7	139			
7	DIN 1.7225	12	188			2
8	DIN 1.6523	15	197			
9	DIN 1.8550	8	175			
10	DIN 1.7225	0	107	Type 2 (40 wt per cent potassium cyanate)	520	1
11	DIN 1.6523	0	74			
12	DIN 1.8550	0	82			
13	DIN 1.7225	2	130			2
14	DIN 1.6523	2	154			
15	DIN 1.8550	0	133			
16	DIN 1.7225	5	79		590	0,5
17	DIN 1.6523	4	95			
18	DIN 1.8550	0	74			
19	DIN 1.7225	10	119			1
20	DIN 1.6523	11	121			
21	DIN 1.8550	6	121			
22	DIN 1.7225	17	170			2
23	DIN 1.6523	18	185			
24	DIN 1.8550	11	164			
25	DIN 1.7225	13	227		630	0,5
26	DIN 1.6523	10	183			
27	DIN 1.8550	6	123			
28	DIN 1.7225	19	236			1
29	DIN 1.6523	20	238			
30	DIN 1.8550	11	190			
31	DIN 1.7225	21	321			1,5
32	DIN 1.6523	26	349			
33	DIN 1.8550	22	214			

and maximal case thickness. As can be seen from Table 4.1, specimens 16, 17, 18 and 31, 32, 33 have yielded respectively the minimum and maximum cases of both compound layer and nitriding case thicknesses.

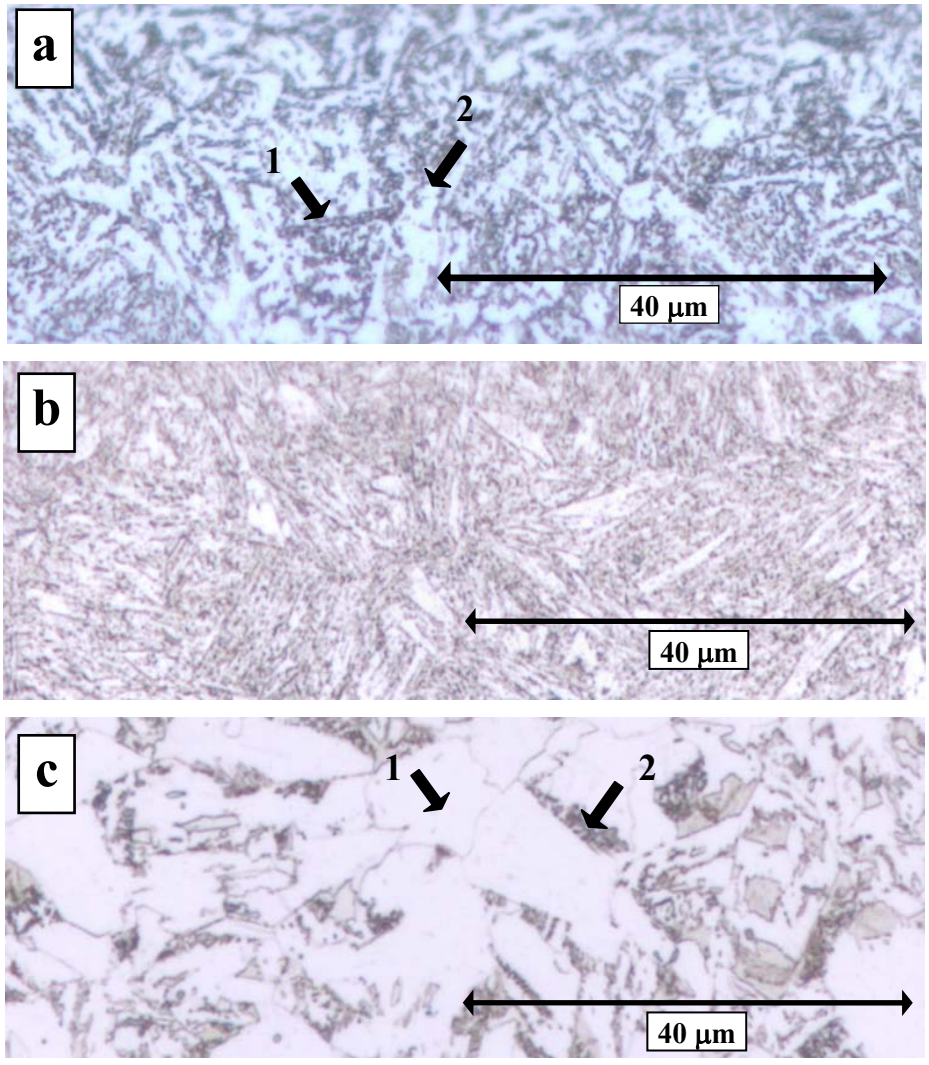

Figure 4.1. The optical microscopy of core microstructures of unnitrided alloys - 1000X (a) DIN 1.7225 (1-cementite, 2-ferrite). (b) DIN 1.8550 - martensite. (c) DIN 1.6523 (1- primary ferrite, 2-pearlite).

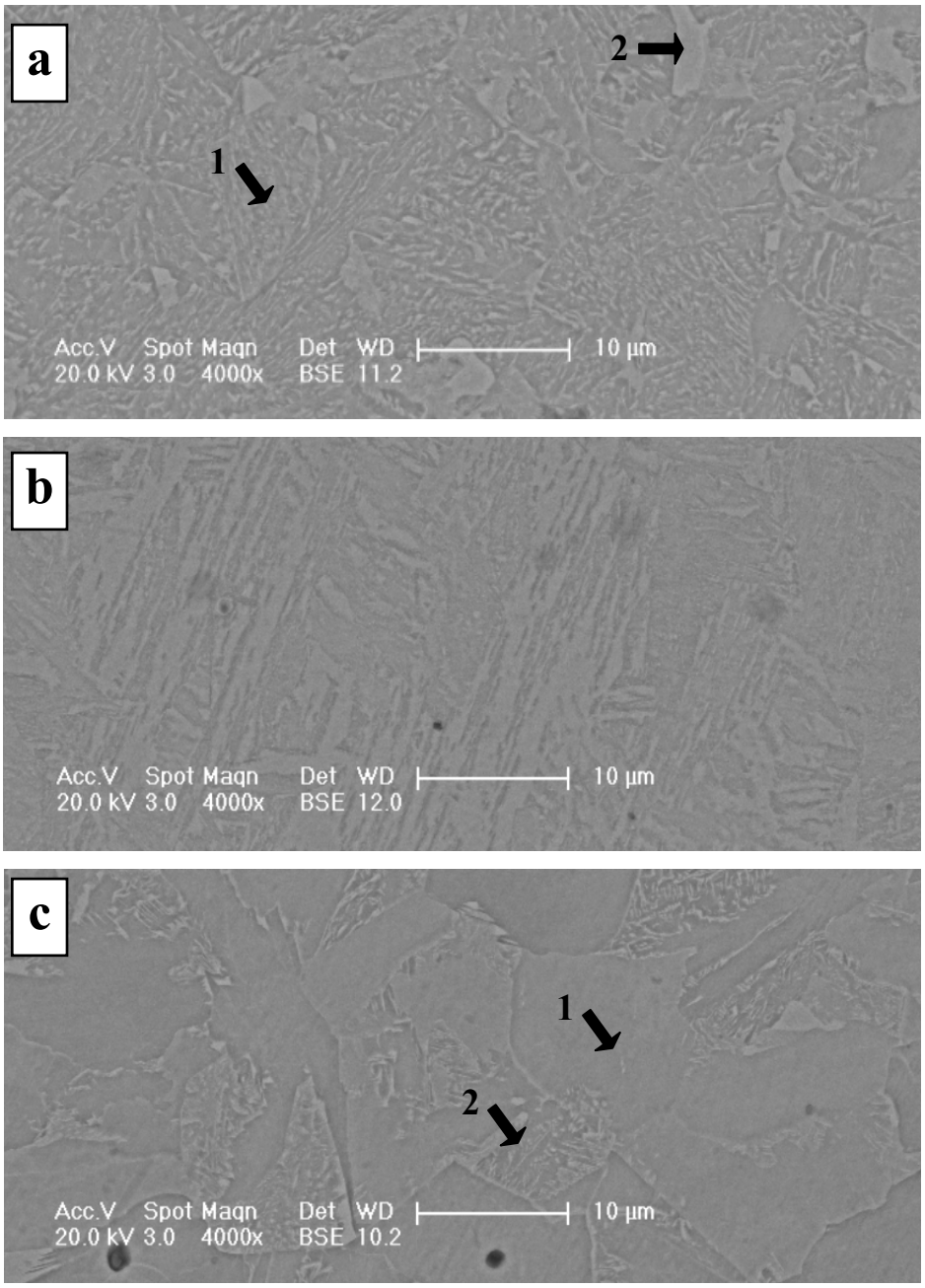

Figure 4.2. The SEM photos of core microstructures of unnitrided alloys (a) DIN 1.7225 (1- cementite, 2-ferrite). (b) DIN 1.8550 - martensite. (c) DIN 1.6523 (1- primary ferrite, 2- pearlite).

In the figures, coloration results from the diffusion of nitrogen and carbon into the specimens. The nitriding case, composed of the compound layer (γ' and/or ε) and the diffusion

layer, can be seen by the optical microscope and SEM. The compound layer is differentiated by its white layer. Due to the nature of the nitriding process, amount of the nitrogen reduces from surface towards the core of the material, and it approaches to zero at the end of the nitriding case. Diffusion rate of nitrogen varies from alloy to alloy under the same nitriding conditions. For instance, at the end of 0,5 h nitriding in Type 2 bath at 590°C, there is a 5 µm continuous compound layer formation on the surface of DIN 1.7225 (Figure 4.3b), but under the same conditions, there is a thinner and discontinuous compound layer formed on the surface of DIN 1.6523 alloy (Figure 4.4b). On the other hand, there is not a compound layer formation at all on the DIN 1.8550 steel (Figure 4.5b). The reason for this lies in the difference between the diffusion kinetics of nitrogen these different alloys as explained in the following sections.

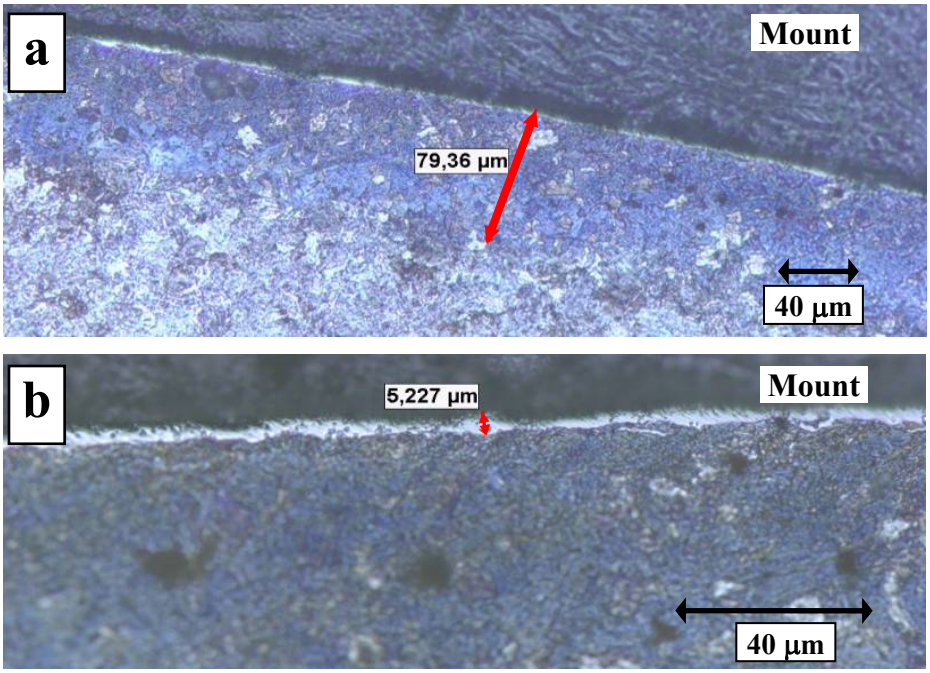

Figure 4.3. Microstructure of specimen no 16 (DIN 1.7225, nitrided in Type 2 bath at 590°C for 0,5h). (a) 200X close-up on the nitriding case. (b) Continuous compound layer on the surface – 500X

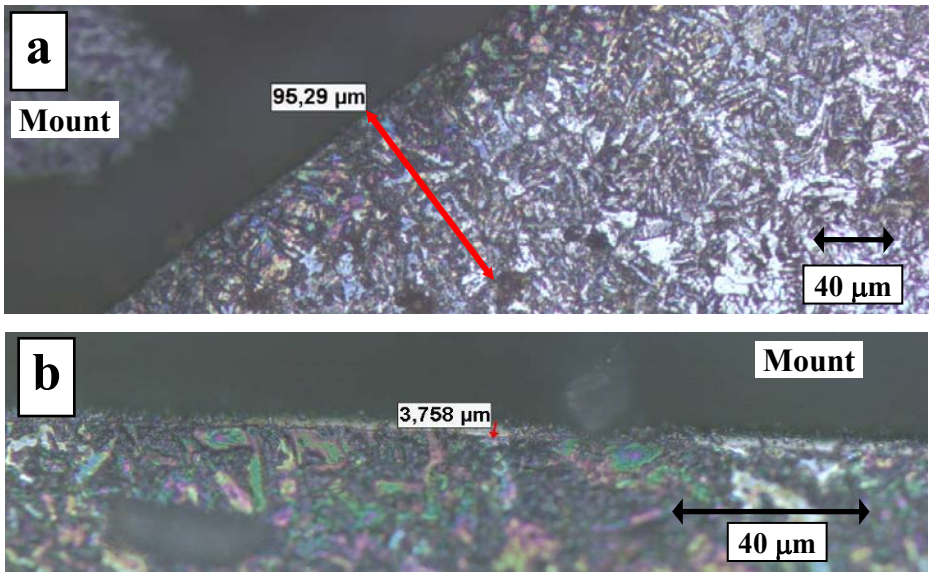

Figure 4.4. Microstructure of specimen no 17 (DIN 1.6523, nitrided in Type 2 bath at 590°C for 0,5h). (a) 200X close-up on the nitriding case. (b) Discontinuous compound layer on surface – 500X

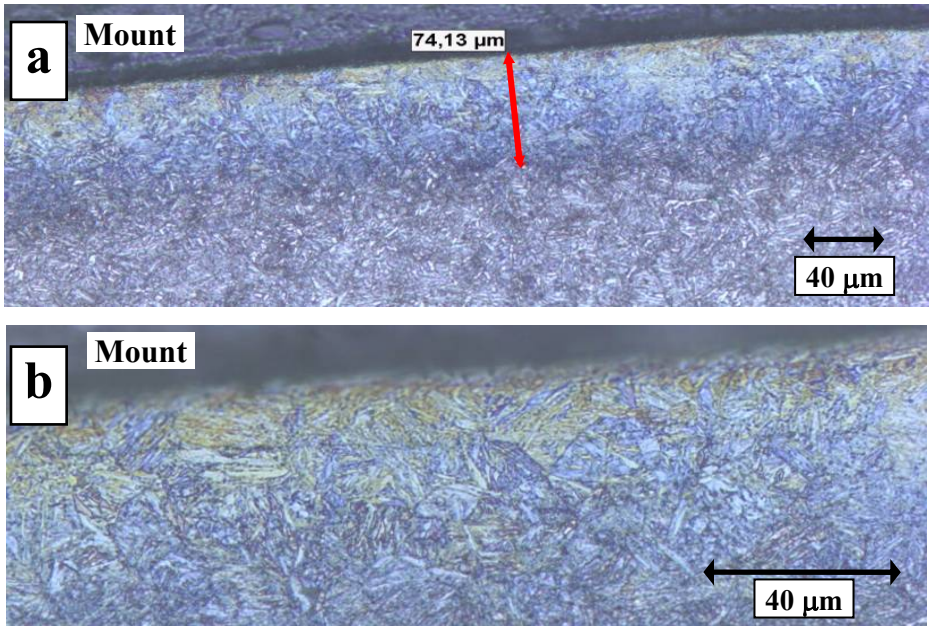

Figure 4.5. Microstructure of specimen no 18 (DIN 1.8550, nitrided in Type 2 bath at 590°C for 0,5h). (a) 200X close-up on the nitriding case after nitriding. (b) No compound layer formation on surface – 500X

In contrast to previous combination (low temperature and short duration), specimens no 31, 32, and 33 are nitrided in Type 2 bath at 630°C for 1,5 h (high temperature and long duration). Microstructure photos (Figures 4.5 - 4.7) show that the nitriding case and compound layer thickness are excessively higher than those of the previously explained combination.

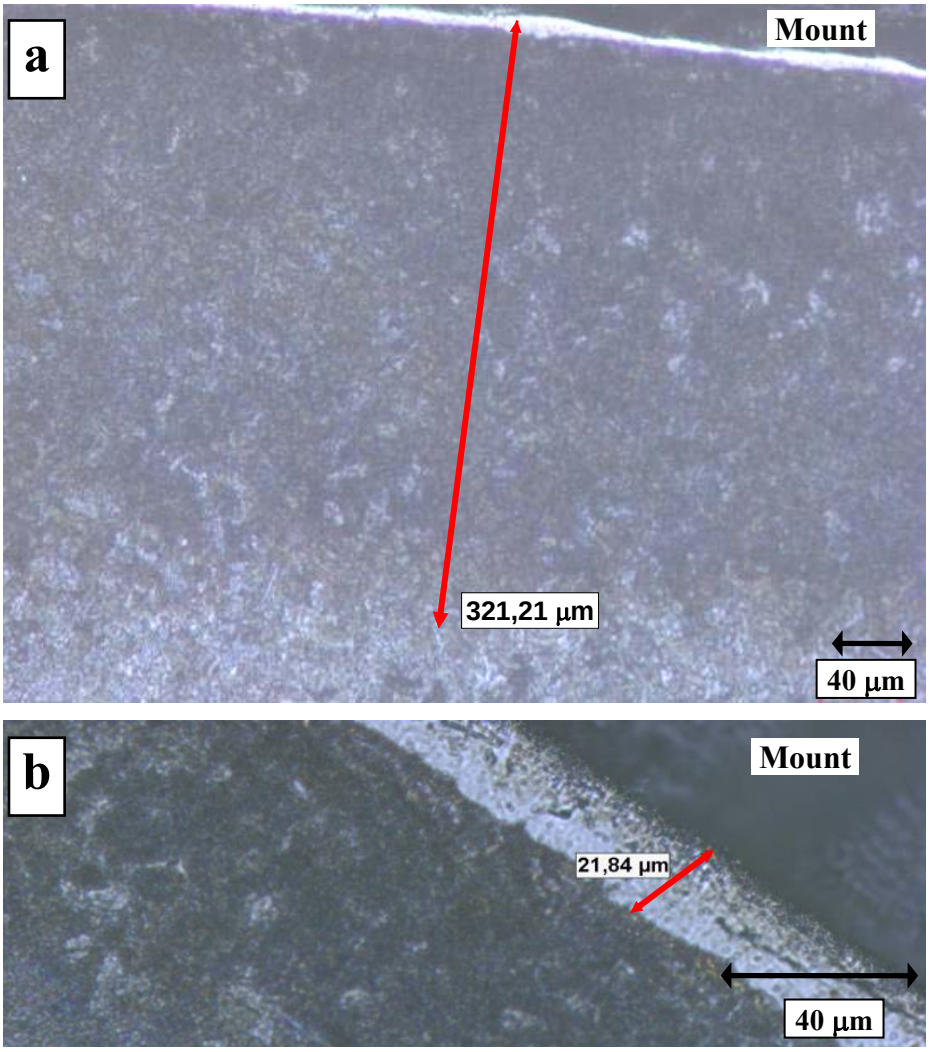

Figure 4.6. Microstructure of specimen no 31 (DIN 1.7225, nitrided in Type 2 bath at 630°C for 1,5h). (a) 200X close-up on the nitriding case. (b) Compound layer on the specimen surface – 500X

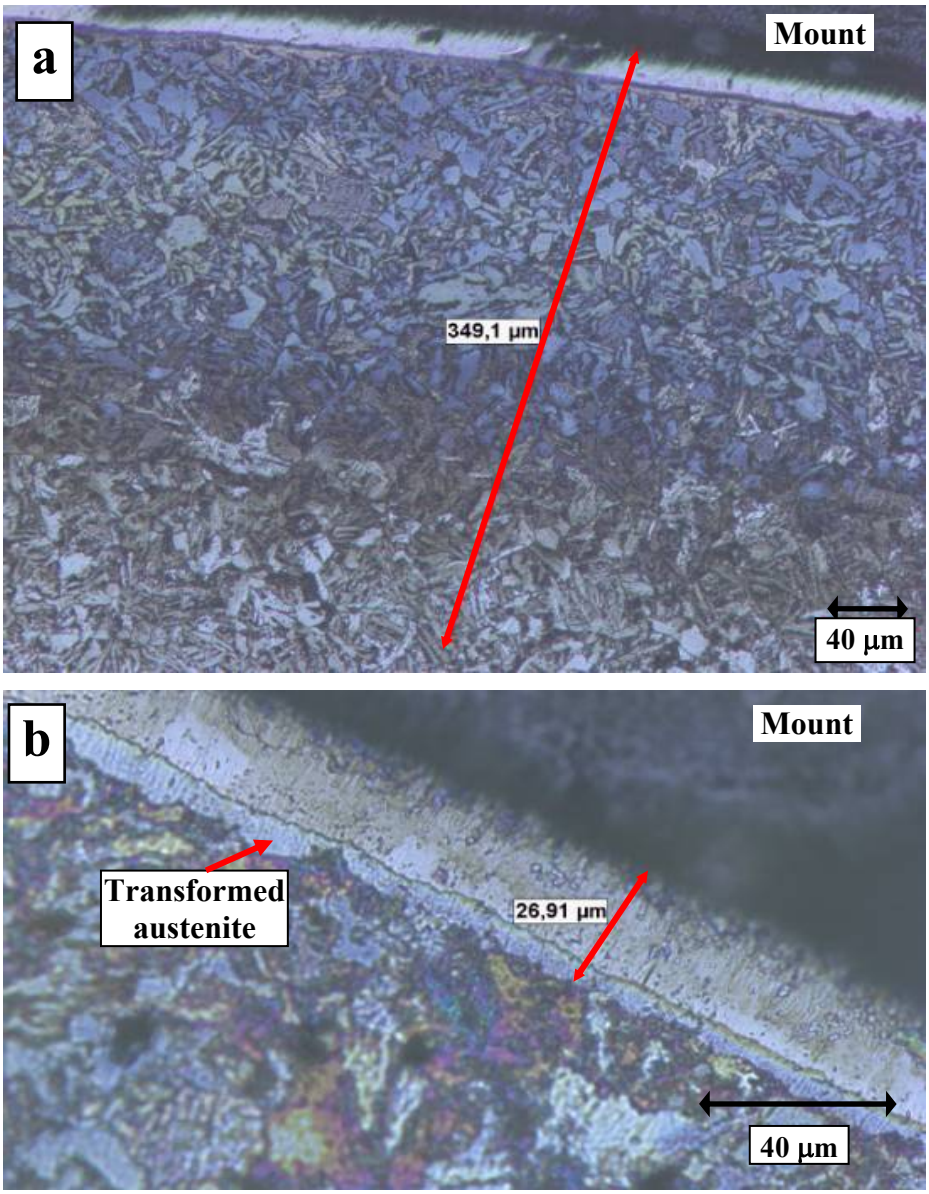

Figure 4.7. Microstructure of specimen no 32 (DIN 1.6523, nitrided in Type 2 bath at 630°C for 1,5h). (a) 200X close-up on the nitriding case. (b) Compound layer and transformed austenite layer in the specimen – 500X

It is interesting to note that, in specimen 32, a light colored layer is also formed below the compound layer. These two layers are separated by a thin, dark line as seen in Figure 4.7b. The light colored layer has been observed only in this particular specimen treated at 630°C, which is in the austenitic range. Hence, the formed layer is claimed to be the transformed

austenite (eg.; Bainite and/or Martensite) layer. As Krishnaraj et al. [44] have explained, the transformed austenite phase forms due to the quenching of the nitrided specimens from treatment temperatures since nitrogen and carbon lower the martensite start temperature and result in the retention of austenite in the transition zone from the compound layer to the diffusion layer. However, this layer is not determined in DIN 1.8550 and DIN 1.7225 specimens (Figures 4.5 and 4.7) because of a higher eutectoid transformation temperature. For example, the eutectoid transformation temperature for DIN 1.8550 is reported to be around 640-650°C [45].

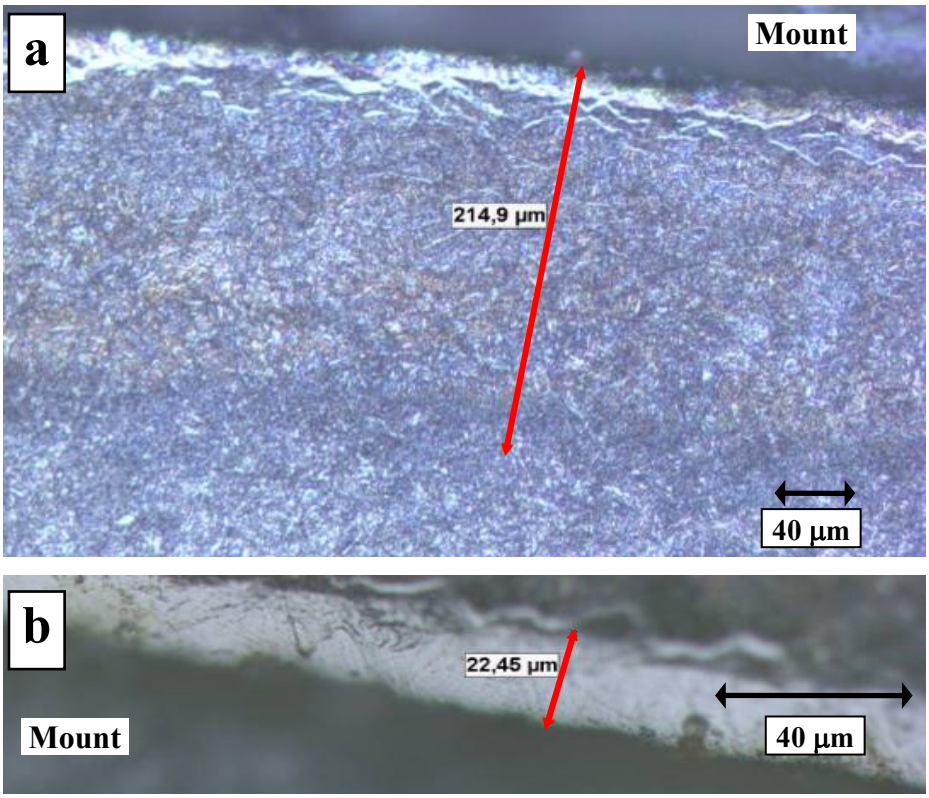

Figure 4.8. Microstructure of specimen no 33 (DIN 1.8550, nitrided in Type 2 bath at 630°C for 1,5h). (a) 200X close-up on the nitriding case (b) Compound layer on the specimen surface – 500X

In Figure 4.9, an SEM photo of specimen no 33 is given. The EDS analysis shows the nitrogen content near the surface of nitrided specimen to be 8,97 wt per cent at 5 µm depth

from the surface, which indicates that the compound layer is basically ε-Fe_3N nitride (See the equilibrium phase diagram, Figure 1.2). The EDS analysis has been repeated towards the core of the material. The nitrogen content has a decreasing trend (See Figure 4.10). Nitrogen content falls to 4,41 wt per cent near the end of the compound layer and to 4 wt per cent at 45 μm depth. The reduction of nitrogen content signals to the γ'-Fe_4N formation as suggested by the Fe-N equilibrium phase diagram. The formation of different layers is discussed in Section 4.1.1.2.

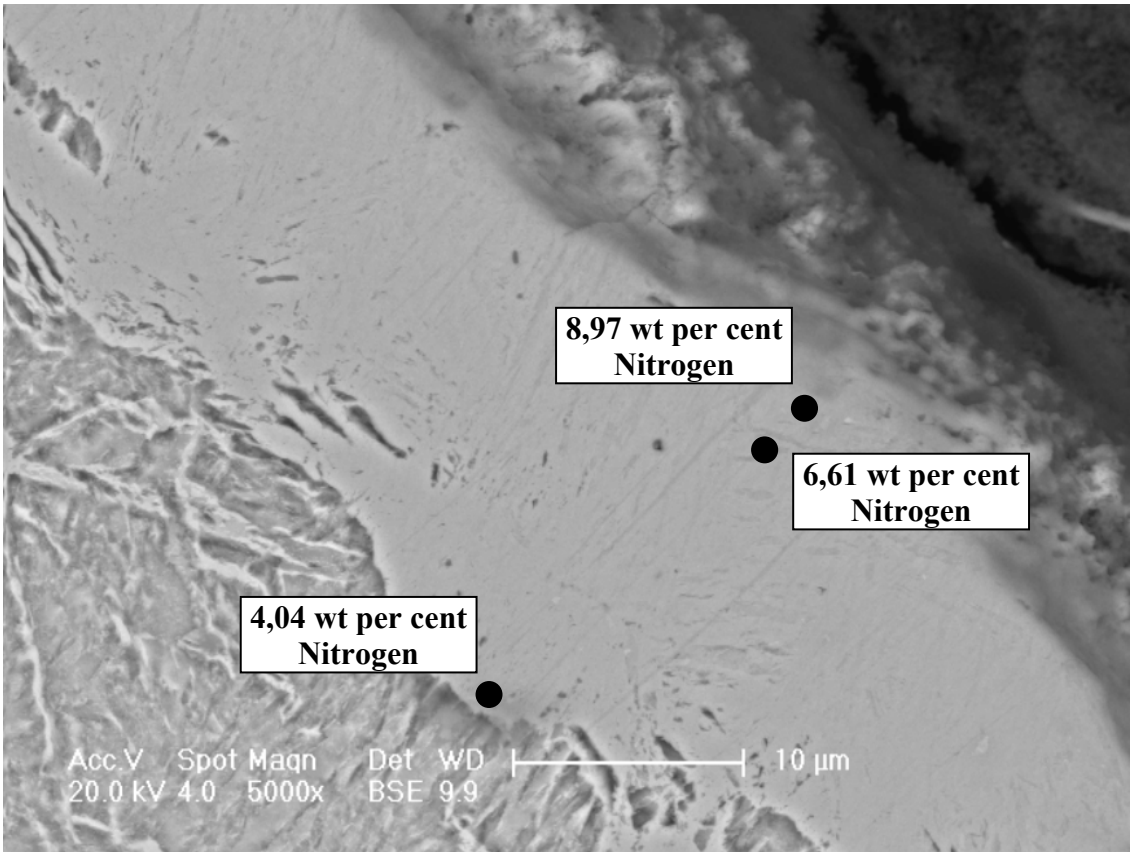

Figure 4.9. SEM and EDS analysis results of the compound layer of specimen no 33 under 5000X magnification (DIN 1.8550, nitrided in Type 2 bath at 630°C for 1,5h). Dark spots show the locations of EDS measurements.

As explained in Section 2.6.1, usually, there is porosity in the compound layer after the nitriding process. Two types of porosity can be seen in the compound layer. Figure 4.11

presents an example for the discontinuous porosity formation in the compound layer. However, there is also possibility to form porosity channels parallel to the surface in the compound layer (See Figure 4.12). Krishnaraj et al. [44] have also explained that size of pore increases at higher treatment temperatures and they form as a result of the accumulation of the interstitially dissolved nitrogen atoms at sites, such as grain boundaries, to form molecular nitrogen. The channel porosity formation is triggered by the pressure which reaches several kilobars applied by the interstitially dissolved nitrogen. The pressure results in the elongation of a pore into a pore channel.

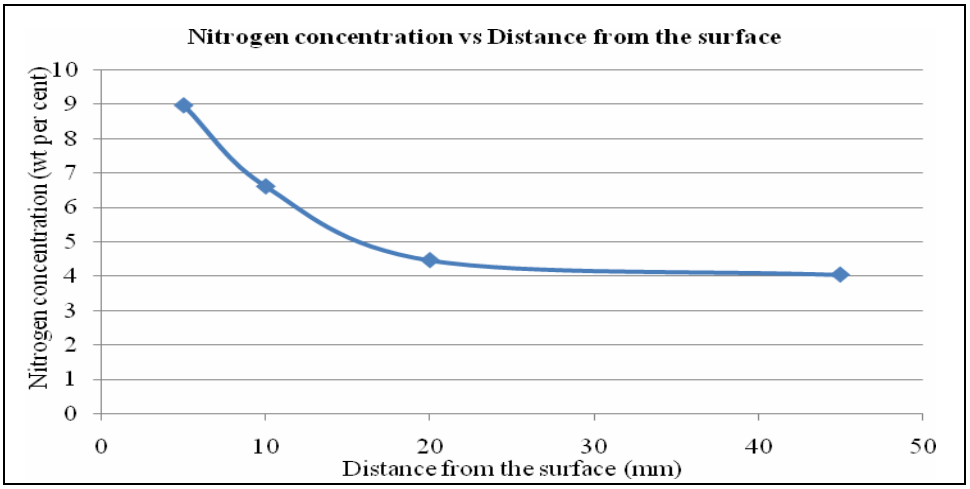

Figure 4.10. Nitrogen concentration change in specimen no 33 from the surface towards the core (DIN 1.8550, nitrided in Type 2 bath at 630°C for 1,5h)

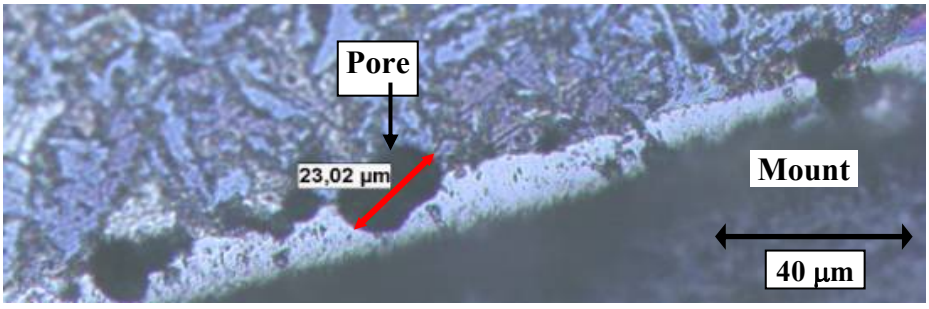

Figure 4.11. Discontinuous porosity formation in the compound layer in specimen no 5 (DIN 1.6523, nitrided in Type 1 bath at 570°C for 1h).

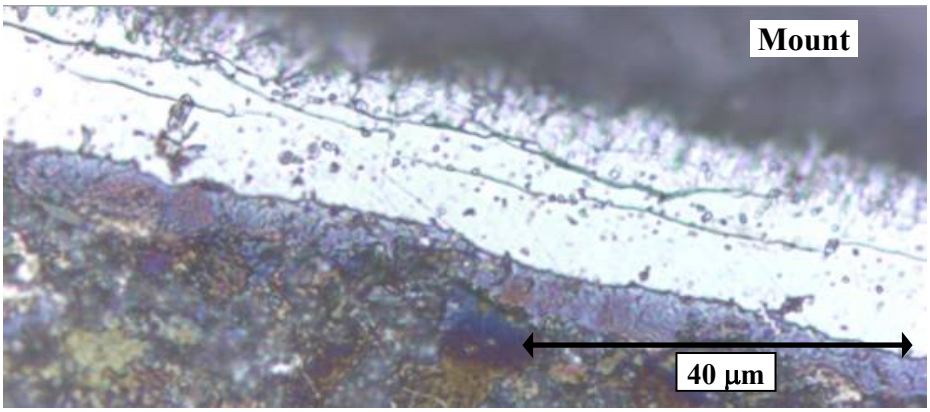

Figure 4.12. Channel porosity formation (dark lines) in the (white) compound layer parallel to the surface in specimen no 29 (DIN 1.6523, nitrided in Type 2 bath at 630^{o}C for 1 h).

4.1.1.2. XRD Verification of Surface Phases**.** X-Ray diffraction is a reliable method for identifying the phases on nitrided surfaces. Somers et al. [46] have produced the X-Ray powder diffraction peaks that are possible for the ε and γ' nitrides as seen in Figure 4.13. The XRD data obtained in the current study have been evaluated on the basis of the above mentioned reference powder diffraction analysis.

The XRD diffraction pattern of specimens no 5, 11, 17, and 32 are given in Figures 4.13 – 4.16. Specimens are selected from DIN 1.6523 steel in terms of compound layer thickness. Specimen no 5 is selected from Type 1 bath (80 wt per cent KCNO) having ~13μm compound layer. The rest of the specimens are taken from Type 2 bath (40 wt per cent KCNO) nitrided at different temperatures and having different compound layer thickness (See Table 4.1).

Specimen no 5 has been nitrided at 570^{o}C which is below the eutectoid temperature, but this bath has high cyanate concentration. Therefore, nitrogen penetration in this bath is very high. Accordingly, this specimen has 13 μm thick compound layer, and the XRD analysis result given in Figure 4.14 shows that the nitride phases on the surface are completely ε-nitride.

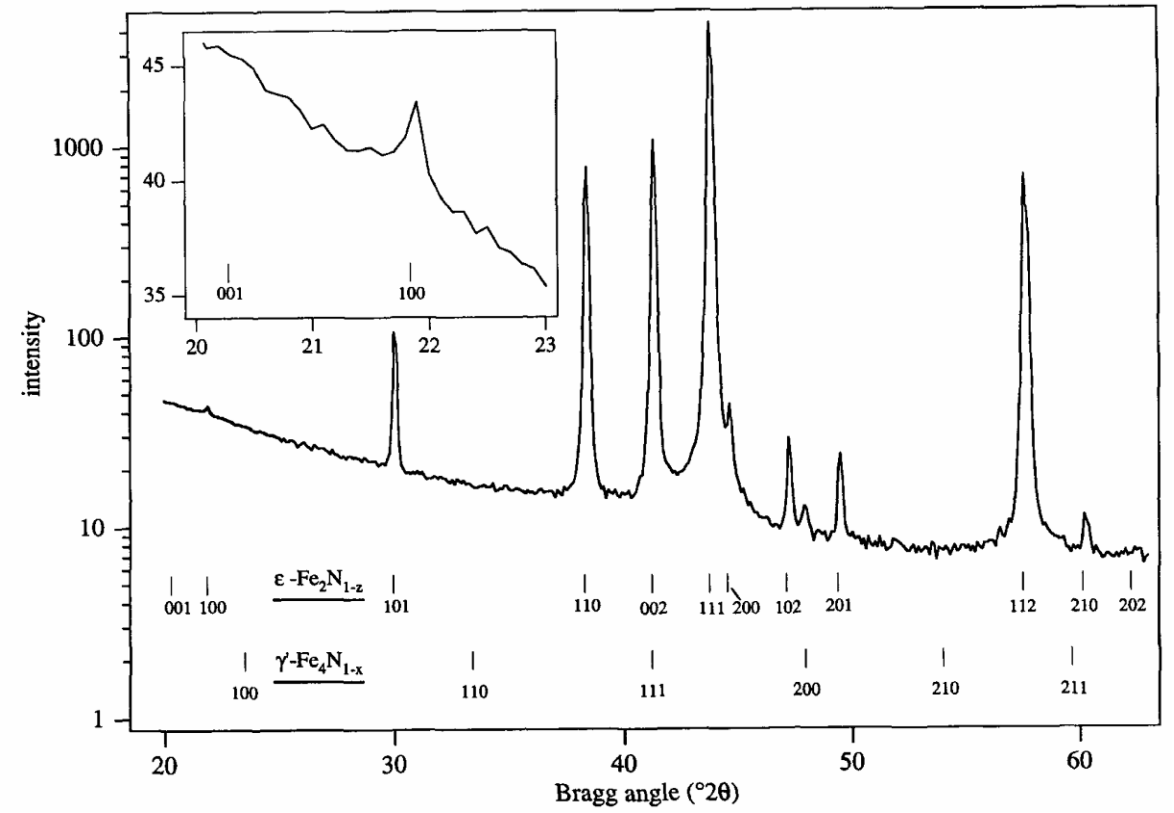

Figure 4.13. The XRD analysis of reference nitride phases in terms of 2θ positions [46]

Specimen no 11 has been nitrided in Type 2 bath at 520^{o}C and it has been observed by the optical microscope that there is only the diffusion layer without a compound layer formed at this temperature. XRD analysis of this specimen is given in Figure 4.15, and it is seen that the surface is composed dominantly of ε-nitride and with very weak peaks of γ'-nitride.

Specimen no 17 has been nitrided at 590^{o}C which is just below the eutectoid temperature of Fe-N phase equilibrium and still in the ferritic zone. This specimen has only 4 μm compound layer since it has been nitrided only for 0,5 h. However, due to the nitriding temperature, nitrogen diffused into the steel more than that in specimen no 11 nitrided at 520^{o}C. The higher diffusion rate brings about more nitride formation in the steel. The XRD analysis given in Figure 4.16 exhibits the nitride formation on the surface of this specimen and

it is indicated that ε-nitrides are dominant on the surface but there is still a single peak corresponding to γ'.

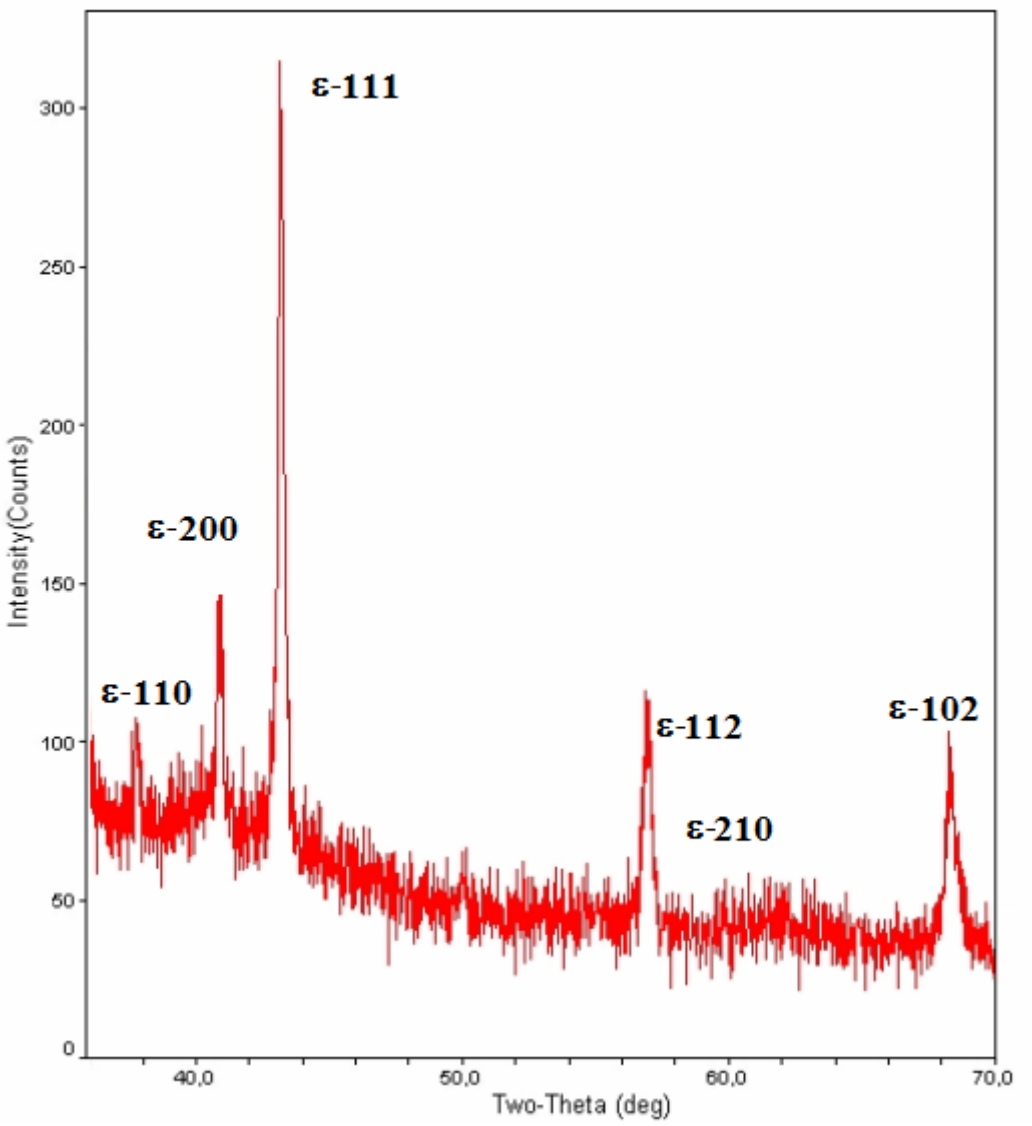

Figure 4.14. XRD analysis of specimen no 5 (DIN 1.6523 nitrided in Type 1 bath at 570°C for 1h)

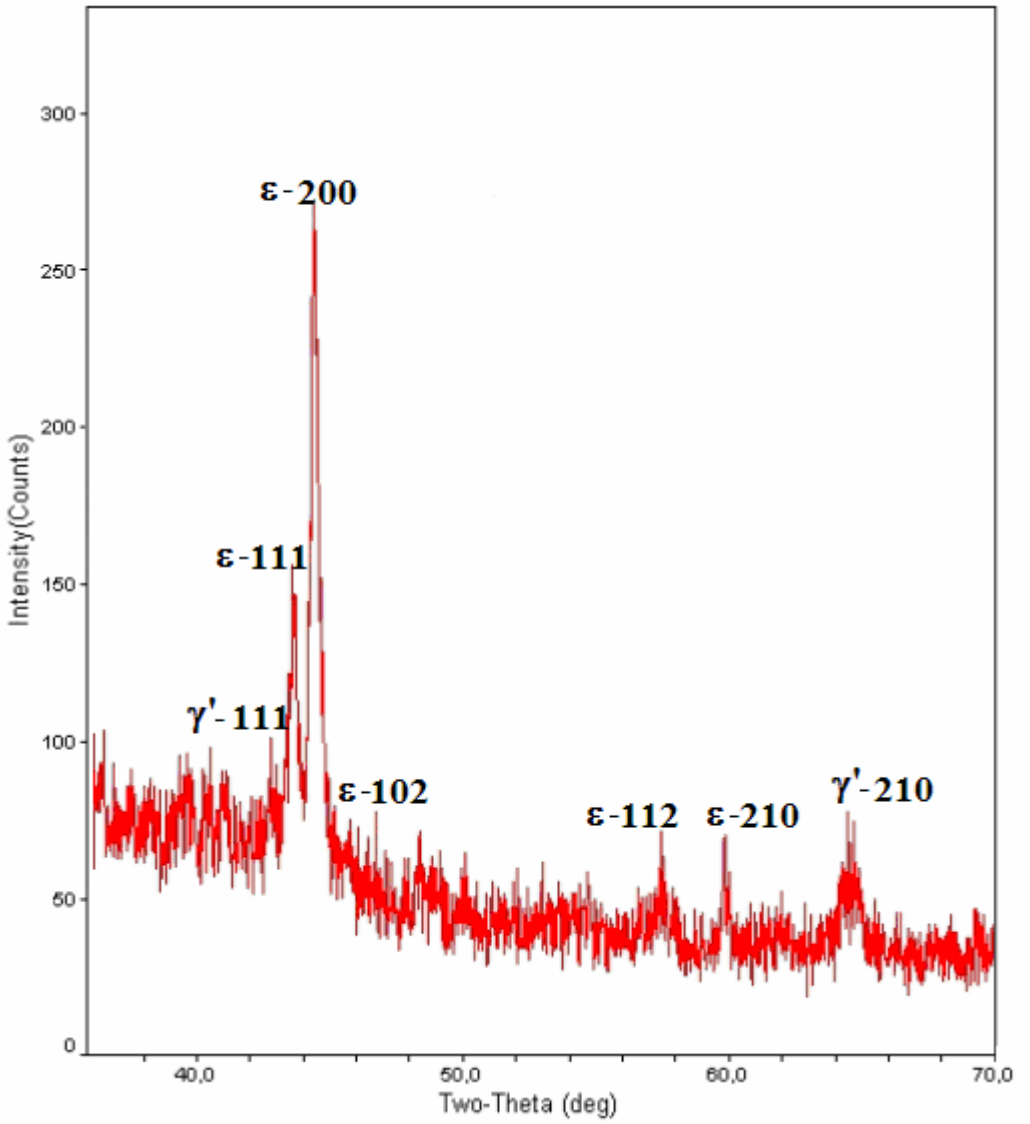

Figure 4.15. XRD analysis of specimen no 11 (DIN 1.6523 nitrided in Type 2 bath at 520^{o}C for 1h)

The compound layer (27 μm thick) of specimen no 32, however, is found to be only the ε-nitrides as presented in Figure 4.17. The nitriding temperature of this specimen is 630^{o}C, and this temperature is in austenitic phase field of Fe-N-C system. As Krishnaraj et al. [44] has explained when the process temperature increases, the ε-nitride phase region extends towards the lower nitriding concentrations. Therefore, it is easy to get specimen without γ'- nitride phase at higher process temperatures.

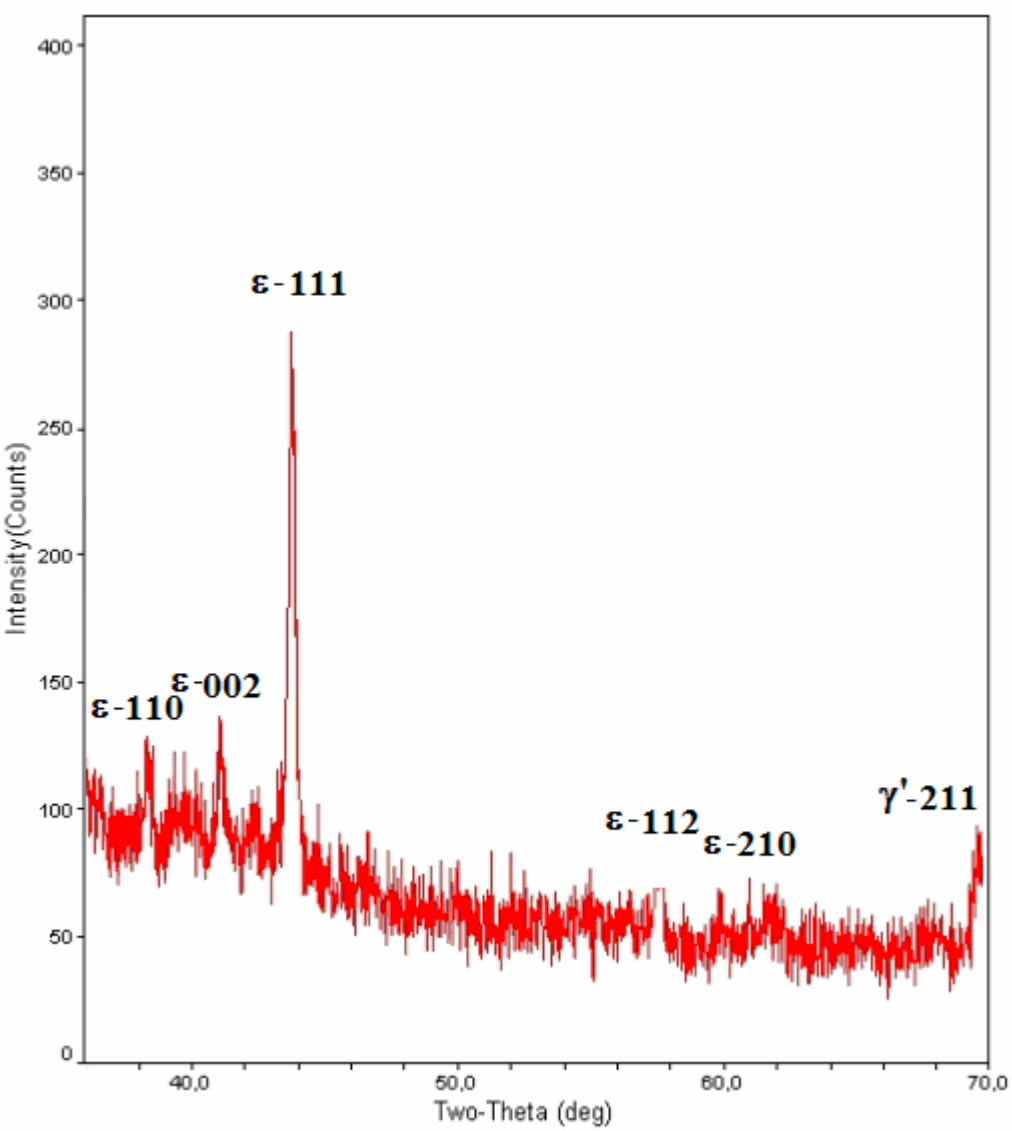

Figure 4.16. XRD analysis of specimen no17 (DIN 1.6523 nitrided in Type 2 bath at 590^{o}C for 0,5h)

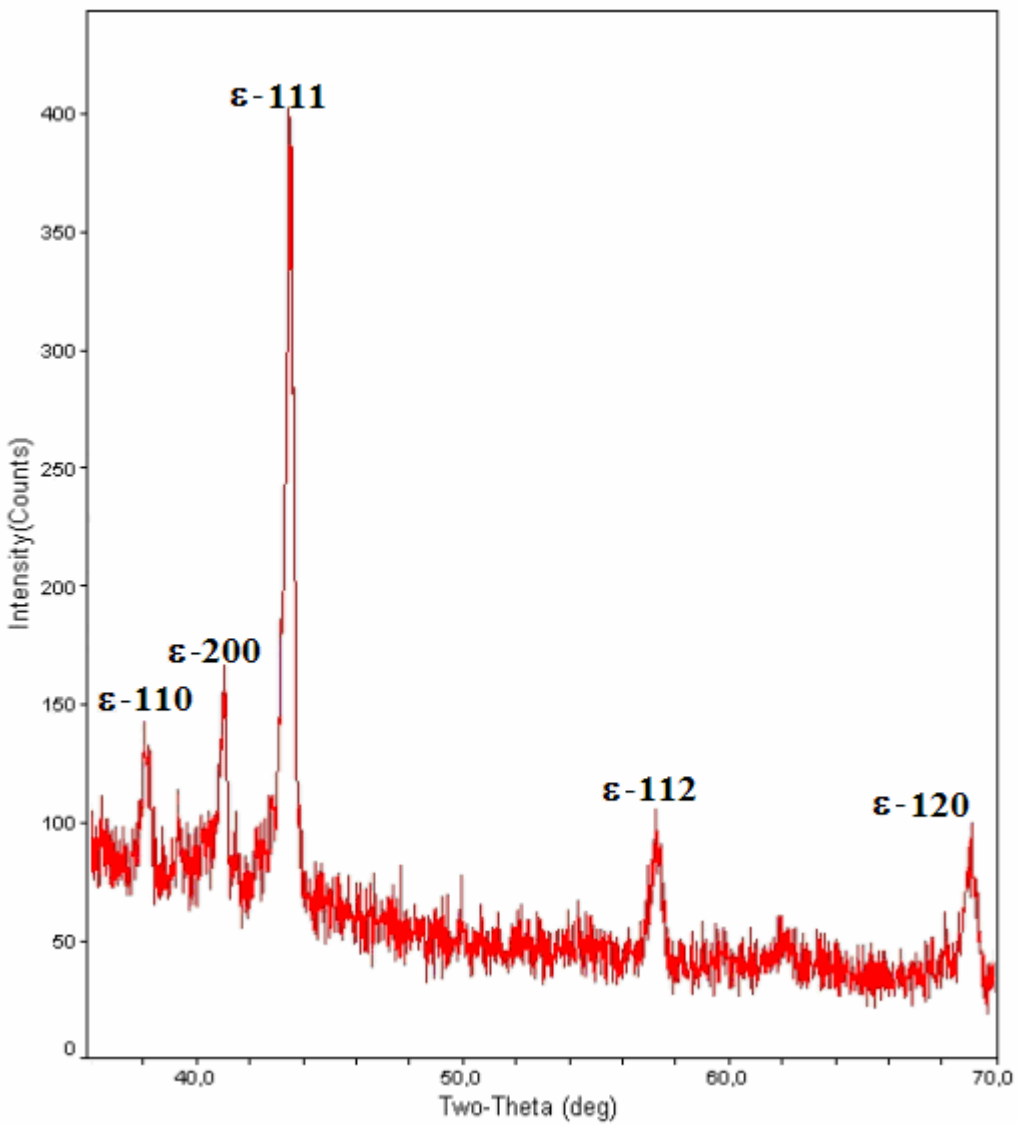

Figure 4.17. XRD analysis of specimen no 32 (DIN 1.6523 nitrided in Type 2 bath at 630^{o}C for 1,5h)

The obtained results from the XRD analysis suggest that depending on the process temperature and bath composition, the nitrided surface consists of both ε-nitride and γ'-nitride as a result of nitriding in ferritic zone. Nonetheless, the XRD results also show that the intensity of the ε-nitride phase increases as the temperature increase. Processing in austenitic phase field results in completely ε-nitride since more nitrogen diffuses into steel, so

completely ε-nitride phase (which is a high nitrogen content phase) forms [44]. This is completely in line with diffusion kinetics of nitrogen into the steel matrix.

4.1.2. Effects of Temperature on Nitriding

An increase in the nitriding process temperature results in an extended nitride case thickness. Figure 4.18 presents the effect of temperature on the nitriding case thickness. The presented specimens in this figure have been nitrided in Type 2 bath for 1h. It is clear that an increase in the process temperature brings about deeper nitriding case thicknesses. Additionally, increasing the process temperature results in a thicker compound layer formation (See Figure 4.19). The both are affected exponentially by the temperature. The Fick's law given in Section 2.1 clarifies that the diffusion depth is affected by diffusion coefficient (D) of an element (e.g.; nitrogen) in the matrix ($x \sim \sqrt{Dt}$; x: diffusion distance, t: time). As the diffusion coefficient is exponentially tied to temperature, an increased temperature raises the diffusion and hence the diffusion layer thickness, which also increases case thickness. This is the main reason for the sharp increase of nitriding case thickness from 590°C to 630°C. As explained above and in Section 2.1, diffusion coefficient depends on temperature. However, it changes from material to material due to different diffusion activation energies of nitrogen in selected alloys. Therefore, this explains the lower compound and nitriding case thickness of DIN 1.8550 ($D_{DIN\ 1.8850}$=298x10^{-14} m^2/s [47]) than those of DIN 1.7225 ($D_{DIN\ 1.7225}$=525x10^{-14} m^2/s [47]) and DIN 1.6523.

Optical microscopy photos given in Figure 4.20 clarify the effect of temperature in the micro scale. A temperature increase results in extended diffusion of nitrogen into the alloy and formation of nitrides in it. In Figure 4.20, it can be seen that there is a thin (82,68 μm) nitriding case developed on the surface of the specimen nitrided at 520°C. Nevertheless, Figure 4.20b shows that the nitriding case is thicker (121.4 μm) for the specimen nitrided at 590°C than that of the specimen nitrided at 520°C. Furthermore, Figure 4.20c displays significantly thicker (190.1 μm) nitriding case after nitriding process at 630°C; this value is more than twice that measured for the specimen nitrided at 520°C.

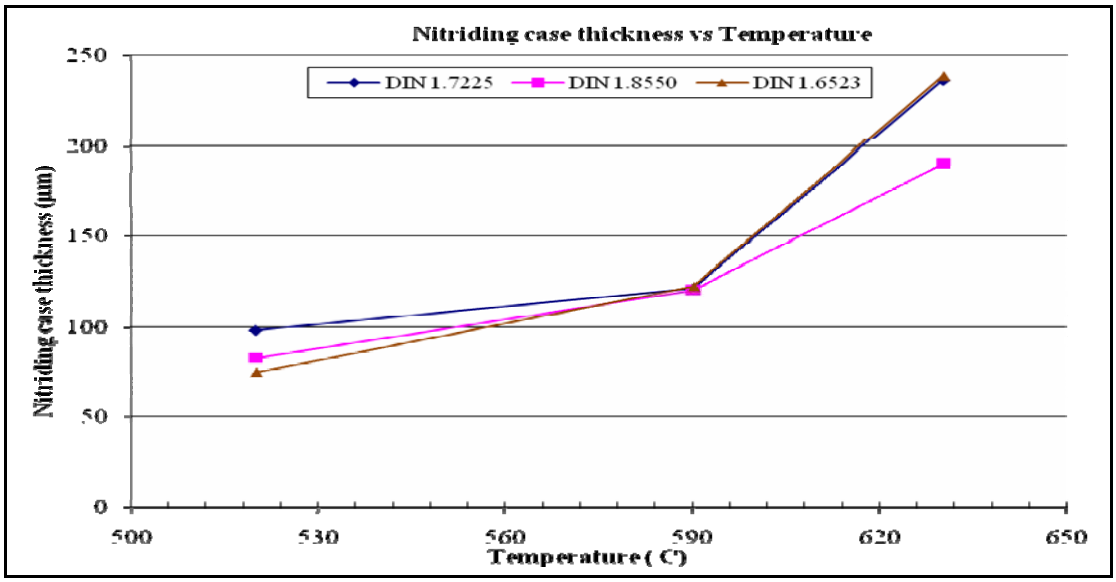

Figure 4.18. Nitriding case thickness of specimens nitrided in Type 2 bath at 520°C, 590°C, and 630°C for 1 h

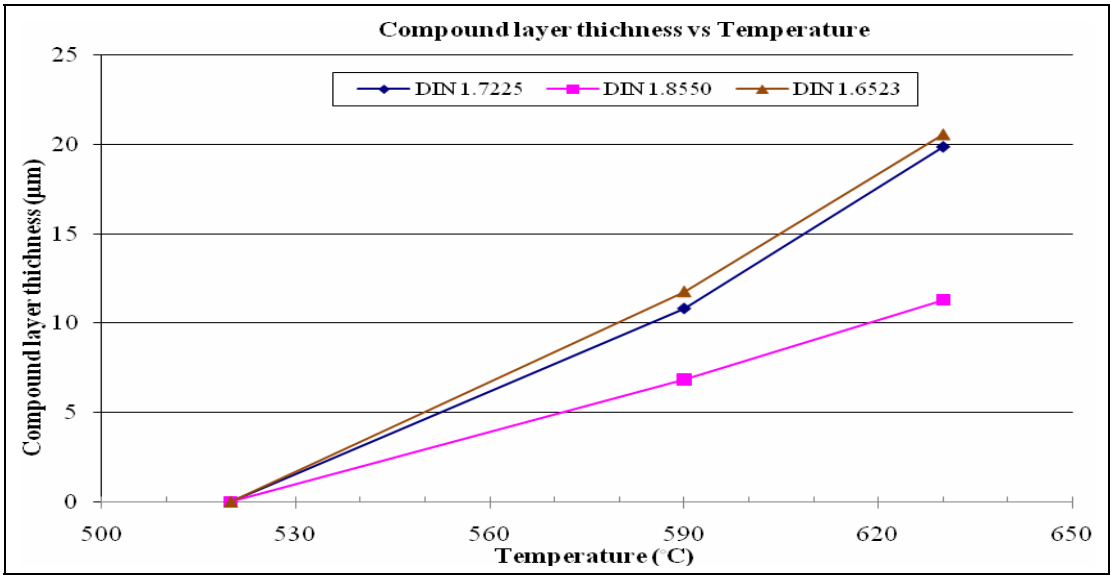

Figure 4.19. Compound layer thickness of specimens nitrided in Type 2 bath at 520°C, 590°C, and 630°C for 1 h

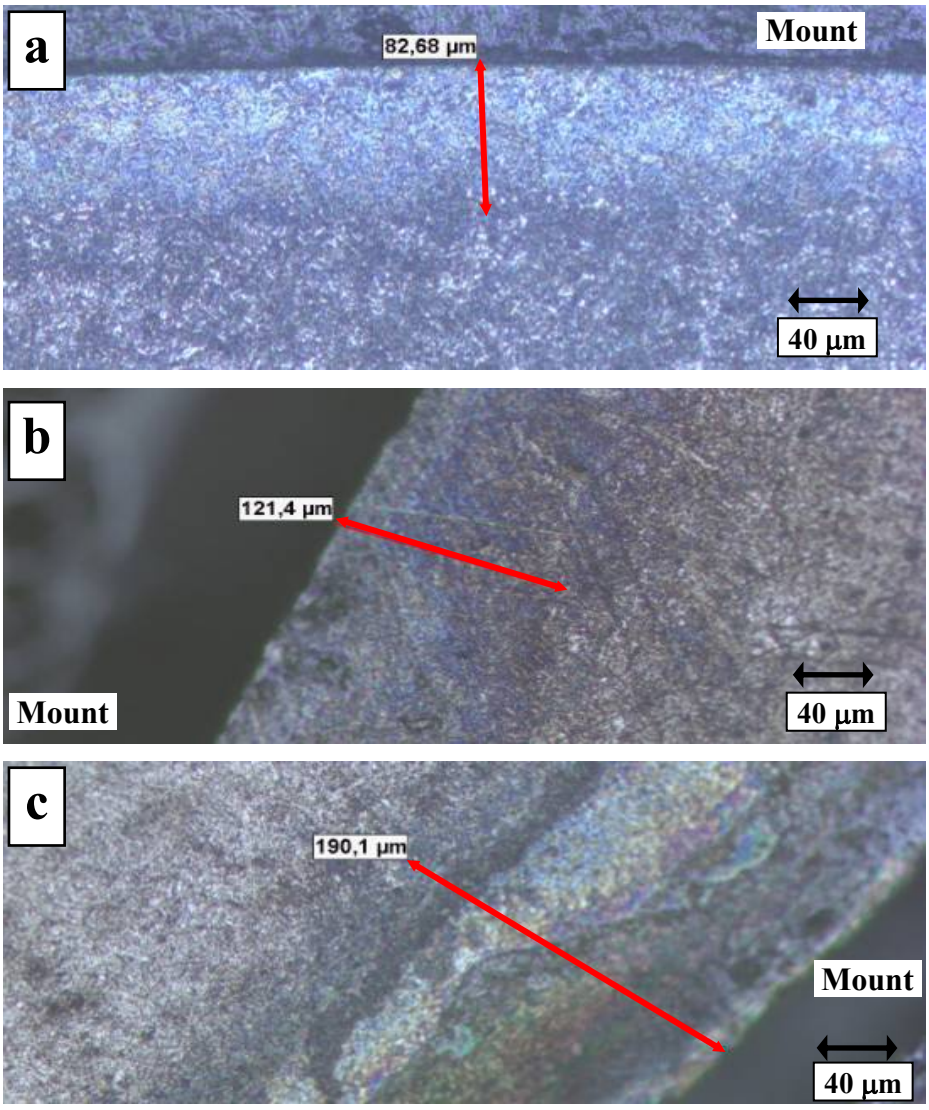

Figure 4.20. Nitriding case thickness of DIN 1.8550 specimens nitrided at various temperatures in Type 2 bath for 1 h – 200X. (a) Nitrided at 520°C. (b) Nitrided at 590°C. (c) Nitrided at 630°C

4.1.3. Effect of Time on Nitriding

As explained in Section 2.1, the Fick's Law also describes the effect of time on the nitriding. According to this law, diffusion of nitrogen is proportional to process duration. The examination of Figure 4.21 and 4.22 shows that diffusion depth increases in line with nitriding duration.

Although time is one of the major nitriding parameter, the nitride case formation depends on many factors. For instance, the diffusion depth of specimens nitrided in Type 2 bath (40 wt per cent KCNO) at 590°C for 2 h is less than those of nitrided in the same bath at 630°C for 1,5 h as expected. This conforms to the explanation in Section 4.1.2 that travel distance of the diffusing species depends exponentially on the temperature; however, it depends on the time as $t^{1/2}$. Similarly, the compound layer formation has analogous trend to diffusion depth; Figure 4.23 and Figure 4.24 have similar trends as in Figure 4.21 and Figure 4.22. This trend is additionally supported by the microphotographs as presented in Figure 4.25. The comparison of microstructures of the alloy DIN 1.6523 shows clearly that the diffusion depth and compound layer thickness have increased with the nitriding time since a longer nitriding time allows more of nitrogen to diffuse into the alloy.

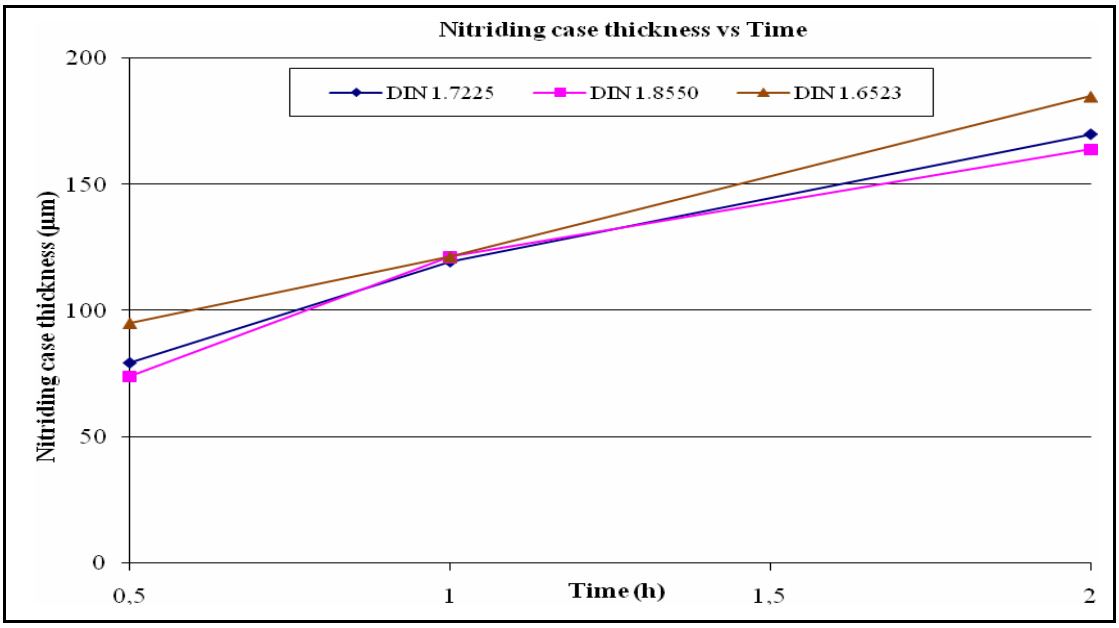

Figure 4.21. Nitriding case thickness of specimens nitrided in Type 2 bath at 590°C for 0,5h, 1h, and 2h

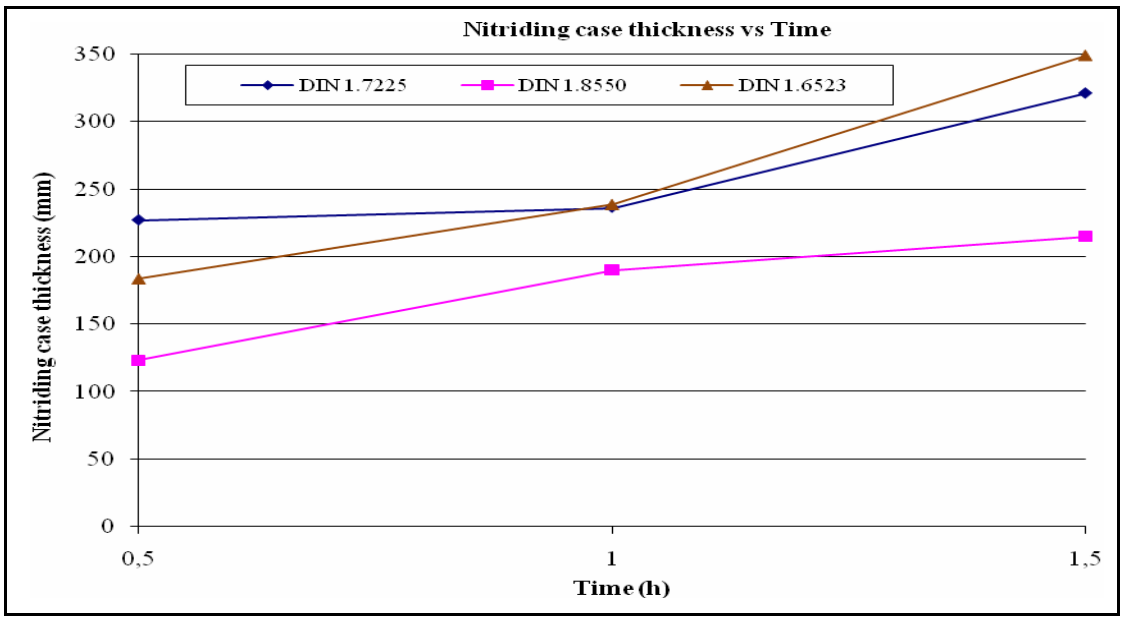

Figure 4.22. Nitriding case thickness of specimens nitrided in Type 2 bath at 630°C for 0,5h, 1h, and 1,5h

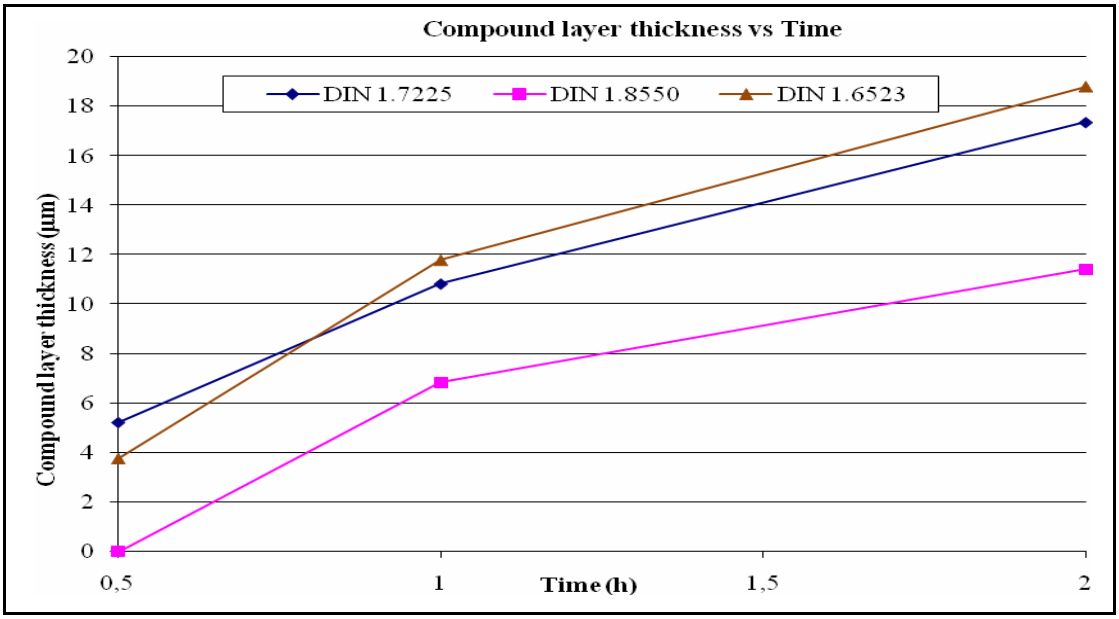

Figure 4.23. Compound layer thickness of specimens nitrided in Type 2 bath at 590°C for 0,5h, 1h, and 2h

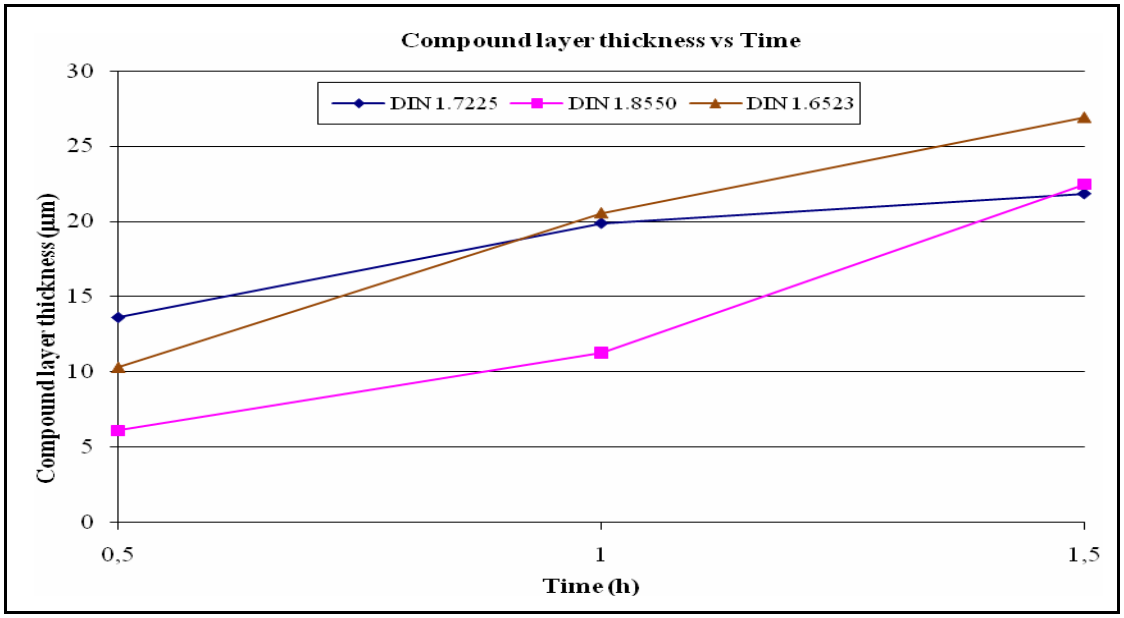

Figure 4.24. Compound layer thickness of specimens nitrided in Type 2 bath at 630°C for 0,5h, 1h, and 1,5h

4.1.4. Effects of Bath Composition

During the trials, two different bath compositions have been used. The first bath (80 wt per cent potassium cyanate) contains higher amount of potassium cyanate than the second bath (40 wt per cent potassium cyanate). It is also described in Section 2.4.1 that cyanate content is responsible for nitriding process. A high cyanate content gives rise to diffusion of more nitrogen through the surface and forms nitrides. For this reason, higher surface hardness, greater hardness depth, and thicker nitriding cases are possible in this type of bath.

Figure 4.26 and Figure 4.27 present the nitriding case and compound layer thickness obtained in these two bath combinations. Specimens nitrided in Type 1 bath at 570°C for 1h and specimens nitrided in Type 2 bath at 590°C for 1h have been selected to show the effect of bath composition. Thus, the comparison of nitriding case thickness resulting from nitriding shows clearly that the nitriding case thickness in specimens nitrided in Type 1 bath is considerably higher than those nitrided in Type 2 bath, even though the bath temperature is lower in Type 1. This indicates the positive effect of high cyanate content on nitrogen

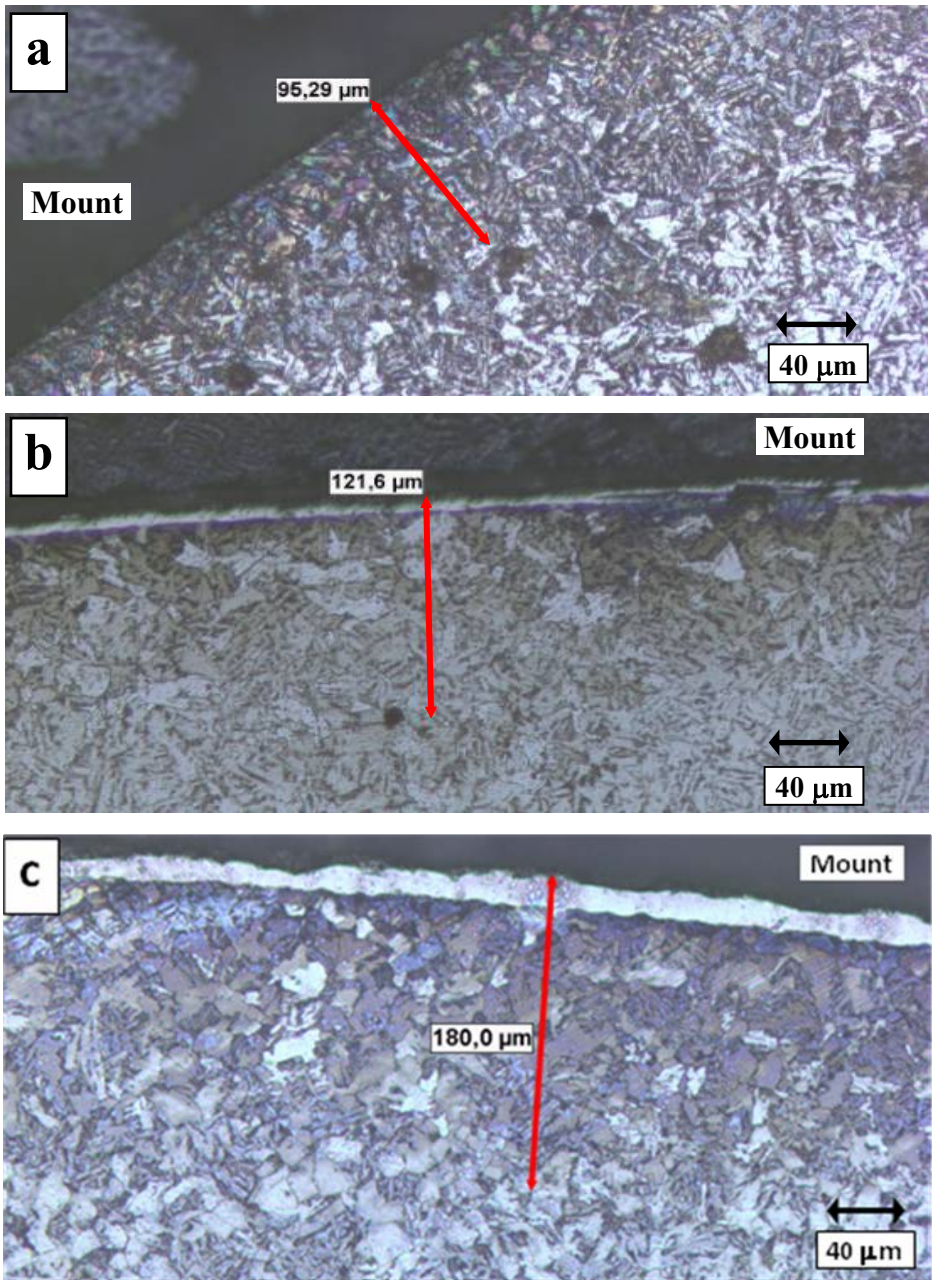

Figure 4.25. Nitriding case thickness of DIN 1.6523 specimens nitrided in Type 2 bath at 590°C for various duration – 200X. (a) Nitrided for 0,5h. (b) Nitrided for 1h. (c) Nitrided for 2h.

diffusion into a deeper region in the core material. The reason for different diffusion rates is the difference in the cyanate contents of the baths; in Type 1 bath, there is more cyanate

content and this enriches the surface concentration to a higher value and sets a higher concentration gradient. Thus, more nitrogen diffuses towards the core of the alloy in this bath. Spies et al. [48] have studied the effects of nitriding potential in their study and presented that the increase of the nitriding potential increases thickness of the layer of chemical compounds (compound layer and diffusion layer) as found in this research.

Figures 4.25 and 4.26 also show the differences of compound layer and nitriding case thicknesses for DIN 1.8550, DIN 1.7225, and DIN 1.6523. The reason for this difference comes from the differences in the diffusion coefficients of nitrogen in these specimens. The measurement results are in line with expectations. The specimens (DIN 1.7225 and DIN 1.6523) having higher diffusion constant (See Section 4.1.5) bring about thicker nitriding cases after nitriding operation.

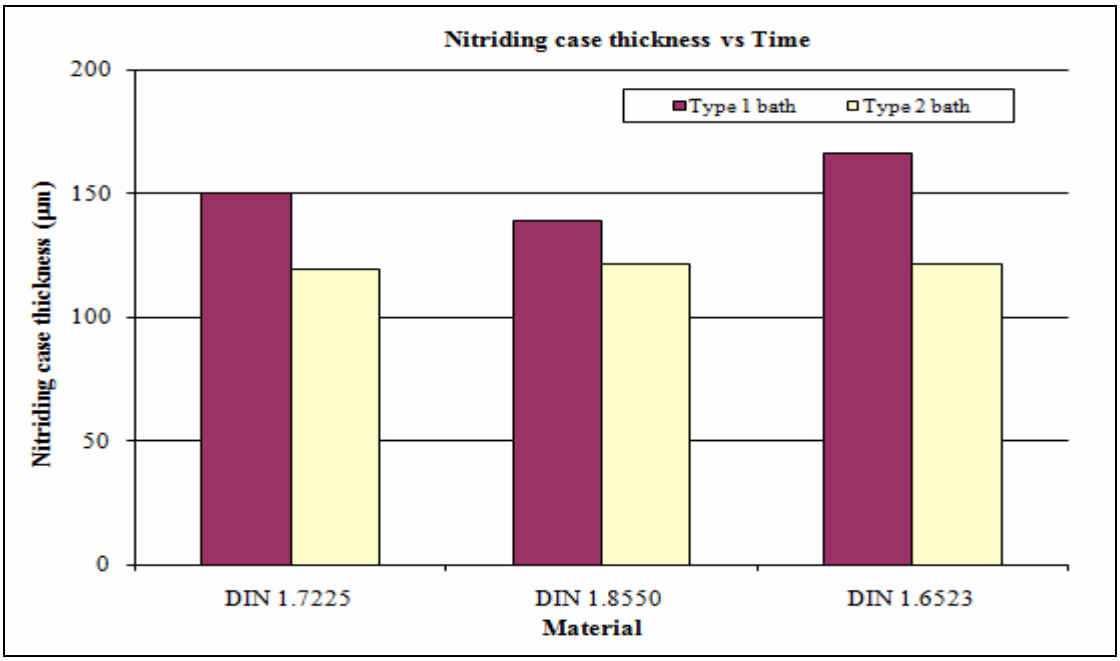

Figure 4.26. Nitriding case thickness of the alloys in the two baths. Specimens nitrided in Type 1 bath at 570^{o}C for 1h and in Type 2 bath at 590^{o}C for 1h.

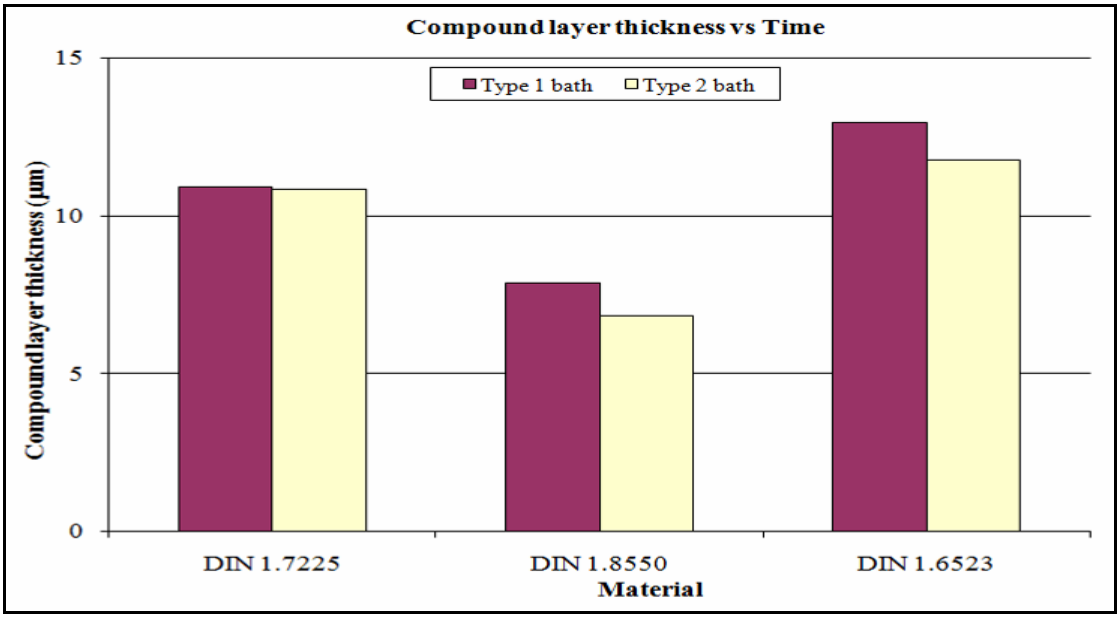

Figure 4.27. Compound layer thickness of the alloys in the two baths. Specimens nitrided in Type 1 bath at 570°C for 1h and in Type 2 bath at 590°C for 1h.

Figure 4.28 shows an SEM microphotograph of specimen no 5 which is nitrided in Type 1 bath. The compound layer thickness was measured as 13 µm on the microphotographs taken both by the light microscope and SEM. The EDS analysis shows that near the surface of this specimen, nitrogen content reaches up to 8,23 wt per cent. The repeated measurements show that the nitrogen content decreases towards the core smoothly (See Figure 4.29). Although, this specimen has been nitrided in Type 1 bath at 570°C for 1h, a high amount of nitrogen can diffuse into the material. Moreover, the comparison of the EDS analyses given in Figures 4.10 and 4.29 shows that the diffused nitrogen amounts in specimens no 5 and 33 are similar, even though the process temperature of specimen no 5 (570°C) is less than that of specimen no 33 (630°C). This indicates the role of cyanate content in the bath.

Additionally, comparison of the compound layer thicknesses as given in Figure 4.27 clarifies that Type 1 forms slightly thicker compound layer than Type 2.

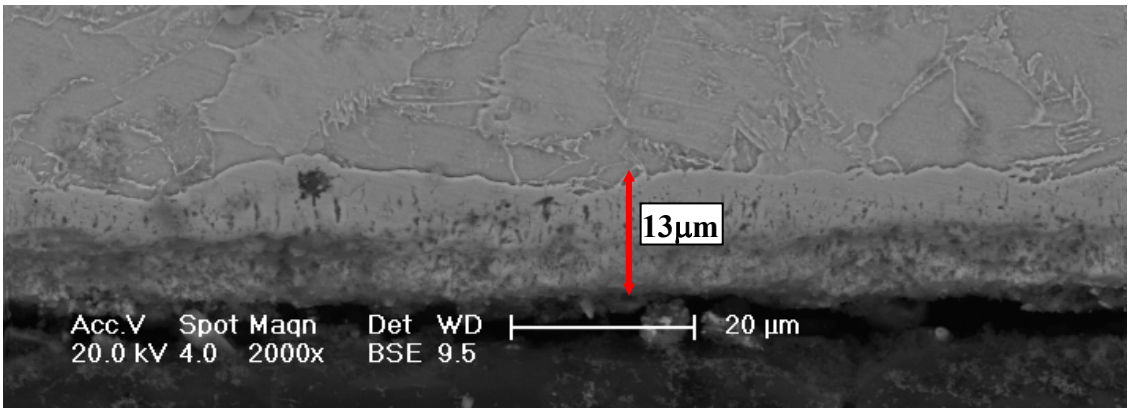

Figure 4.28. An SEM view of specimen no 5 having 13 µm compound layer. (DIN 1.6523 nitrided in Type 1 bath at 570°C for 1h)

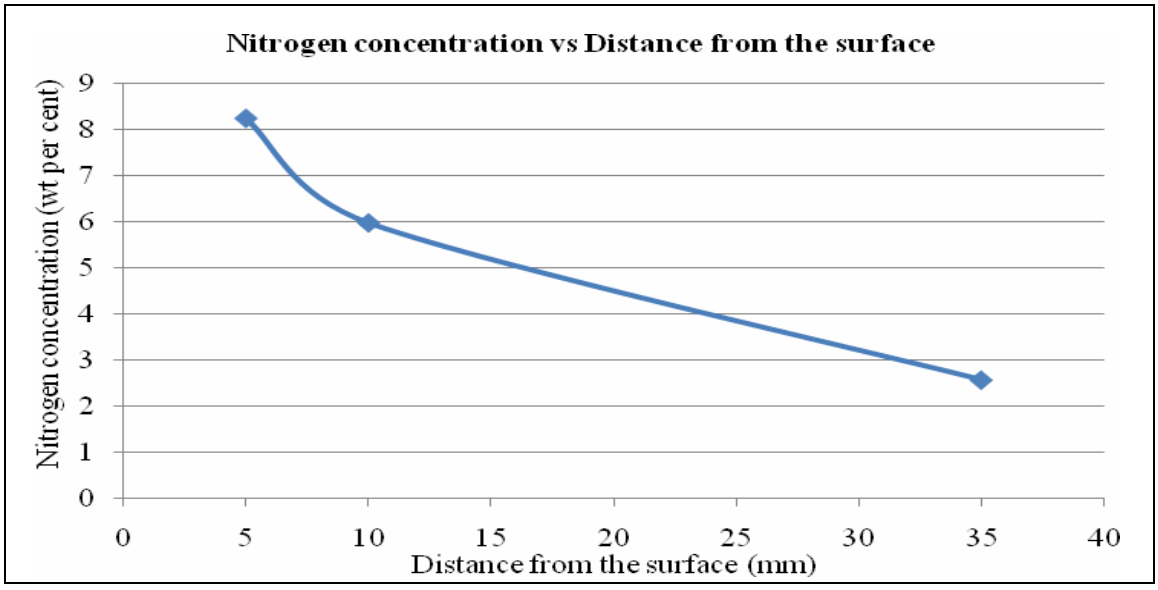

Figure 4.29. Nitrogen concentration changes towards the core of specimen no 5 (DIN 1.6523 nitrided in Type 1 bath at 570°C for 1h)

4.1.5. Effect of Elements in Steel

It is a known fact that aluminum and chromium individually increase surface hardness capability during nitriding process of steel whereas nickel alone keeps hardness on a stable

trend as shown in Figure 2.9. On the other hand, nickel with chromium and aluminum allows excellent surface hardness to be obtained [27]. However, these three elements together reduce nitriding case thickness as expected since they reduce diffusivity of nitrogen in the base alloy. The specimen no 28 (DIN 1.7225) and 30 (DIN 1.8550) show the combined effect of chromium, nickel, and aluminum content on the hardness and nitriding case thickness (DIN 1.7225 does not have Ni and Al while DIN 1.8550 does). Evaluation of the hardness measurements (See Table 4.2) show that the surface hardness of specimen no 30 is 949 $HV_{0,1}$ and that of specimen no 28 is 861 HV0,1. Obviously, alloying elements increase the hardness capability of specimen no 30, which possesses a lower core hardness than that of specimen no 28 (See Table 3.1). Conversely, compound layer and nitriding case thickness analyses explain the adverse effects of these nitride formers (Ni, Al, and Cr) on diffusion (See Figures 4.21, 4.22, 4.23, and 4.24). Spies et al. [48] have pointed out that an increase in the chromium content decreases the diffusion layer thickness excessively. Furthermore, they have showed that the aluminum content has similar effects as chromium. Therefore, this explains the reason for thinner compound layer and nitriding case formation in DIN 1.8550 alloy than those in the other alloys. Additionally, diffusion coefficient of nitrogen in DIN 1.8550 is less than that for DIN 1.7225 as already given in Section 4.1.2.

Effect of carbon and nickel can be seen by comparing DIN 1.7225 (0,41 wt per cent C) and DIN 1.6523 (0,19 wt per cent C). As Karaoglu [49] has explained the carbon amount in the material affects the hardness, hardness depth, and diffusion depth. In high carbon cases, carbon combines with the alloying elements as carbide, so this limits the number and amount of elements to form nitrides. Thus, hardness of the material decreases. Additionally, more carbon atoms make nitrogen diffusion harder and hence hardness depth and nitriding case thickness reduce. The analyses of Figures 4.18 and 4.19 show that DIN 1.7225 and DIN 1.6523 have nearly same compound layer and nitriding case thickness trends within the temperature range of the experiments for 1 h of nitriding. On the other hand, slightly lower compound layer thicknesses are observed for DIN 1.7225 especially for higher treatment temperatures. In fact, the reason for this slight difference is explained by Leppänen et al. [50]; they have indicated that carbon content is the major factor for diffusion and the diffusion

coefficient for low carbon alloys is higher than that for high carbon alloys as implied in Figures 4.21 and 4.22.

In contrast to the diffusion, if the hardness is concerned (See Table 4.2), DIN 1.7225 (Specimens no 13, 16, 25, 28, and 31) alloys has higher hardness than that of DIN 1.6523 (Specimens no 14, 17, 26, 29, and 32) as expected due to high chromium composition.

The comparison of DIN 1.6523 and DIN 1.8550 gives the effect of aluminum, chromium, and carbon elements. High chromium content and other alloying elements in DIN 1.8550 prevent nitrogen diffusion into deeper zones [51]. Thus, diffusion depth of DIN 1.8550 is less than that of DIN 1.6523 in all application conditions. The nitriding case thickness measurements as given in Table 4.1 is in line with this finding especially at the high temperature nitriding application. This can be explained by dependence of the diffusion coefficient on temperature and concentration as stated in Section 2.1. However, the microhardness measurements show that generally hardness of DIN 1.8550 alloys are found to be higher than that of DIN 1.6523 and this is a result of high chromium and aluminum content of DIN 1.8550 alloys as explained above.

4.1.6. Change in Surface Roughness

A stylus profilometer has been used to measure the change in the surface roughness caused by nitriding. The measurement results show that after nitriding, the average roughness value (R_a) has increased. The degree of increase in surface roughness varied with material types. In the case of Type 2 bath nitriding, the average surface roughness of DIN 1.6523 (specimen no 5) steel has increased 10 per cent from 0,7 μm to approximately 0,77 μm, the average surface roughness of DIN 1.7225 (specimen no 4) steel increased 50 per cent from 0,52 μm to approximately 0,78 μm, and average surface roughness of DIN 1.8550 (specimen no 6) steel has increased 30 per cent from 0,56 μm to 0,73 μm. The reason for the different initial surface roughness of unnitrided specimens comes from the difference on the hardness of specimens; harder specimens are machined easily and smoothly. However, after the nitriding

process, a similar surface roughness value has been measured for the three alloys due to the property of the compound layer. As Totten [34] discussed in detail, the reason for high surface roughness after nitriding is nonuniform nucleation and growth of nitride grains in the compound layer. The compound layer thickness as determined by light microscopy show that specimen no 4, 5, and 6 have around 10 μm thick compound layer. Therefore, the surface roughness of specimens after nitriding is similar as expected.

4.2. Microhardness Studies

Microhardness measurements have been performed to identify the hardness and hardness depth profile of nitrided specimens. Besides the nitrided specimens, unnitrided specimens' microhardness values have been also measured and given in Table 3.1 and Table 4.2.

Selected hardness data is plotted in Figures 4.30 – 4.32. Comparison of these figures makes clearly visible the effect of nitriding on hardness. Presence of high chromium and other nitride forming elements brings about high amount of strong nitride phases. On account of high affinity between nitrogen and other alloying elements, nitrogen-rich nitride phases form which hinder further nitrogen diffusion into the core. This immobilization of nitrogen gives rise to only a thin nitriding case formation [51].

As a result of nitriding in Bath Type 2 at 630^{o}C for 1,5 h, measured surface hardness values have increased more than three times for all nitrided specimens with respect to core hardness values of unnitrided specimen given in Table 3.1. Maximum surface hardness of DIN 1.7225 has been measured to be around 1000 $HV_{0,1.}$ Furthermore, the surface hardness of DIN 1.8550 and DIN 1.6523 have reached around 1300 $HV_{0,1}$ and 969 $HV_{0.1}$, respectively. However, the results suggest that the maximum hardness in DIN 1.6523 has been found below the surface of the specimen in contrast to the other alloys (See Figure 4.30). As indicated by Krishmaraj et al. [44] and Schneider et al. [45], the main reason for the increased hardness in DIN 1.6523 alloy is the transformed austenite that exists in the microstructure due to high

nitriding process temperature as explained in Section 4.1.1.1. Hardness profile of this specimen shows a sudden decrease after the peak in the transformed austenite phase field towards the core material. The hardness change in the transformed austenite field is related with the mixture of the precipitation-hardened ferrite and transformed austenite [45].

Table 4.2. Microhardness values (HV0.1) of selected specimens

		Distance from the surface (μm)							
		10	20	50	100	150	200	300	400
Specimen	5	811	713	527	439	250			
	13	653	602	523	434	300			
	14	530	443	402	329	252			
	16	726	643	418	300				
	17	702	417	351	185				
	18	639	543	439	268				
	25	816	795	716	589	464	332	300	
	26	759	714	640	375	214	185		
	27	804	645	531	330	268			
	28	861	651	579	530	495	471	300	
	29	846	681	605	533	408	263	185	
	30	949	769	700	613	362	268		
	31	1023	954	897	747	583	509	348	300
	32	969	1178	746	650	528	484	363	185
	33	1300	1241	812	679	501	368	268	

The optical microscopy observations have not shown any transformed austenite inside the DIN 1.8550 specimens, since Schneider et al. [45] have identified that the eutectoid temperature for DIN 1.8550 alloy is between 640-650^{o}C. However, the hardness decreases sharply towards the core of the material as seen in Figure 4.31. The sharp decrease results from relatively thin nitriding case after nitriding process. The low diffusion coefficient and

high amount of chromium and aluminum which are strong nitride formers prevent nitrogen from diffusing towards the core of the specimen. Therefore, the hardness falls down sharply. On the contrary, DIN 1.7225 specimen has a gradual decrease from maximum hardness to the core hardness as shown in Figure 4.32. This gradual decrease is caused by the thicker compound layer and nitriding case thickness since diffusion coefficient of DIN 1.7225 alloys is quite higher than that of DIN 1.8550 alloys. Therefore, more nitrogen diffuses into the material and more nitrides can form in deeper locations.

In contrast to the high hardness values of specimens nitrided at the high temperature (630^{o}C), the hardness values of specimens nitrided at the low temperatures are relatively lower. During the evaluation of the measured data, it is found that the maximum hardness of the specimens depend on the nitriding temperature and nitriding duration. Especially, the hardness values of specimens nitrided for 0,5 h at various temperatures have been found to be around 600 $HV_{0,1}$ which is comparably low. However, the increase of hardness even in these specimens is more than twice compared to the hardness of the unnitrided specimens.

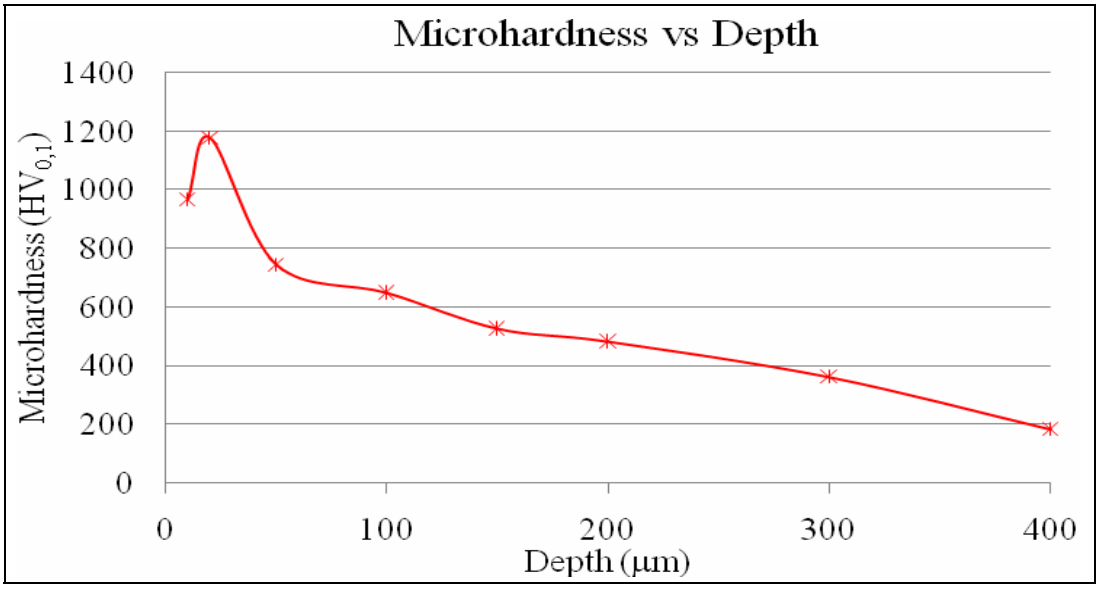

Figure 4.30. Microhardness profile of specimen no 32 (DIN 1.6523, nitrided in Type 2 bath at 630^{o}C for 1,5h)

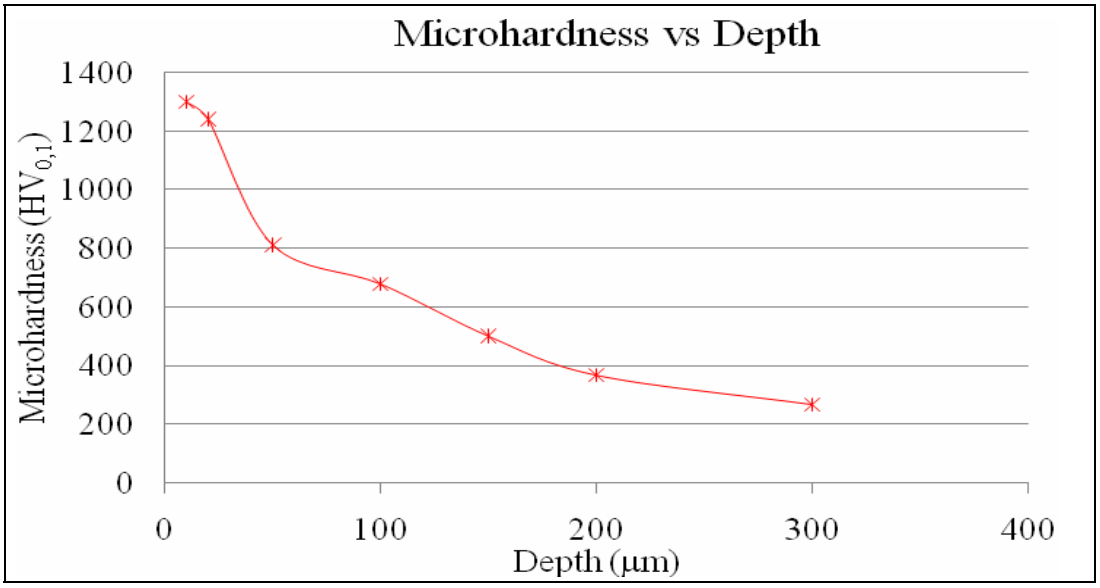

Figure 4.31. Microhardness profile of specimen no 33 (DIN 1.8550, nitrided in Type 2 bath at 630°C for 1,5h)

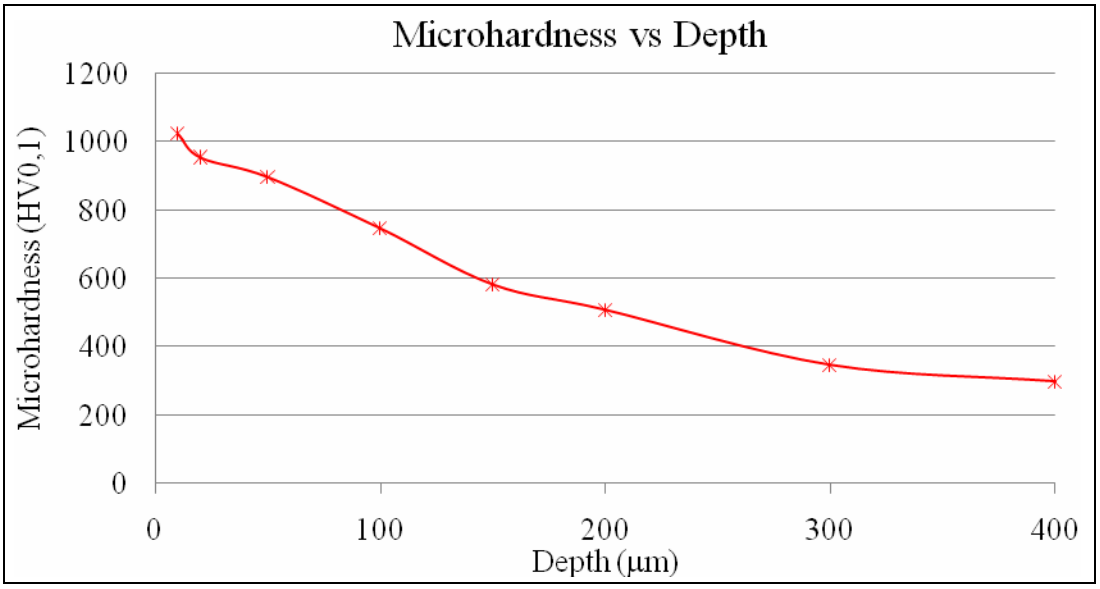

Figure 4.32. Microhardness profile of specimen no 31 (DIN 1.7225, nitrided in Type 2 bath at 630°C for 1,5h)

4.3. Pin-on-Disc Wear Test Results

The pin and disc specimens have been investigated by an optical microscope to understand the wear mechanism (See Figures 4.33, 4.34, and 4.36). The evaluation of these figures shows that there are signs for abrasive and adhesive wear modes on the pin and disc pairs. Figure 4.33 shows the worn surfaces of the specimen no 32 (DIN 1.6523) possessing the highest compound layer thickness as well as the largest nitriding case. Due to the nitrogen diffusion and nitride formation, surface hardness of this specimen (969 $HV_{0.1}$) is excessively higher than that of the disc material (263 $HV_{0.1}$). Therefore, as it is expected, wear is mainly on the disc. From Figure 4.33d, it can be seen that main wear type is abrasion and the channel formations on the disc result from the breakage of hard and brittle compound layer particles. This is in line with the study performed by Karamış and Gerçekçioğlu [52] in which they explain that compound layer breaks down at the early stage of the wear test and this causes an increased material loss. Additionally, Podgornik et al. [53] agree with this opinion; they have found that the thick compound layer breaks down during sliding contact and the broken parts act as abrasive particles between the sliding surfaces, so excessive wear is observed in the contact area.

Microstructure analysis of specimen no 12 (DIN 1.8550, nitrided in Type 2 bath for 1h at 520^{o}C) shows that it has nearly no compound layer on the surface of the specimen after nitriding. Hence, it is assumed that the disc material is in contact with the diffusion layer of the pin directly. In this direct contact, as seen in Figure 4.34, the wear type is adhesion on the disc. The SEM photo (see Figures 4.36) and EDS analysis indicate that the material has been transferred from the pin to the disc since some amount of nitrogen (2,13 wt per cent) has been found on the adhesive wear zone on the disc, and this nitrogen basically should come from the worn nitriding case of the pin. Although the main wear type is adhesion, from Figure 4.34, the abrasive wear marks can be seen on the disc and pin specimens. The abrasive wear forms due to the loose worn material behaving as particles between the contact surfaces, which results in abrasive wear on the disc and pin specimens.

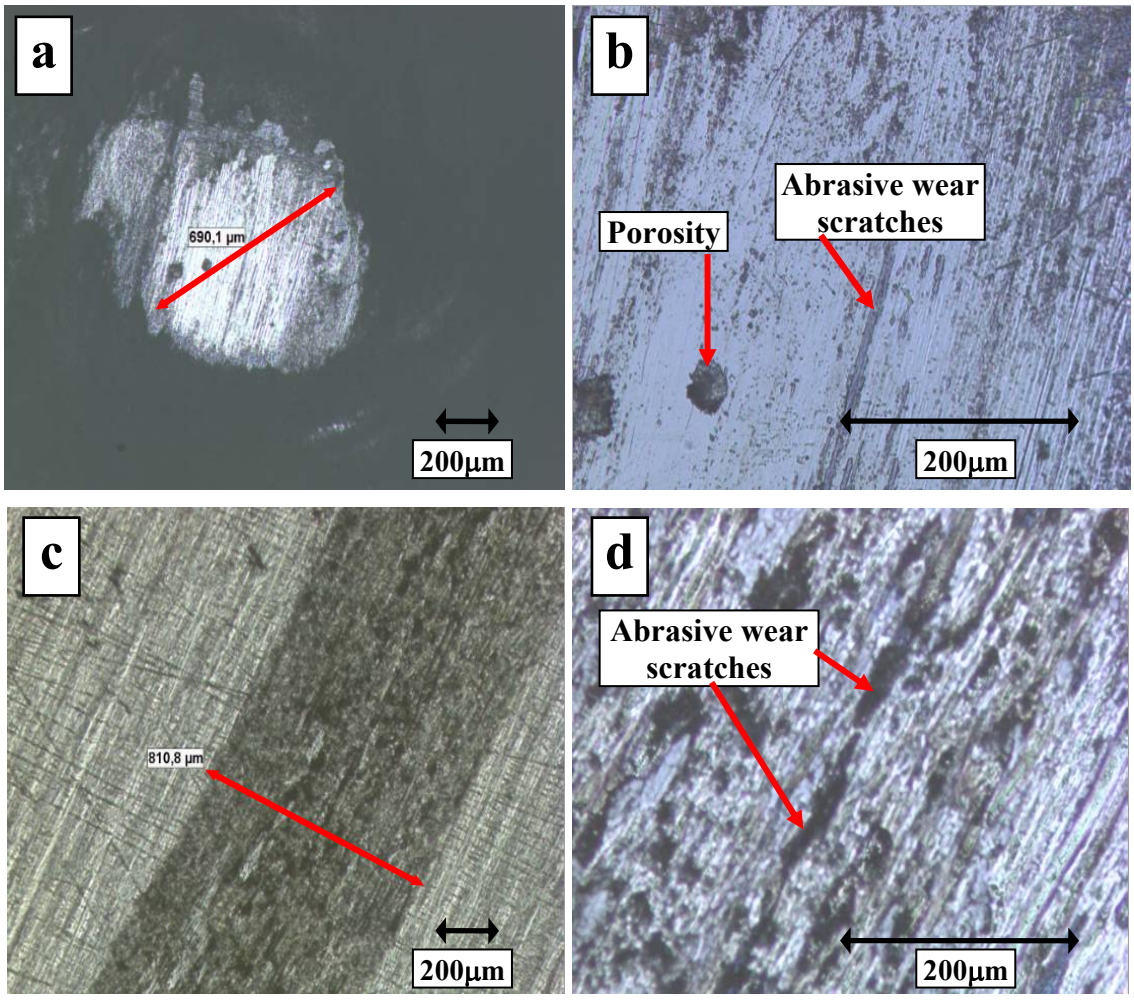

Figure 4.33. Photographs taken after wear test of specimen no 32 (DIN 1.6523, nitrided in Type 2 bath for 1,5h at 630°C) (a) Wear scar diameter of the pin – 50X. (b) Abrasive wear scratches and porosity on the pin – 200X. (c) Track width on the disc – 50X. (d) Abrasive wear marks on the disc – 200X

Comparison of Figure 4.33 and Figure 4.34 clearly shows that the disc pair of specimen no 32 with a thick compound layer on it gets worn more than that of specimen no 12 without compound layer. This demonstrates that the wear resistance of the specimen is increased with thick compound layer due to high surface hardness.

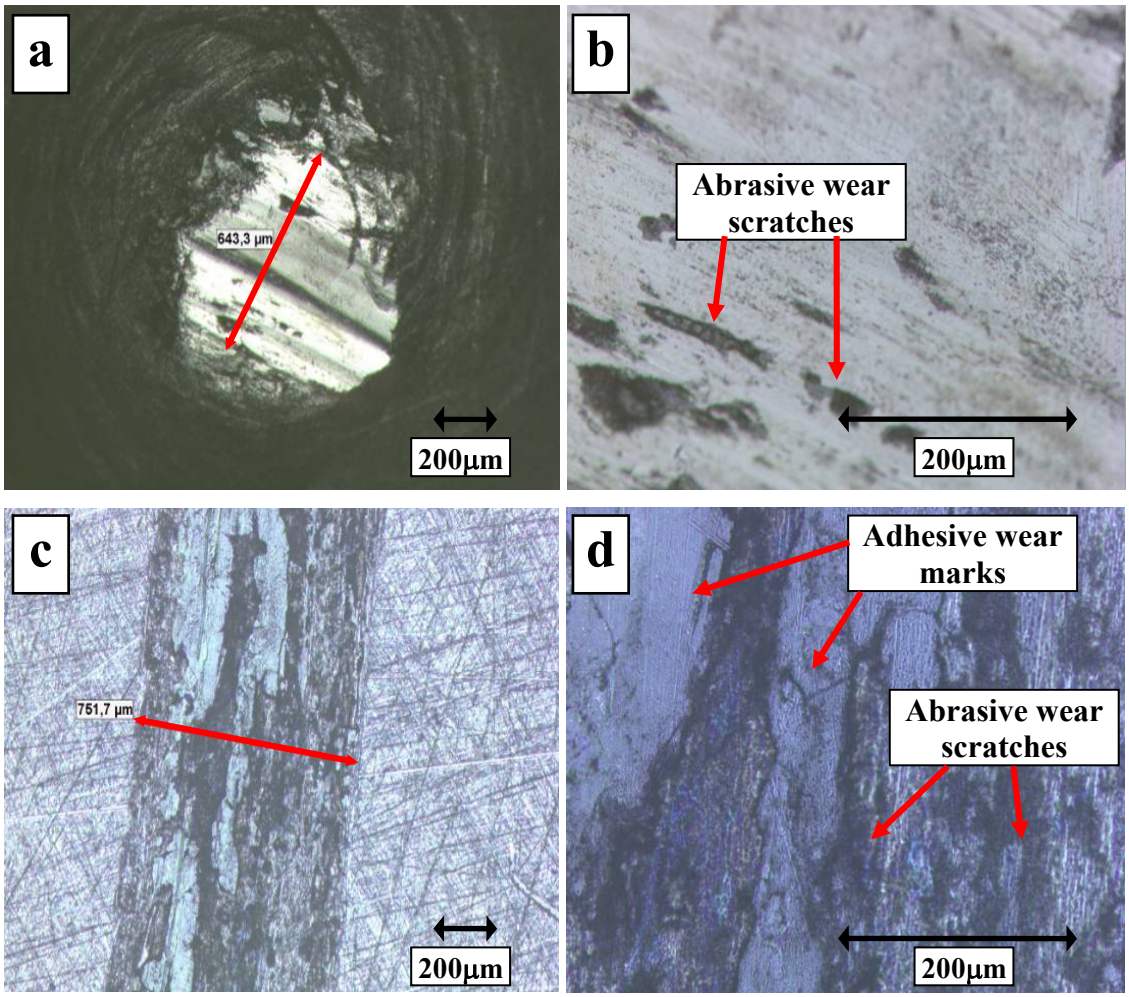

Figure 4.34. Photographs taken after wear test of specimen no 12 (DIN 1.8550, nitrided in Type 2 bath for 1h at 520°C) (a) Wear scar diameter of the pin – 50X. (b) Abrasive wear scratches on the pin – 200X. (c) Track width on the disc – 50X. (d) Abrasive and adhesive wear marks on the disc – 200X

Figure 4.36 shows surfaces of unnitrided DIN 1.6523 alloy and corresponding disc after wear test. This steel (185 $HV_{0.1}$) is relatively softer than the disc (263 $HV_{0.1}$) and as expected, wear is mainly on the pin material. Thus, the scar width on the disc is nearly half that of the other specimens tested in this study. In this case, pin wears very rapidly and the wear type is clearly abrasion on the pin. Abrasive wear scratches on the pin are seen in Figure 4.36b. The pin scar diameter is 1150µm. However, the disc scar diameter is 451 µm in this particular

pair. In contrast to expectations, the scar diameters do not match. The reason for this mismatch is thought to be a misalignment of the pin and disc before the wear test during assembling the pin and disc pair.

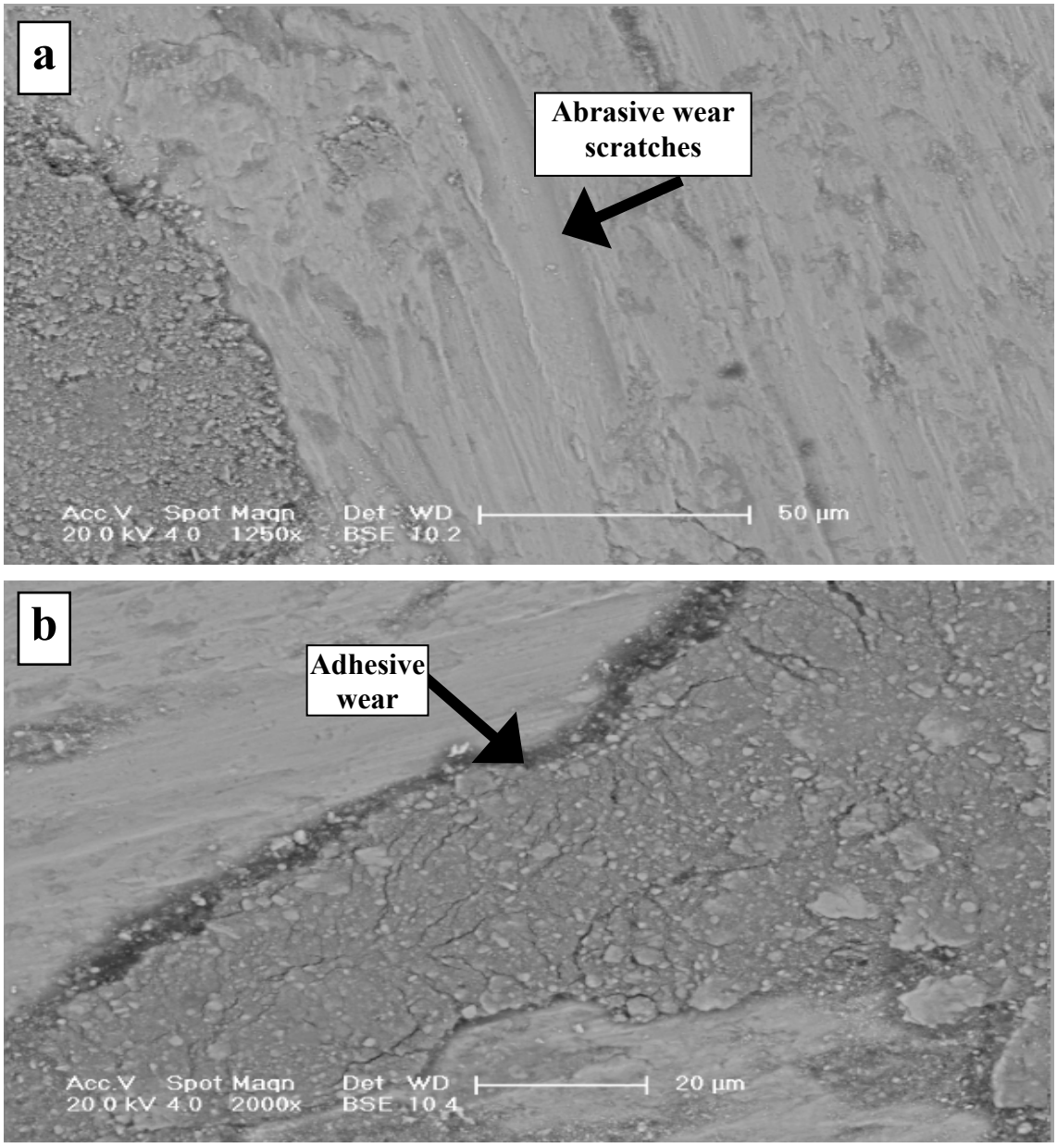

Figure 4.35. SEM photos of specimen no 12 disc pair. (a) 1250X magnification of worn zone of disc. Adhesive and abrasive wear failures on the surface are identified. (b) Close-up view of adhesive wear zone - 2000X magnification

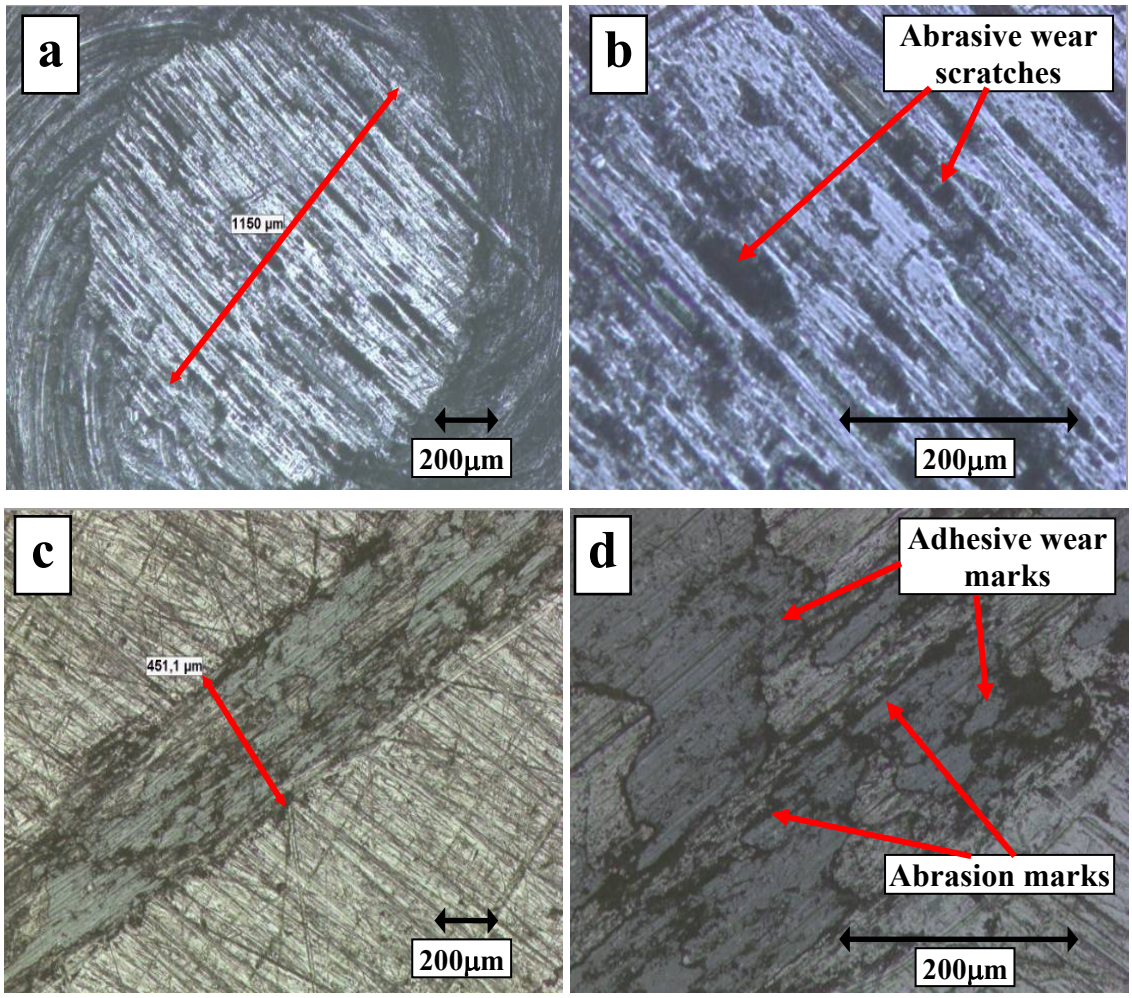

Figure 4.36. Photographs taken after wear test of unnitrided DIN 1.6523 alloy (a) Wear scar diameter of the pin – 50X. (b) Adhesive wear scratches – 200X. (c) Track width on the disc – 50X. (d) Abrasive and adhesive wear marks on the disc – 200X

Besides microscopic analysis, volumetric losses due to wear have been also calculated to judge the wear performance of the nitrided specimens. The volumetric loss on the pins is considerably lower than that on the discs. Additionally, before and after wear test measurements show that the weight reduction in the pin materials is around 0,001g except for the pins which have adhesion type wear and are unnitrided. (The mass loss has been recorded around 0,004 or 0,005 g in adhesion type wear, and around 0,012g in unnitrided pins.) Therefore, volumetric loss in pins is neglected during calculation and comparison. The

volumetric loss in the disc has been calculated according to the formula given by Equation 3.2 (See Section 3.5). Figures 4.37 and 4.38 show the relationship between the disc volume loss and compound layer and nitriding case thickness, respectively.

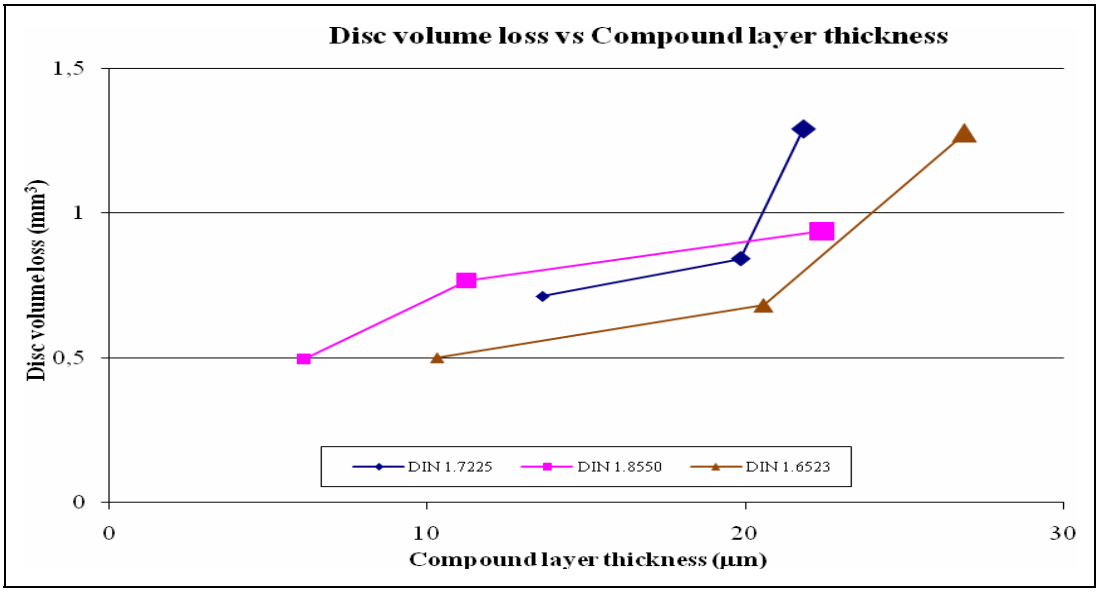

Figure 4.37. Effect of the compound layer thickness on the disc volume loss (Specimens nitrided in Type 2 bath at 630°C for 0.5h, 1h, and 1,5h) (Note: The growing legend symbols indicate increasing nitriding duration)

It is inferred from Figure 4.37 (Specimens nitrided in Type 2 bath at 630°C for 0,5 h, 1 h, and 1,5 h) that the increase in the compound layer thickness results in an increase ,n the disc volume loss as expected. The nitriding case thickness and hardness measurements of these samples show that these specimens have high surface hardness and thick nitriding case thicknesses than those nitrided under different conditions. Therefore, the high surface hardness results in higher wear resistance and high volume loss on the discs.

Conversely, Figure 4.38 shows that increasing nitriding case gives reduced wear on the disc material. (These specimens have been nitrided at 520°C and there is hardly any compound layer on the surface of these specimens.) Disc volume loss is considerably lower than the previous case shown in Figure 4.37. Additionally, the increase of nitriding duration has not

improved the wear resistance of the pins. As indicated previously, the main wear type on these pins is adhesion. The main reason for the unsatisfactory wear performance of these specimens is the shortage of the interstitial nitrogen in the matrix due to the low nitriding temperature. The absence of the nitrogen prevents the formation of an enough compressive stress on the surface and surface hardness of these samples cannot reach required levels which decrease the wear resistance of these specimens.

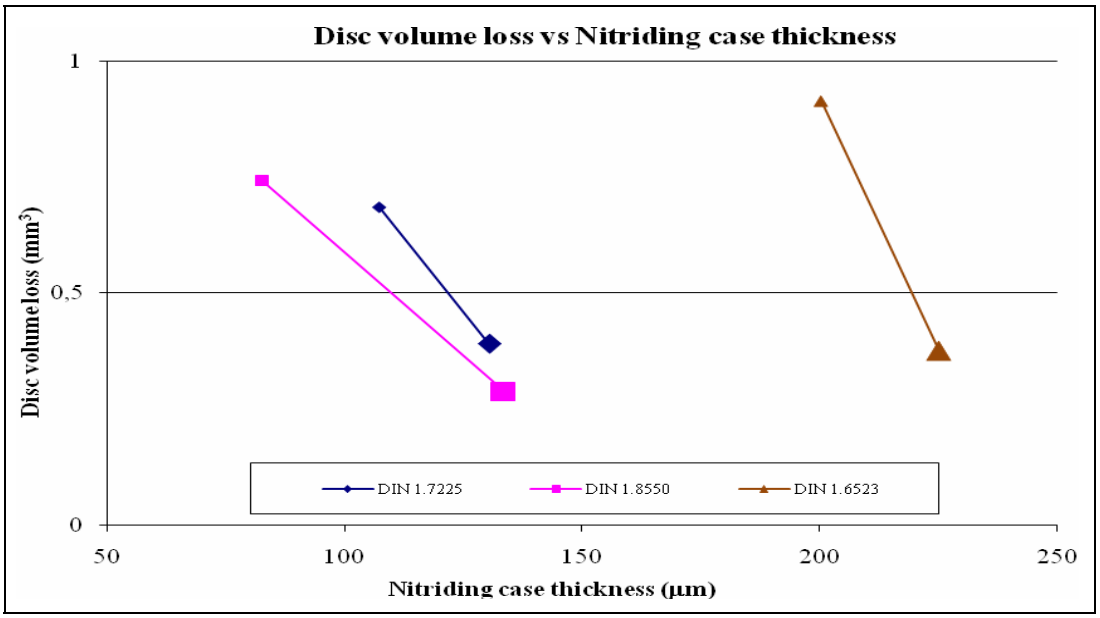

Figure 4.38. Effect of nitriding case thickness on the disc volume loss (Specimens nitrided in Type 2 bath at 520°C for 1h, and 2h) (Note: The larger legend symbols indicate increased nitriding duration)

In contrast to the expectations, for the specimens nitrided in Type 2 bath at 590°C for 0,5h, 1h, and 2h, a different trend than that in Figure 4.37 is seen as shown in Figure 4.39. Volumetric loss measurement of DIN 1.6523 specimens gives an increasing trend with respect to compound layer thickness. In contrast, DIN 1.7225 and DIN 1.8550 specimens' volumetric loss slightly decrease after 1h nitriding, even when compound layer thickness increases. This undesirable result may have been the result of the pore formation in a thick compound layer. In accordance with the explanation in Section 4.1.1.1, channel porosity formation has been

observed in a thick compound layer at high temperature nitriding process (630°C) (See Figure 4.12). However, an equiaxed pore formation has been identified at a low temperature application with a decrease in compound layer thickness (See Figure 4.11). It is possible that an equiaxed pore in the compound layer may wear out easily to become an open pore which reduces the effective contact area between the disc and the compound layer on the pin. Therefore, this may be a reason for lower wear resistance of specimens nitrided at 590°C which have equiaxed pore formations. Furthermore, uneven distribution of compound layer may be also another reason for the wear resistance decrease as it is known that continuous white layer increases wear resistance of the specimens.

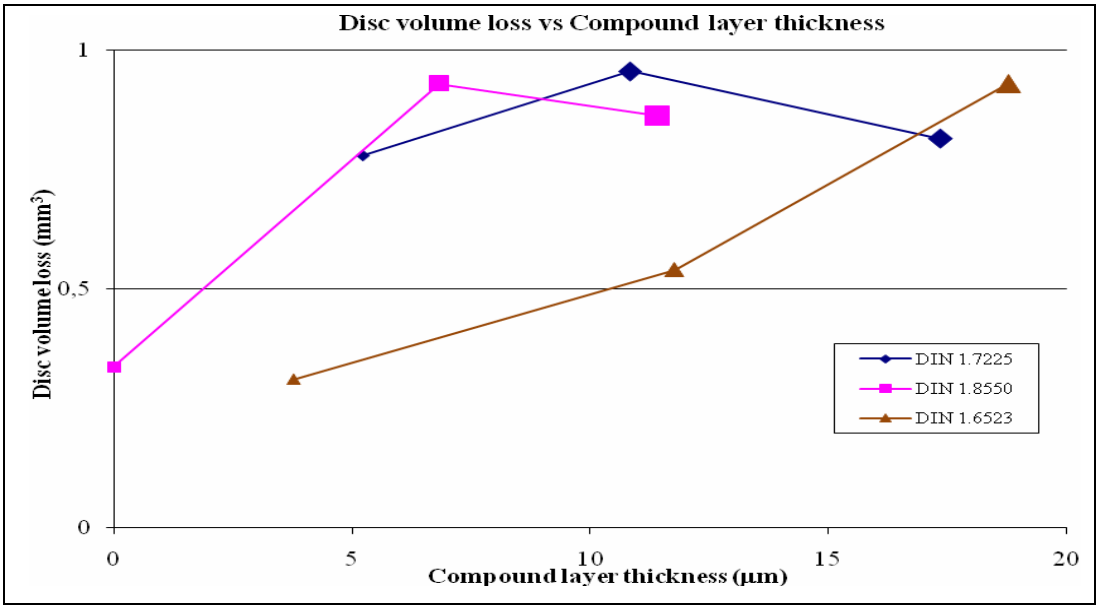

Figure 4.39. Effect of compound layer thickness on the disc volume loss (Specimens nitrided in Type 2 bath at 590°C for 0,5h, 1h, and 2h) (Note: The growing symbols indicate increasing nitriding duration)

The overall evaluation of wear tests has indicated that nitriding increases wear resistance greatly in comparison to unnitrided specimens. Additionally, the wear resistance of the low alloy steel (DIN 1.6523) has been found to be nearly as good as that of the high alloy steel (DIN 1.8550) in this particular test carried out in this thesis. For example, a 0,76 mm^3 disc

volume loss for specimen no 30 (DIN 1.8550) and a 0,68 mm^3 disc volume loss for specimen no 29 (DIN 1.6523) have been measured as plotted in Figure 4.37.

5. CONCLUSIONS

In this thesis, effects of nitriding parameters such as nitriding temperature and duration, nitriding bath composition, and alloy composition on wear and hardness performance have been investigated in detail. Three different alloys have been chosen and nitrided in two different salt baths for four different nitriding durations at four different process temperatures according to a predetermined nitriding test matrix. Microstructures and microhardness of nitrided and unnitrided specimens have been identified by using OM, SEM, EDS, XRD, surface roughness, and microhardness indentations. After that, all specimens have been tested on a pin-on-disc wear setup to identify the change in the wear resistance after nitriding. The following results have been drawn after detailed data analysis.

The OM observations have shown that the compound and diffusion layer formation depend mainly on process temperature and nitriding duration. The higher nitriding temperature results more nitrogen diffusion and hence in a thicker compound layer and nitriding case. Compound layer thickness ranging from 0 to 27 μm has been obtained as a result of nitriding trials. Observations have shown that the nitriding case thickness has a similar trend to the compound layer thickness, and it varies from 70 to 350 μm. Nitriding duration has also been found very important in terms of compound layer and nitriding case formation although its effects have been determined less than that of temperature. This is in consistent with the Fick's 2^{nd} law of diffusion since diffusion depends on temperature exponentially.

Compound and diffusion layer formation are basically triggered by the cyanate content of the salt bath since salt bath composition has a major effect on diffusion. Analyses have shown that Type 1 bath (80 wt per cent potassium cyanate) results in larger diffusion zone than that Type 2 bath (40 wt per cent potassium cyanate) although the process temperature in Type 1 bath is less than that of Type 2 bath which is in line with the diffusion kinetics.

The selected alloys have been compared to differentiate effects of the alloying elements. The analyses have identified that especially aluminum and chromium decrease the diffusion of nitrogen whereas they increase hardness of the specimen. The diffusion depth has been found to depend on the carbon content as well. For example, DIN 1.6523 specimens having low carbon content have always yielded the thickest diffusion layer after the nitriding.

During the analyses, it has been found that the surface roughness of specimens has increased significantly. This increase depends on the core material hardness since harder material can be machined more smoothly but, generally, surface roughness after nitriding is measured around to be 0.7 μm. Therefore, at design stage the dimensions and surface roughness variation due to nitriding should be considered.

Pin on disc wear test result have been evaluated to find the wear resistance of specimens. According to the observations, the compound layer on the surface has a major role on the wear. The increase in the compound layer has reduced the wear on the pin and raised the wear on the disc as expected. Wear test results have also indicated that wear on the disc mating with a specimen without compound layer is less than those with compound layer. In this case, however, the decrease in the compound layer thickness in the pin gives rise to adhesive wear. The softer material gets worn out more rapidly. SEM photos and EDS analysis show clearly that the material deposits from relatively soft pin onto the disc. However, very thick compound layer has triggered abrasive wear on the disc and pin due to its brittle structure.

The combination of microhardness and pin-on-disc wear test results point out that a really high surface hardness (~1000 $HV_{0.1}$) brings about more volume loss on the disc because high surface hardness increases the wear resistance of pin specimens. The decrease in the hardness gives rise to higher amount of wear.

In conclusion, the observations show that nitriding is an effective diffusional surface hardening method to increase wear resistance of specimens. Moreover, by this method, it is possible to use low alloy steels in applications which require high surface hardness and wear

resistance since the surface hardness of the low alloy specimens can be increased to a value twice that of the unnitrided reference specimens.

6. SUGGESTED FUTURE WORKS

In this thesis, the wear performance of nitrided specimens has been studied. However, it is a known fact that nitriding process increases the fatigue and corrosion resistance of alloys. Therefore, the corrosion resistance and fatigue resistance should be studied to understand nitriding process completely. Additionally, the wet wear performance of nitrided specimens has not been studies during this research. This topic is another important application area of nitrided specimens. Thus, wear resistance with lubricant is also needed to be investigated. The change in the core material matrix structure is also affected due to the application temperature of the nitriding process. Thus, changes in the matrix can be analyzed.

7. REFERENCES

1. Stephen, M. C. (Editor), "ASM Handbook Volume 4: Heat Treatment", 1st ed., ASM International, pp.607-978, Detroit, Michigan, 1991.

2. S. Mridha and A.A. Khan, "The Effects of Process Variables on the Hardness of Nitrided 3% Chromium Steel", Journal of Materials Processing Technology, Vol. 201, pp. 325–330, Elsevier, Amsterdam, 2008.

3. "Nitreg Potential-Controlled Gas Nitriding", Nitrex Metal, http://www.nitrex.com/english/ technologies_extra.htm, 2008.

4. "Nitriding, Surface Hardening", Matter, University of Liverpool, http://www.matter.org.uk/steelmatter/manufacturing/surface_hardness/7_2_4.html, 2009.

5. Pye, D., "Practical Nitriding and Ferritic Nitrocarburizing", ASM International, pp. 3-11 and 219-229, Ohio, 2003.

6. Shoemaker, R. H. and Wood, W. G., "Improvement in Wear and Fatigue Properties of Structural Metals through Liquid Nitriding", Journal of Spacecraft and Rockets, Vol. 12, No. 1, pp. 51-53, Detroit, Michigan, 1975.

7. Totten, G. E and Howes, M.A.H. (Editors), "Steel Heat Treatment Handbook", CRC Press, 1st Ed., pp. 721-725, New York, 1997.

8. Langford, G. Sc.D., "Microstructures", Massachusetts Institute of Technology, Cambridge, MA, 1966.

9. "History of Nitriding", http://www.badgermetal.com/nitriding/nitriding-history.htm, 2009.

10. "Modern Methods of Ferritic Nitrocarburizing (FNC)", Badger Metal Tech, Inc, http://nadca.org/committees/die_materials/111401/DM%2011%2014%2001%20Attachment%20G.PDF, 2009.

11. Campbell, F. C., "Elements of Metallurgy and Engineering Alloys", ASM International, pp. 64-71 and 403-405, Ohio, 2007.

12. Bannykh, O. A., Zinchenko, V. M., Prusakov, B. A., and Syropyatov, V. Y., "Advancement Of Nitriding In Russia", Metal Science and Heat Treatment, Vol. 41, No. 7, pp. 287-291, Springer, New York, 1999.

13. Asthana, R., Kumar, A., and Dahotre, N.B., "Materials Processing and Manufacturing Science", pp. 368, Butterworth-Heinemann, Elsevier, Amsterdam, 2006.

14. " Carburizing", http://steel.keytometals.com/Articles/Art114.htm , 2009.

15. "Carburization", http://en.wikipedia.org/wiki/Carburization, 2009.

16. Semiatin, S.L., Cahill, L., Verma, R., and Kovacs, B., "Techcommentary Ion Nitriding" EPRl Center for Materials Fabrication, Vol. 2, No. 5, California, 1994.

17. Souza, C.X. and Pinedo, C.E., "The use of selective plasma nitriding on piston rings for performance Improvement", Materials and Design Vol. 24, pp 131–135, , Elsevier, Amsterdam 2003.

18. "ALLCARB Low Pressure Carburizing for Gears", Fours Industrials B.M.I internal publication, Lyon, 2008.

19. "Boriding / Boronizing", http://metlabheattreat.thomasnet.com/item/all-categories/boriding-boronizing/pn-1010?&plpver=10&forward=1, Metlab Potero, 2009.

20. Davis, J.R., "Surface Hardening of Steels: Understanding the Basics", ASM International, pp. 178-214, Ohio, 2002.

21. Cotell, C.M., Sprague, J.A., and Schmidt, F.A., Jr. (Editors), "ASM Handbook Volume 5: Surface Engineering", 1st ed., ASM International, pp. 1698, Ohio, 1994.

22. Davis, J.R., "Surface Engineering for Corrosion and Wear Resistance: for Corrosion and Wear Resistance", ASM International, pp. 119, Ohio, 2001.

23. Mezlini, S., Tkaya, M.Bb, El Mansori, M., Zahouani, H., and Kapsa, P., "Correlation Between Tribological Parameters and Wear Mechanisms of Homogeneous and Heterogeneous Material", Tribology Letters,Vol. 33, pp. 153–159, Springer, New York, 2008.

24. Liliental, W.K., Maldzinski, L., Morawski, C.D., and Tymowski, G.J., "Potential - Controlled Gas Nitriding Applied to Gears", Nitrex Metal, Inc internal publication, Québec, 2000.

25. Trotter, D., Varcoe, D., Reeves, R., and Anderson, S.H., "Use of HBI and DRI for Nitrogen Control in Steel Products", The Hot Briquetted Iron Association, North Carolina, 2002.

26. K. Yurtışık, "Wear Behaviour of H10A AISI/SAE Steel Nitrided by Various Methods", Master Thesis, METU, Ankara, 2002.

27. Hawkins, D.T., "ASM Source Book on Nitriding", American Society for Metals, pp. 3-120, Cleveland, OH, 1977.

28. Uzun, M.Y., Mühendis ve Makina Dergisi, Vol. 29, No. 338, Türkiye, 1988.

29. Pantazopoulos, G. and Antoniou, S., "Wear-Related Failures of Nitrocarburized Steels: Some Microstructural and Morphological Observations", Journal of Failure Analysis and Prevention, Vol. 4, No. 6, pp. 51-57, Springer, New York, 2004.

30. Huiliang, C., Luo, C.P., Liu, J., and Zou, G., "Phase Transformations in Low-Temperature Chromized 0.45 wt.% C Plain Carbon Steel", Surface & Coatings Technology Vol. 201, no.18, pp. 7970-7977, Elsevier, Amsterdam, 2007.

31. Easterday, J.R., "Liquid Ferritic Nitrocarburizing", Nitromet Division of Kolene Corporation, Detroit, MI 2005.

32. "Industrial Process of Low Pressure Nitriding", Fours Industrials BMI internal publication, Lyon, 2009.

33. "Anhydrous Ammonia", Material Safety Data Sheet, Tanner Industries, Inc., Southampton, PA, 2000.

34. Totten, G.E., Funatani, K., and Xie, L., "Handbook of Metallurgical Process Design", CRC Press, pp. 545-588, New York, 2004.

34. Blau, P.J. (Editor), "ASM Handbook Volume 18: Friction, Lubrication and Wear Technology", 1st ed., Metals and Ceramics Division, Oak Ridge National Laborator, ASM International, Cleveland, OH, 1992.

35. Larbi, A.B.L., Cherif, A., and Tarres, M.A., "Improvement of the Adhesive Wear Resistance of Steel by Nitriding Quantified by the Energy Dissipated in Friction", Wear, Vol. 258, pp. 712–718, Elsevier, Amsterdam, 2005.

36. Toro, A.D., Tanaka, D.K., Sinatora, A., and Tschiptschin A.P., "Improvement of Corrosion-Erosion Resistance of Martensitic Stainless Steels by Nitrogen Addition at High Temperature", Special Issue of the Journal of Materials Processing Technology - Section B4, Vol. 117, no. 3, São Paulo 2001.

37. Ülker, Ş., "PULS Nitrürleme Cihazının Tasarımı ve AISI 52100 Çeliğinin Plazma Nitrürlenmesi", Master Thesis, Afyonkarahisar Kocatepe Üniversitesi, Metal Education Department, Afyonkarahisar, 2006.

38. Güneş, İ., "Plazma Nitrürleme ile Çelikler Üzerinde Kompleks Kaplamaların Oluşturulması", Master Thesis, Afyonkarahisar Kocatepe Üniversitesi, Metal Education Department, Afyonkarahisar, 2006.

39. "Wear", http://en.wikipedia.org/wiki/Wear, 2009.

40. "Fatigue Wear", http://www.pall.com/Aerospace_18167.asp, 2009.

41. Becker, W.T., "ASM Handbook Volume 11: Failure Analysis and Prevention", 1st ed., ASM International, pp.607-978, Detroit, Michigan, 2002.

42. "Tribometers - Friction and Wear Testers", http://www.azonano.com/nanotechnology-equipment.asp?cat=14, 2009.

43. "Nano & Micro Range for Tribological Studies", CSM Tribometers, CMS Instruments Inc, http://www.csm-instruments.com/en/webfm_send/5, 2009.

44. Krishnaraj, N., Iyer, K.J.L., and Sundaresan, S., "Scuffing Resistance of Salt Bath Nitrocarburized Medium Carbon Steel", Wear, Vol: 210, pp. 237-244, Elsevier, Amsterdam, 1997.

45. Schneider, R.S.E. and Hiebler, H., "Influence of Increased Nitriding Temperatures on the Hardness Profile of Low-Alloy Steels", Journal of Materials Science, Vol. 33, No. 7, Springer, New York, 1998.

46. Somers, M. A. J., Kooi, B. J., Maldzinskf, L., Mittemeijer, E. J., Van Der Horst, A. A., Van Der Kraan, A. M., and Van Der Pers, N. M., "Thermodynamics and Long-Range Order of Interstitials in an H.C.P. Lattice: Nitrogen in $\varepsilon - Fe_2N_{1-Z}$", Acta Mater., Vol. 45, No. 5, pp. 2013-2025, Elsevier Science, Oxford, 1997.

47. Türk, A., Ok, O. and Bindal, C., "Structural Characterization of Fluidized Bed Nitrided Steels", Vacuum, Vol. 80, pp. 332–342, Elsevier, Amsterdam, 2005.

48. Spies, H.J., Le Thien, H. and Biermann, H. B., "Nitriding and Carbonitriding of Steels, Controlled Nitriding", Metal Science and Heat Treatment, Vol. 46, No. 7, pp. 7-11, Springer, New York, 2004.

49. Karaoğlu, S., "Az Alaşimli Çeliklerde Karbon Miktarinin Plazma Nitrürasyonu Davranişina Etkisi", Dokuz Eylül Üniversitesi Mühendislik Fakültesi Fen ve Mühendislik Dergisi, Vol. 6, No. 2, pp. 47-52, İzmir, 2004.

50. Leppänen, R., Jonsson, H., "Properties of Nitrided Components – A Result of the Material and the Nitriding Process" Ovako Steels Technical Report 1, Hofors, 1999.

51, Spalvlns, T., "Frictional and Structural Characterization of Ion-Nitrided Low and High Chromium Steels", NASA Technical Memorandum prepared for 12th International Conference on Metallurgical Coatings, Los Angeles, California, 1985.

52. Karamis, M.B., Gercekcioglu, E., "Wear Behaviour of Plasma Nitrided Steels at Ambient and Elevated Temperatures" Wear, Vol. 243, pp.76-84, Kayseri, 2000.

53. Podgornik, B., Vižintin, J., Wänstrand, O., Larsson, M., Hogmark, S., Ronkainen, H., and Holmberg, K., “Tribological Properties of Plasma Nitrided and Hard Coated DIN 1.7225 Steel”, Wear, Vol. 249, pp. 254–259, Elsevier, 2001.